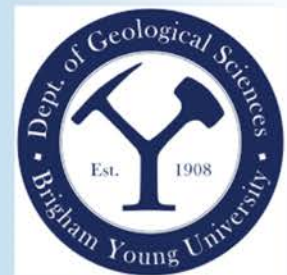
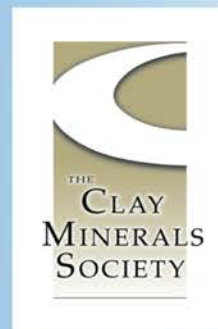


Program and Abstracts



IONIC
MINERAL TECHNOLOGIES





63rd Annual Meeting The Clay Minerals Society

Held at:
Brigham Young University
Conference Center
July 7-11, 2026

CMS 2026 Organizing Committee

Chair: Barry R. Bickmore (BYU)
Vice Chair: Emily J. Evans (BYU)
Scientific Program Chair: Julia A. McIntosh (USGS)
Social Program Coordinator: Joseph W. Stucki (U. Illinois)
Logistics Coordinator: Kevin Rey (BYU)
Tech Support Coordinator: Eric Tingey (BYU)
Field Trip Coordinator: Eric Christiansen (BYU)

The Clay Minerals Society Administration

Mary S. Gray
The Clay Minerals Society
3635 Concorde Parkway, Suite 500
Chantilly, VA 20151-1125 USA
Phone: 703-652-9960 | Fax: 703-652-9951 | Email: cms@clay.org

The Clay Minerals Society

Executive Committee (2025 – 2026)

President: Youjun Deng (Texas A&M)
Vice President: Yuji Arai (U. Illinois)
Secretary: Katerina M. Dontsova (U. Arizona)
Past President: Ian Bourg (Princeton U.)
Treasurer: Wouter Ijdo (Elementis Specialties)
Editor-In-Chief: Joseph W. Stucki (U. Illinois)
Vice-President Elect: Janice Bishop (SETI Institute & NASA-ARC)

Council Members

Through 2026:

Geoffrey Bowers
Branimir Segvic

Through 2027:

Hendrik Heinz
Prakash Malla
Christophe Tournassat

Through 2028:

David Bish
Michael Cheshire
Georgios Chryssikos

2025 Contribution Sustaining Members

Richard K. Brown
Wen-An Chiou
Randall T. Cygan
Will P. Gates
Mary and David Gray
Stephen Guggenheim
William C. Hood
Warren D. Huff
Shelley Roberts (in memory of Dewey Moore)
Paul A. Schroeder
Joseph W. Stucki
Michael A. Velbel

Awards

Marilyn and Sturges W. Bailey Distinguished Member Award

The Marilyn and Sturges W. Bailey Award, the highest honor of The Clay Minerals Society (CMS), is awarded solely for scientific eminence in clay mineralogy as evidenced primarily by the publication of outstanding original scientific research and by the impact of this research on the clay sciences. Service to clay mineralogy, teaching, and administrative accomplishments are not considered in the evaluation of nominees.

| | | |
|----------------------------|----------------------------|-----------------------------------|
| 1968 – Ralph E. Grim | 1990 – John Hower | 2009 – Joseph W Stucki |
| 1969 – C. S. Ross | 1991 – Joe B. Dixon | 2010 – J. M. Serratos |
| 1970 – Paul F. Kerr | 1992 – Philip F. Low | 2011 – Sridhar Komarneni |
| 1971 – Walter D. Keller | 1993 – Thomas J. Pinnavaia | 2012 – Akihiko Yamagishi |
| 1972 – G. W. Brindley | 1995 – W. D. Johns | 2013 – Stephen Guggenheim |
| 1975 – William F. Bradley | 1996 – Victor A. Drits | 2015 – James Kirkpatrick |
| 1975 – Sturges W. Bailey | 1997 – Udo Schwertmann | 2016 – Lisa Heller-Kallai |
| 1975 – Jose J. Fripiat | 1998 – Brij L. Sawhney | 2018 – Gordon “Jock” Churchman |
| 1977 – M. L. Jackson | 2000 – Boris Zvyagin | 2019 – Dennis “Denny” Eberl |
| 1979 – Toshio Sudo | 2001 – Keith Norrish | 2020 – Eduardo Ruiz-Hitzky |
| 1980 – Haydn H. Murray | 2002 – Gerhard Lagaly | 2021 – David L. Bish |
| 1984 – C. Edmund Marshall | 2004 – Benny K. G. Theng | 2022 – Jin-Ho Choy |
| 1985 – Charles E. Weaver | 2005 – M. Jeff Wilson | 2023 – Randall T. Cygan |
| 1988 – Max M. Mortland | 2006 – Frederick J. Wicks | 2024 – Jan Srodon |
| 1989 – R. C. Reynolds, Jr. | 2007 – No Award Made | 2025 – Hailiang Dong |
| 1990 – Joe L. White | 2008 – Norbert Clauer | 2026 – Michael A. Velbel |

George W. Brindley Clay Science Lecture

The G. W. Brindley Clay Science Lecture recognizes a clay scientist who will infuse the Society with new ideas, someone who is both a dynamic speaker and involved in innovative research. Dr. Brindley himself approved the concept of the Lecture, and the speaker should deliver a lecture that Brindley himself would applaud.

| | | |
|----------------------------|---------------------------|----------------------------|
| 1984 – Walter Keller | 1997 – Paul H. Nadeau | 2018 – Cliff T. Johnston |
| 1985 – J. J. Fripiat | 1998 – Bruce Velde | 2019 – Bruno Lanson |
| 1986 – Ralph E. Grim | 1999 – Richard Eggleton | 2020 – No Award Made |
| 1987 – S. W. Bailey | 2000 – D. M. Moore | 2021 – No award Made |
| 1988 – M. L. Jackson | 2001 – Robert Schoonheydt | 2022 – Lynda B. Williams |
| 1989 – W. D. Johns | 2002 – David L. Bish | 2023 – No Award Made |
| 1990 – Alain Baronnet | 2003 – Alain Manceau | 2024 – Prakash B. Malla |
| 1991 – Thomas J. Pinnavaia | 2005 – Maria F. Brigatti | 2025 – No Award Made |
| 1992 – Philip Low | 2008 – Robert Gilkes | 2026 – W. Crawford Elliott |
| 1993 – Dennis D. Eberl | 2009 – M. F. Hochella Jr | |
| 1994 – R. C. Reynolds, Jr. | 2010 – Randall T. Cygan | |
| 1995 – Gerhard Lagaly | 2013 – Andrey Kalinichev | |
| 1996 – Samuel M. Savin | 2017 – Sridhar Komarneni | |

Marion L. and Chrystie M. Jackson Mid-Career Clay Scientist Award

The Jackson Award is to recognize mid-career scientists for excellence in the contribution of new knowledge to clay minerals science through original and scholarly research.

| | | |
|---------------------------|---------------------------|------------------------------|
| 1992 – Joseph W. Stucki | 2001 – Cliff T. Johnston | 2014 – Will P. Gates |
| 1993 – Jan Srodon | 2002 – Sridhar Komarneni | 2015 – Balwant Singh |
| 1994 – Stephen Guggenheim | 2003 – Peter Komadel | 2016 – Janice Bishop |
| 1995 – David L. Bish | 2004 – Fred J. Longstaffe | 2018 – Stephen Hillier |
| 1996 – Darrell G. Schulze | 2005 – Samuel J. Traina | 2019 – Colleen M. Hansel |
| 1997 – Jerry M. Bigham | 2006 – J. Theo Klopprogge | 2020 – Eric E. Roden |
| 1998 – Murray McBride | 2007 – Paul A. Schroeder | 2021 – Hongping He |
| 1999 – Stephen Boyd | 2010 – Toshihiro Kogure | 2022 – Young-Shin Jun |
| 2000 – Jillian Banfield | 2011 – Douglas K. McCarty | 2023 – Christophe Tournassat |
| 2008 – Hailiang Dong | 2012 – Jeffery Post | 2024 – Eric Ferrage |
| 2009 – Lynda B. Williams | 2013 – George Christidis | 2025 – Yuanzhi Tang |
| | | 2026 – Yunfei Xi |

Warren Huff Clay Science Pathway Award

The Warren Huff Clay Science Pathway Award is a newly endowed award of The Clay Minerals Society, intended to support the development of the next generation of clay scientists as they begin to build their careers in clay science research by encouraging their involvement in CMS activities and in the annual meeting.

2025 – Xiaojin Zheng
2026 – Karolina Rybka

Pioneer in Clay Science Lecture Award

The purpose of this award is to recognize at the annual meeting an individual who has made pioneering contributions to clay science.

| | | |
|---------------------------|---------------------------|------------------------------|
| 1987 – Marion L. Jackson | 2000 – William F. Moll | 2013 – Thomas J. Pinnavaia |
| 1988 – R. M. Barrer | 2001 – Don Scafe | 2014 – Douglas W Ming |
| 1989 – H. van Olphen | 2002 – Victor Drits | 2015 – Reinhard Kleeberg |
| 1990 – John W. Jordan | 2003 – Vernon J. Hurst | 2016 – Donald L. Sparks |
| 1991 – Charles E. Weaver | 2004 – Hideomi Kodama | 2017 – Fred J. Longstaffe |
| 1992 – Udo Schwertmann | 2005 – Jillian Banfield | 2018 – Jan Srodon |
| 1993 – Linus Pauling | 2006 – Jean-Maurice Cases | 2019 – Laurent J. Michot |
| 1994 – Joe L. White | 2007 – Spencer G. Lucas | 2020 – James D. Kubicki |
| 1995 – Rustum Roy | 2008 – Emilio Galan | 2021 – No Award Made |
| 1996 – Max M. Mortland | 2009 – Haydn H. Murray | 2022 – Michael Hochella |
| 1997 – Koji Wada | 2010 – No Award Made | 2023 – Susan Brantley |
| 1998 – Robert C. Reynolds | 2011 – Glenn Waychunas | 2024 – Toshihiro Kogure |
| 1999 – V. Colin Farmer | 2012 – No Award Made | 2025 – Christopher Greenwell |
| | | 2026 – Dennis Eberl |

Meeting Sponsors



IONIC
MINERAL TECHNOLOGIES



BYU Conference Center

Interactive BYU Campus Map: <https://map.byu.edu/?parking=true>



- ★ **2254–Room 1**
- ★ **2265–Room 2**
- ★ **2267–Room 3**
- ★ **2295–Poster Hall**
- ★ **2279–Speaker Ready Room**
- ★ **2287–Coffee/Tea**
- ★ **Pavilion (Snack Breaks)**

Parking

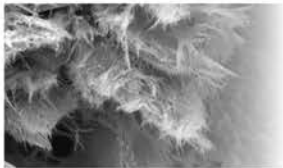
Free parking in the first three rows of parking spaces next to the BYU Conference Center. If you cannot find parking there, there are other Visitor lots on campus where you can park for free. To see an interactive map of campus, visit <https://map.byu.edu>.



Other

For questions about travel, public transportation, lodging, food, activities, and more, see:

<https://clayconferences.org/clay-minerals-society-2026-meeting/>



CLAY 2027
Madrid - Spain
20-26 June



Our next meeting will be in Madrid with clay scientists from around the world!

<https://icc.aipea.org/clay-2027/>

CLAY 2027 Conference Chairs

Jaime Cuevas (CyGQ, UAM)

Pilar Aranda (ICMM-CSIC)

Ana Isabel Ruiz (CyGQ, UAM)

Margarita Darder (ICMM-CSIC)

Sociedad Española de Arcillas

Departamento de Geología y Geoquímica | Facultad de Ciencias
Universidad Autónoma de Madrid · Campus de Cantoblanco
Calle Francisco Tomás y Valiente, 7, 28049, Madrid, Spain

Events

Concurrent events and social program activities are listed below.

| Day | Time | Event | Location |
|-------------------|-------------|--|--|
| Tuesday, July 7 | 07:45-17:00 | SLC Tour | Meet on the West side of the BYU Conference Center |
| Tuesday, July 7 | 09:00-15:00 | Executive Committee and Council Meeting | 2279 Conference Center |
| Tuesday, July 7 | 20:00-22:00 | Opening Social | Provo Marriott Hotel |
| Wednesday, July 8 | 09:00-10:00 | BYU Campus Tour #1 | Meet on the West side of the BYU Conference Center |
| Wednesday, July 8 | 10:00-11:00 | BYU Campus Tour #2 | Meet on the West side of the BYU Conference Center |
| Wednesday, July 8 | 11:00-12:00 | BYU Campus Tour #3 | Meet on the West side of the BYU Conference Center |
| Wednesday, July 8 | 14:00-16:00 | Geologic Tour of Rock Canyon #1 | Meet on the West side of the BYU Conference Center |
| Wednesday, July 8 | 16:00-18:00 | Geologic Tour of Rock Canyon #2 | Meet on the West side of the BYU Conference Center |
| Wednesday, July 8 | 18:30-20:30 | C&CM Editorial Board Dinner | Meet on the West side of the BYU Conference Center at 5:45 pm. We will be going to a restaurant in Lehi, UT. |
| Wednesday, July 8 | 20:00-21:00 | Planetarium Show | BYU, Eyring Science Center, 4th Floor |
| Thursday, July 9 | 08:30-12:30 | Timpanogos Cave Guided Tour | Meet on the West side of the BYU Conference Center |
| Thursday, July 9 | 18:00-22:00 | Conference Banquet | Provo Marriott Hotel |
| Friday, July 10 | 11:30-13:00 | BYU Paleontology Museum Tour | Meet on the West side of the BYU Conference Center |
| Friday, July 10 | 14:00-16:00 | Geologic Tour of Rock Canyon #3 | Meet on the West side of the BYU Conference Center |
| Friday, July 10 | 16:00-18:00 | Geologic Tour of Rock Canyon #4 | Meet on the West side of the BYU Conference Center |
| Friday, July 10 | 17:00-21:00 | CMS Business Meeting | 2279 Conference Center |
| Saturday, July 11 | 08:00-17:00 | Field Trip | Meet on the West side of the BYU Conference Center |

At-a-Glance Schedule

Room key: Room 1 = CONF 2254; Room 2 = CONF 2265; Room 3 = CONF 2267; Poster Session = CONF 2295

Tuesday

| Time | Room 1 CONF 2254 | Room 2 CONF 2265 | Room 3 CONF 2267 | Events 1 | Events 2 |
|-------------|---------------------|---------------------|---------------------|----------------------------|---|
| 07:45-09:00 | | | | 07:45-17:00 SLC Tour | |
| 09:00-15:00 | | | | SLC Tour (cont.) | 09:00-15:00 Executive Committee and Council Meeting |
| 15:00-17:00 | | | | SLC Tour (cont.) | |
| 20:00-22:00 | | | | 20:00-22:00 Opening Social | |

Wednesday

| Time | Room 1 CONF 2254 | Room 2 CONF 2265 | Room 3 CONF 2267 | Events 1 | Events 2 |
|-------------|--|----------------------------|--|--------------------------------|----------|
| 08:40-09:00 | Welcome | | | | |
| 09:00-09:05 | Introduction: Barry Bickmore for Eberl | | | 09:00-10:00 BYU Campus Tour #1 | |
| 09:05-09:45 | Plenary 1: Pioneer Lecture: Eberl | | | BYU Campus Tour #1 (cont.) | |
| 09:45-09:50 | Break | Break | Break | BYU Campus Tour #1 (cont.) | |
| 09:50-10:00 | Session 14: Ishimwe; Lam | Session 1: Nguyen; Donahoe | Session 7: Sanchez-Avellaneda; Barbosa | BYU Campus Tour #1 (cont.) | |
| 10:00-10:30 | | | | 10:00-11:00 BYU Campus Tour #2 | |
| 10:30-10:50 | Break | Break | Break | BYU Campus Tour #2 (cont.) | |
| 10:50-11:00 | Session 14: Liu; Ryan | Session 1: Kang; Zeng | Session 7: Rybka; Xu | BYU Campus Tour #2 (cont.) | |
| 11:00-11:30 | | | | 11:00-12:00 BYU Campus Tour #3 | |

| Time | Room 1 CONF 2254 | Room 2 CONF 2265 | Room 3 CONF 2267 | Events 1 | Events 2 |
|-------------|--------------------------------|--------------------------------|-----------------------------------|---|------------------------------|
| 11:30-11:50 | | Session 1: Zhong | Session 7: Morii | BYU Campus Tour #3 (cont.) | |
| 11:50-12:00 | Lunch | Lunch | Lunch | BYU Campus Tour #3 (cont.) | |
| 12:00-13:50 | | | | | |
| 13:50-14:00 | Session 9: Ma; Dong; Liang | Session 12: Legg; Cho; Oladele | Session 7: Kuligiewicz; Derkowski | | |
| 14:00-14:50 | | | | 14:00-16:00 Geologic Tour of Rock Canyon #1 | |
| 14:50-15:10 | | Session 12: Chipman | Session 7: Skiba | Geologic Tour of Rock Canyon #1 (cont.) | |
| 15:10-15:30 | Break | Break | Break | Geologic Tour of Rock Canyon #1 (cont.) | |
| 15:30-16:00 | Session 9: Bouchelaghem; Trung | Session 12: Xi; Yang | Session 7: Chuang; Bourg | Geologic Tour of Rock Canyon #1 (cont.) | |
| 16:00-16:10 | | | | 16:00-18:00 Geologic Tour of Rock Canyon #2 | |
| 16:10-16:50 | | Session 12: Zhang; Xu | | Geologic Tour of Rock Canyon #2 (cont.) | |
| 16:50-18:00 | | | | Geologic Tour of Rock Canyon #2 (cont.) | |
| 18:30-20:00 | | | | 18:30-20:30 C&CM Editorial Board Dinner | |
| 20:00-20:30 | | | | C&CM Editorial Board Dinner (cont.) | 20:00-21:00 Planetarium Show |
| 20:30-21:00 | | | | Planetarium Show (cont.) | |

Thursday

| Time | Room 1 CONF 2254 | Room 2 CONF 2265 | Room 3 CONF 2267 | Events 1 | Events 2 |
|-------------|--|--------------------------------|--|---|----------|
| 08:30-08:35 | Introduction: Janice Bishop for Michael Velbel | | | 08:30-12:30 Timpanogos Cave Guided Tour | |
| 08:35-09:15 | Plenary 2: Bailey Lecture: Velbel | | | Timpanogos Cave Guided Tour (cont.) | |
| 09:15-09:20 | Introduction: Prakash Malla for Crawford Elliott | | | Timpanogos Cave Guided Tour (cont.) | |
| 09:20-10:00 | Plenary 3: Brindley Lecture: Elliott | | | Timpanogos Cave Guided Tour (cont.) | |
| 10:00-10:05 | Break | Break | Break | Timpanogos Cave Guided Tour (cont.) | |
| 10:05-11:05 | Session 8: Bose; Vierling; Bishop x2 | Session 3: Holmboe; Swai; Legg | Session 2: McIntosh; Smolen; Döbelin (Kanik) | Timpanogos Cave Guided Tour (cont.) | |
| 11:05-11:25 | Break | Break | Break | Timpanogos Cave Guided Tour (cont.) | |
| 11:25-12:05 | Session 8: Hendrickson; M. Elwood Madden | Session 3: Ho; Underwood | Session 2: Andrzejewski; Burgener | Timpanogos Cave Guided Tour (cont.) | |
| 12:05-12:25 | | Session 3: Heinz | | Timpanogos Cave Guided Tour (cont.) | |
| 12:25-12:30 | Lunch | Lunch | Lunch | Timpanogos Cave Guided Tour (cont.) | |

| Time | Room 1 CONF 2254 | Room 2 CONF 2265 | Room 3 CONF 2267 | Events 1 | Events 2 |
|-------------|-----------------------------|------------------------|----------------------|--------------------------------|----------|
| 12:30-14:25 | | | | | |
| 14:25-14:45 | | | | | |
| 14:45-15:05 | Session 8: A. Elwood Madden | Session 4: Meyer | Session 11: Smolen | | |
| 15:05-15:25 | Session 8: Sluder | Session 4: Day-Stirrat | Session 11: Hudson | | |
| 15:25-15:45 | Session 8: Sahai | Session 4: Ogunsunlade | Session 11: Stokes | | |
| 15:45-16:05 | Break | Break | Break | | |
| 16:05-16:25 | Session 6: Rytwo | Session 4: Molnar | Session 11: Fischer | | |
| 16:25-16:45 | | Session 4: Ellis | Session 11: Cheshire | | |
| 16:45-17:05 | | Session 4: Schroeder | | | |
| 17:05-17:25 | | Session 4: Wei | | | |
| 18:00-22:00 | | | | 18:00-22:00 Conference Banquet | |

Friday

| Time | Room 1 CONF 2254 | Room 2 CONF 2265 | Room 3 CONF 2267 | Events 1 | Events 2 |
|-------------|---|--------------------------|--------------------------|---|----------|
| 08:55-09:00 | Introduction: Michal Skiba for Karolina Rybka | | | | |
| 09:00-09:40 | Plenary 4: Huff Lecture: Rybka | | | | |
| 09:40-09:45 | Introduction: Youjun Deng for Yunfei Xi | | | | |
| 09:45-10:25 | Plenary 5: Jackson Award Lecture: Xi | | | | |
| 10:25-10:30 | Break | Break | Break | | |
| 10:30-11:30 | Poster Session CONF 2295 | Poster Session CONF 2295 | Poster Session CONF 2295 | | |
| 11:30-12:40 | | | | 11:30-13:00 BYU Paleontology Museum Tour | |
| 12:40-13:00 | Lunch | Lunch | Lunch | BYU Paleontology Museum Tour (cont.) | |
| 13:00-14:00 | | | | | |
| 14:00-14:20 | | | | 14:00-16:00 Geologic Tour of Rock Canyon #3 | |
| 14:20-15:00 | Session 10: Foyсал; Matusik | Session 1: Wong; Liu | | Geologic Tour of Rock Canyon #3 (cont.) | |

| Time | Room 1 CONF 2254 | Room 2 CONF 2265 | Room 3 CONF 2267 | Events 1 | Events 2 |
|-------------|------------------------|---------------------|---------------------|---|----------------------------------|
| 15:00-15:20 | Session 10: Phillips | | | Geologic Tour of Rock Canyon #3 (cont.) | |
| 15:20-15:40 | Break | Break | Break | Geologic Tour of Rock Canyon #3 (cont.) | |
| 15:40-16:00 | Session 10: Dziewiatka | Session 1: Bickmore | | Geologic Tour of Rock Canyon #3 (cont.) | |
| 16:00-16:20 | Session 10: Zolzaya | Session 1: Wang | | 16:00-18:00 Geologic Tour of Rock Canyon #4 | |
| 16:20-16:30 | Break | Break | Break | Geologic Tour of Rock Canyon #4 (cont.) | |
| 16:30-17:00 | Closing/Awards | | | Geologic Tour of Rock Canyon #4 (cont.) | |
| 17:00-18:00 | | | | Geologic Tour of Rock Canyon #4 (cont.) | 17:00-21:00 CMS Business Meeting |
| 18:00-21:00 | | | | CMS Business Meeting (cont.) | |

Saturday

| Time | Room 1 CONF 2254 | Room 2 CONF 2265 | Room 3 CONF 2267 | Events 1 | Events 2 |
|-------------|---------------------|---------------------|---------------------|------------------------|----------|
| 08:00-17:00 | | | | 08:00-17:00 Field Trip | |

Plenary and Award Lectures

| Day | Time | Lecturer | Lecture |
|-----------|-------------|-----------|--|
| Wednesday | 09:05-09:45 | Eberl | My Half Century as a Clay Scientist |
| Thursday | 08:35-09:15 | Velbel | Bailey Lecture: From Earth to Mars: A framework for interpreting Martian clay minerals and ancient Mars |
| Thursday | 09:20-10:00 | Elliott | Brindley Lecture: Occurrences and Distributions of the Rare-Earth Elements in the Georgia Kaolins and Enclosing Sands, Upper Coastal Plain, Georgia. |
| Friday | 09:00-09:40 | Rybka | Huff Lecture: Rehydration Behaviour of Smectites and Bentonites |
| Friday | 09:45-10:25 | Yunfei Xi | Jackson Award Lecture: Structure and Reactivity of Clay Minerals and Its Environmental and Engineering Applications |

Session Descriptions

Descriptions are summarized from the CMS 2026 Sessions page. Folded/defunct sessions are omitted from this list.

| Session | Title | Summary |
|---------|--|--|
| 1 | General Session | Clay science presentations that do not fit neatly into one of the specialized sessions, including talks folded in from undersubscribed topics. |
| 2 | Clays as Paleoclimate Indicators | Paleosol clay mineralogy, geochemistry, microscopy, and modeling as tools for reconstructing past terrestrial environments and climates. |
| 3 | Clays in the Computer | Computational, atomistic, continuum, machine-learning, and data-driven approaches to clay structure, reactivity, transport, swelling, and related processes. |
| 4 | Clay-hosted Critical Mineral Resources | Occurrences, speciation, extraction, and resource evaluation of critical minerals in clay-rich rocks and sedimentary systems. |
| 5 | Software for Clays | Software packages and computational tools for analyzing clay-related data and supporting clay science workflows. |
| 6 | Clays, Organoclays, and Nanocomposites for Water Treatment | Clay-based materials and technologies for water purification, pollutant removal, disinfection, and sustainable water treatment. |
| 7 | Science and Engineering of Bentonites and Other Clays for Nuclear Waste Disposal | Characterization, monitoring, and prediction of clay behavior in engineered and natural nuclear-waste barrier systems. |
| 8 | Investigating Clays on Planetary Bodies | Laboratory, remote-sensing, returned-sample, analog, and modeling studies of phyllosilicates on Mars, asteroids, Ceres, and ocean-world environments. |
| 9 | Sorption, Transport, and Remediation of Emerging Contaminants by Natural and Engineered Clays | Clay-contaminant interactions, molecular mechanisms, engineered barriers, field performance, and predictive tools for sustainable remediation. |
| 10 | Clay-Based Strategies for Mitigating Toxins | Clay and layered-material strategies for microbial control, toxin adsorption or degradation, health applications, and regulatory/safety considerations. |

| Session | Title | Summary |
|---------|---|---|
| 11 | Clays and Zeolites in the Oil and Gas Industry | Roles of clays and zeolites in petroleum systems, drilling, refining, rock properties, and energy production. |
| 12 | Advanced Characterization of Clay Minerals | High-resolution, in situ, spectroscopic, synchrotron, microscopy, and porosimetry methods that advance clay-mineral characterization. |
| 14 | Clay-sized Minerals in Soils | Characterization, reactivity, nutrient cycling, pollutant immobilization, and agro-environmental behavior of the soil clay fraction. |

Abstract Indices

By Day and Session

Wednesday Morning

Plenary and Award Lectures | Room 1 (CONF 2254) | 09:00-09:45

| | |
|--|----|
| 09:00-09:05 - Introduction: Barry Bickmore for Eberl | |
| 09:05-09:45 - Eberl: My Half Century as a Clay Scientist | 29 |

Session 14: Clay-sized Minerals in Soils | Room 1 (CONF 2254) | 09:50-11:30

| | |
|--|----|
| 09:50-10:10 - Ishimwe: Formation of Halloysite in Volcanic Soils: Insights for Podoconiosis | 30 |
| 10:10-10:30 - Lam: Characterizing the Clay Mineralogy of the Pu'u 'Ōhi'a Andisol from O'ahu, Hawai'i | 34 |
| 10:50-11:10 - Liu: Mg-Fe Layered Double Hydroxide as a Controlled-Release Phosphorus Fertilizer: Improving Plant P Uptake and Reducing Soil P Loss | 37 |
| 11:10-11:30 - Ryan: Soil Heterogeneity and the Influence of Clay Minerals on Landslide Risk in Hilly Tropical Landscapes | 40 |

Session 1: General Session | Room 2 (CONF 2265) | 09:50-11:50

| | |
|--|----|
| 09:50-10:10 - Nguyen: Synthesis of Smectite-Like Clays from Biotite in Mine Waste for Acid Mine Drainage Prevention | 32 |
| 10:10-10:30 - Donahoe: Clay Minerals and Fe-Oxyhydroxides as Controls on Trace Metal Attenuation in an Acid Mine Drainage-Impacted Watershed, Alabama, USA | 35 |
| 10:50-11:10 - Kang: Selective Microbial Iron Reduction in Nontronite-Maghemite Mixtures Under Repeated Freeze-Thaw Cycles | 38 |
| 11:10-11:30 - Zeng [Remote]: Construction of Sepiolite-Supported Polyamidoxime Composite and Its Uranyl Ion Adsorption Performance | 41 |
| 11:30-11:50 - Zhong [Remote]: Sepiolite-Supported Bimetallic Catalysts for the Oxidation of 5-Hydroxymethylfurfural to 2,5-Furandicarboxylic Acid | 43 |

Session 7: Science and Engineering of Bentonites and Other Clays for Nuclear Waste Disposal | Room 3 (CONF 2267) | 09:50-11:50

| | |
|--|----|
| 09:50-10:10 - Sanchez-Avellaneda [Remote]: A Miniature Device for Studying Swelling Pressure of Smectites | 33 |
| 10:10-10:30 - Barbosa [Remote]: Coupled Thermo-Hydro-Mechanical Modeling of Mx-80 Bentonite Pellets Using a Double-Structure Framework | 36 |
| 10:50-11:10 - Rybka: Is Humidity the Main Control of Hydration in Smectites? | 39 |
| 11:10-11:30 - Xu: Immobilizing Radioactive Iodide and Iodate Using Chrysotile and Halloysite, Respectively | 42 |
| 11:30-11:50 - Morii: In Situ Observation of the Re-Oxidation Behavior of Structural Iron in Montmorillonite by X-Ray Absorption Fine Structure | 44 |

Wednesday Afternoon

Session 9: Sorption, Transport, and Remediation of Emerging Contaminants by Natural and Engineered Clays | Room 1 (CONF 2254) | 13:50-16:10

| | |
|---|----|
| 13:50-14:10 - Ma: Incorporating Clay into Novel Nature-Based Solutions for Emerging Contaminants | 45 |
| 14:10-14:30 - Dong: Tailoring Natural Clays for Selective and Sustainable PFAS Removal: Exploring Cation Exchange, Post-Grafting, and Fluorophilic Interactions | 48 |
| 14:30-14:50 - Liang: The Use of Cationic Clay for Sorption of per- and Poly-Fluoroalkyl Substances and Destruction by Photoreduction | 52 |
| 15:30-15:50 - Bouchelaghem [Remote]: Membrane Efficiency of Montmorillonite Suspensions | 55 |
| 15:50-16:10 - Trung: Optimizing Bentonite Contents in Moraine for Low-Permeability Oxygen Barriers in Mine Waste Cover Systems | 58 |

Session 12: Advanced Characterization of Clay Minerals | Room 2 (CONF 2265) | 13:50-16:50

| | |
|---|----|
| 13:50-14:10 - Legg: Imaging the Formation of Nanostructured Hydroxide Films on Mineral-Water Interfaces | 46 |
| 14:10-14:30 - Cho: Iron Redox-Driven Arsenic Immobilization via Algal Biomineralization Revealed by Synchrotron Spectroscopy | 49 |
| 14:30-14:50 - Oladele: Physicochemical Characterization and Surface Reactivity of Cookeite from Mineral Dissolution, Microscopic and Spectroscopic Studies | 50 |
| 14:50-15:10 - Chipman: A Deep-Learning Approach for Phase Picking in X-Ray Powder Diffraction Analysis of Clay-Bearing Mixtures | 53 |
| 15:30-15:50 - Xi [Remote]: Integrated Micro-To-Atomic Scale Characterization of Complex Phyllosilicates from the Long Valley Rhyolite: A Multi-Technique Approach | 56 |

| | |
|--|----|
| 15:50-16:10 - Yang [Remote]: Three-Dimensional Electron Diffraction: A Revolutionary Technique for Rapid and Non-Destructive Identification of Clay Mineral Structures | 59 |
| 16:10-16:30 - Zhang [Remote]: Accurate Identification of Element Occupancy Within Single Layers of Mg–Ni Saponite by Coupling FTIR and HAADF-STEM-EDXS | 61 |
| 16:30-16:50 - Xu: Incommensurately Modulated Structure of Greenalite with Non-Stoichiometry: Z-Contrast Imaging and iDPC Imaging Study | 62 |

Session 7: Science and Engineering of Bentonites and Other Clays for Nuclear Waste Disposal | Room 3 (CONF 2267) |

13:50-16:10

| | |
|---|----|
| 13:50-14:10 - Kuligiewicz: The Apparent Layer Charge Changes in Dehydrated and Rehydrated Smectites and Bentonites | 47 |
| 14:30-14:50 - Derkowski: Prospecting Raw Clay Materials for Nuclear Waste Repository Buffer Applications | 51 |
| 14:50-15:10 - Skiba: Belchatów Bentonite Deposit: A Unique Case with Distinct Properties | 54 |
| 15:30-15:50 - Chuang: Comparative Mineralogical Characterization of Asian Bentonites for Potential Engineered Clay Barrier Applications | 57 |
| 15:50-16:10 - Bourg: Claycg: Towards a Coarse-Grained Model of Hydrated Clay Minerals | 60 |

Thursday Morning

Plenary and Award Lectures | Room 1 (CONF 2254) | 08:30-10:00

| | |
|--|----|
| 08:30-08:35 - Introduction: Janice Bishop for Michael Velbel | |
| 08:35-09:15 - Velbel: Bailey Lecture: From Earth to Mars: A Framework for Interpreting Martian Clay Minerals and Ancient Mars | 63 |
| 09:15-09:20 - Introduction: Prakash Malla for Crawford Elliott | |
| 09:20-10:00 - Elliott: Brindley Lecture: Occurrences and Distributions of the Rare-Earth Elements in the Georgia Kaolins and Enclosing Sands, Upper Coastal Plain, Georgia | 64 |

Session 8: Investigating Clays on Planetary Bodies | Room 1 (CONF 2254) | 10:05-12:05

| | |
|---|----|
| 10:05-10:25 - Bose: An Overview of Clay-Rich Mudballs in Our Solar System | 65 |
| 10:25-10:45 - Vierling: Alteration Histories of Asteroids Revealed by Clay Chemistry | 68 |
| 10:45-10:55 - Bishop: Spectral Properties of NH₄⁺-Clays and Applications to Asteroids Ceres, Bennu, and Ryugu | 71 |
| 10:55-11:05 - Bishop: Clay Mineral Assemblages Provide Insights into Ancient Aqueous Alteration at Tyrrhena Terra, Mars | 72 |
| 11:25-11:45 - Hendrickson: Evaluating Clay Mineral Ima Species in Gale Crater, Mars, and Maa Model Clay Predictions | 74 |
| 11:45-12:05 - M. Elwood Madden: Clay Alteration in High Salinity Brines: Cation Exchange & Enhanced Aluminum Mobility | 79 |

Session 3: Clays in the Computer | Room 2 (CONF 2265) | 10:05-12:25

| | |
|--|----|
| 10:05-10:25 - Holmboe [Remote]: Atomipy: A Python Framework and Topology Tool for Building Multicomponent Clay Systems for Molecular Simulations | 66 |
| 10:25-10:45 - Swai [Remote]: MD Simulation on Ciprofloxacin-Montmorillonite Interaction: Interfacial Dynamics, Coordination Environment, and Adsorption Free Energy Landscapes | 69 |
| 10:45-11:05 - Legg: The Energetics of Electrical Double Layers Over Heterogeneously Charged Surfaces | 75 |
| 11:25-11:45 - Ho: Unraveling Long-Range Nanoconfinement Effects in Charged Layered Nanopores | 77 |
| 11:45-12:05 - Underwood: When Pores Polarize: A Brownian Dynamics Examination of Membrane Polarization in Heterogeneously Charged Media | 80 |
| 12:05-12:25 - Heinz [Remote]: Simulation of Alumina and Clay Minerals with pH Resolution to Study Electrolyte Interfaces and Organic Binding | 81 |

Session 2: Clays as Paleoclimate Indicators | Room 3 (CONF 2267) | 10:05-12:05

| | |
|--|----|
| 10:05-10:25 - McIntosh: A Review of O-H Stable Isotope Methods for Improved Estimation of Temperature Using Phyllosilicates .. | 67 |
| 10:25-10:45 - Smolen: Kinetic Controls on Clay Hydrogen Isotopes in Paleoclimate Archives | 70 |
| 10:45-11:05 - Döbelin (Kanik): Recent Progress in the Understanding of Smectite-Stable Isotope Systematics: Methodological Considerations for Soil Science | 73 |
| 11:25-11:45 - Andrzejewski: Assessing Paleoclimate Using Pedogenic Minerals from Cretaceous Paleosols of the Dakota Fm. in Kansas | 76 |
| 11:45-12:05 - Burgener: Paleoclimate Reconstructions Using Paleosol Clay and Coarse Sediment Geochemistry: A Machine Learning Approach | 78 |

Thursday Afternoon

Session 8: Investigating Clays on Planetary Bodies | Room 1 (CONF 2254) | 14:45-15:45

| | |
|---|----|
| 14:45-15:05 - A. Elwood Madden: Is There a Smectite Signature of Euxinic Chemical Weathering or Diagenesis? | 82 |
|---|----|

| | |
|--|-----|
| 15:05-15:25 - Sluder: Nano-Phases Formed at Redox Interfaces in a Sulfidic Spring | 84 |
| 15:25-15:45 - Sahai: A Generalized Structure-Chemistry-Activity Relationship for Smectite-Catalyzed RNA Polymerization in Prebiotic Chemistry on Early Earth-Like Planetary Bodies | 86 |
| Session 4: Clay-hosted Critical Mineral Resources Room 2 (CONF 2265) 14:45-17:25 | |
| 14:45-15:05 - Meyer: Differentiating Lithium-Bearing Clays Using Orbital and Airborne Hyperspectral Data | 85 |
| 15:05-15:25 - Day-Stirrat: Lithium-Bearing Clay Mineral Assemblages in the McDermitt Caldera, Oregon-Nevada, USA: An Exploration Framework | 87 |
| 15:25-15:45 - Ogunsunlade: Mechanical Activation of Underclay for Enhanced Lithium Extraction and Amorphous Silica Production | 89 |
| 16:05-16:25 - Molnar: The Effect of pH on the Interactions Between Rare Earth Element Ions and Gibbsite Nanoparticles | 92 |
| 16:25-16:45 - Ellis: Clay Mineral Controls on REE Distribution and Recovery in Georgia Kaolin Mine Tailings | 94 |
| 16:45-17:05 - Schroeder: History of Georgia and Cornwall Kaolin Production and New Insights for Co-Production of Critical Minerals | 96 |
| 17:05-17:25 - Wei [Remote]: The Characteristics and Genesis of Secondary Minerals in the Granitic Rock Regolith in South China .. | 97 |
| Session 11: Clays and Zeolites in the Oil and Gas Industry Room 3 (CONF 2267) 14:45-16:45 | |
| 14:45-15:05 - Smolen: Clay-Organic Interactions: Evolution of N-Alkanes During Early Maturation of Sedimentary Organic Matter | 83 |
| 15:05-15:25 - Hudson: Elemental Geochemistry of the Mowry Shale as a Predictive Tool for Hydrocarbon Exploration | 88 |
| 15:25-15:45 - Stokes: Evaluating the Effects of Smectite Species and Exchangeable Cations on Solid Bitumen Maturation in Hydrous Pyrolysis Experiments | 90 |
| 16:05-16:25 - Fischer: Modeling the Geomechanical Effects of Layered Bentonites in Production of the Mowry Shale | 93 |
| 16:25-16:45 - Cheshire: Smectite–Illite Transformation and Kaolinite Formation from Offshore Africa: Implications for Thermal Evolution and Fluid–Rock Interaction | 95 |
| Session 6: Clays, Organoclays, and Nanocomposites for Water Treatment Room 1 (CONF 2254) 16:05-16:25 | |
| 16:05-16:25 - Rytwo: Application of Clay-Polymer Nanocomposites for the Removal of Toxic Cyanobacteria and Other Phytoplankton from Water | 91 |
| Friday Morning | |
| Plenary and Award Lectures Room 1 (CONF 2254) 08:55-10:25 | |
| 08:55-09:00 - Introduction: Michał Skiba for Karolina Rybka | |
| 09:00-09:40 - Rybka: Huff Lecture: Rehydration Behaviour of Smectites and Bentonites | 98 |
| 09:40-09:45 - Introduction: Youjun Deng for Yunfei Xi | |
| 09:45-10:25 - Yunfei Xi: Jackson Award Lecture: Structure and Reactivity of Clay Minerals and Its Environmental and Engineering Applications | 99 |
| Session 1: General Session Posters (CONF 2295) 10:30-12:40 | |
| 10:30-12:40 - Agada [Remote]: Functional Evaluation of Clay Minerals and Carbon-Based Adsorbents for Antimicrobial and Cytoprotective Effects in a Poultry Disease Model | 104 |
| 10:30-12:40 - Al-Laban [Remote]: Finite Element Analysis of Piled Raft Tunnel Interaction Under Changing Clay Conditions | 115 |
| 10:30-12:40 - Deng: Probing Structural Changes of Sepiolite and Zeolitic Water Dynamics with Temperature-Dependent Infrared Spectroscopy and Molecular Simulations | 105 |
| 10:30-12:40 - Matusik: Evaluating Zinc and Cobalt Doping of Layered Double Hydroxides on Their Efficiency of Lithium Extraction from Brines | 102 |
| 10:30-12:40 - Olorunfemi: Kaolin Membranes for Ethanol Steam Reforming and Gas Separation: Microstructural Evolution and Chemical Modification | 100 |
| Session 2: Clays as Paleoclimate Indicators Posters (CONF 2295) 10:30-12:40 | |
| 10:30-12:40 - Muhammad: Quaternary Reorganization of the Indonesian Throughflow and Its Influence on Regional Sea Level and Monsoon Dynamics | 107 |
| Session 4: Clay-hosted Critical Mineral Resources Posters (CONF 2295) 10:30-12:40 | |
| 10:30-12:40 - Gerratt: The Mineralogy, Geochemistry, and Genesis of the Silicon Ridge Clay Deposit, Utah County, Utah, USA | 109 |
| Session 5: Software for Clays Posters (CONF 2295) 10:30-12:40 | |
| 10:30-12:40 - Bickmore: Emmalab: A Tool for Sediment Unmixing | 113 |
| 10:30-12:40 - Burgener: The Terrestrial Paleoclimate Database: An Open-Access Resource for Sedimentologic and Geochemical Paleoclimate Studies | 114 |
| 10:30-12:40 - Evans: Machine Learning for Mineral Identification | 112 |
| 10:30-12:40 - Kuligiewicz: LC-OD: A Portable R-Based Application for Smectite Layer Charge Calculation Using the OD Method ... | 110 |
| 10:30-12:40 - Teeple: A Peak-Modeling Program for Thermogravimetric Analysis | 111 |

Session 7: Science and Engineering of Bentonites and Other Clays for Nuclear Waste Disposal | Posters (CONF 2295) | 10:30-12:40

[10:30-12:40 - Deng: In-Situ Monitoring of Micro-Morphology and Swelling Pressure of Na-Smectite at Elevated Temperatures...](#) 101

Session 9: Sorption, Transport, and Remediation of Emerging Contaminants by Natural and Engineered Clays | Posters (CONF 2295) | 10:30-12:40

[10:30-12:40 - Hsu: Chromium Oxidation on Ferrihydrite Under Atmospheric Conditions with Ultraviolet Irradiation: Trends and Mechanisms](#)..... 103

Session 10: Clay-Based Strategies for Mitigating Toxins | Posters (CONF 2295) | 10:30-12:40

[10:30-12:40 - Foysal: Develop a Clay-Based Platform as an Antibiotic Alternative to Disarm Pseudomonas Aeruginosa](#) 106

[10:30-12:40 - Oluseyifunmi: Protective Effects of a Bio-Clay Product on Growth, Jejunal Histomorphology, Bacteriome, and Metabolites in Aflatoxin-Challenged Broilers](#)..... 108

Friday Afternoon

Session 10: Clay-Based Strategies for Mitigating Toxins | Room 1 (CONF 2254) | 14:20-16:20

[14:20-14:40 - Foysal: A Clay-Based Platform to Sequester Virulence Factors Produced by Clostridium Perfringens to Regulate the Pathogen's Gene Expression](#)..... 116

[14:40-15:00 - Matusik: Surface and Interlayer Engineering of Smectites for Efficient Removal of Mycotoxins: Zearalenone, Alternariol and Enniatin B](#)..... 118

[15:00-15:20 - Phillips: Edible Clay for the Mitigation of Toxic Environmental Chemicals During Outbreaks, Emergencies and Disasters](#)120

[15:40-16:00 - Dziewiatka: From Mineral Surfaces to Mycotoxin Breakdown: UV-Activated Semiconductors Supported on Kaolin-Group Minerals](#)..... 121

[16:00-16:20 - Zolzaya: Results of the Study on Adsorption Quality of Zeolite by Artificially Increasing Rumen Cud Ammonia Concentration in Lambs](#)..... 123

Session 1: General Session | Room 2 (CONF 2265) | 14:20-16:20

[14:20-14:40 - Wong \[Remote\]: Halloysite-Reinforced Nanocomposite Hydrogel as Multifunctional Injectable Wound Dressing](#) 117

[14:40-15:00 - Liu: Functionalization of Halloysite Nanotubes for Biomedical Application](#)..... 119

[15:40-16:00 - Bickmore: Evaluating and Correcting the Accuracy of the Full-Pattern Summation Method](#)..... 122

[16:00-16:20 - Wang: Interpretable Machine Learning for Predicting Brick Strength from Kaolinite and Illite](#) 124

By Session

Plenary and Award Lectures

| | |
|---|----|
| Wed. 09:00-09:05, Room 1 (CONF 2254) - Introduction: Barry Bickmore for Eberl | |
| Wed. 09:05-09:45, Room 1 (CONF 2254) - Eberl: My Half Century as a Clay Scientist | 29 |
| Thu. 08:30-08:35, Room 1 (CONF 2254) - Introduction: Janice Bishop for Michael Velbel | |
| Thu. 08:35-09:15, Room 1 (CONF 2254) - Velbel: Bailey Lecture: From Earth to Mars: A Framework for Interpreting Martian Clay Minerals and Ancient Mars | 63 |
| Thu. 09:15-09:20, Room 1 (CONF 2254) - Introduction: Prakash Malla for Crawford Elliott | |
| Thu. 09:20-10:00, Room 1 (CONF 2254) - Elliott: Brindley Lecture: Occurrences and Distributions of the Rare-Earth Elements in the Georgia Kaolins and Enclosing Sands, Upper Coastal Plain, Georgia | 64 |
| Fri. 08:55-09:00, Room 1 (CONF 2254) - Introduction: Michał Skiba for Karolina Rybka | |
| Fri. 09:00-09:40, Room 1 (CONF 2254) - Rybka: Huff Lecture: Rehydration Behaviour of Smectites and Bentonites | 98 |
| Fri. 09:40-09:45, Room 1 (CONF 2254) - Introduction: Youjun Deng for Yunfei Xi | |
| Fri. 09:45-10:25, Room 1 (CONF 2254) - Yunfei Xi: Jackson Award Lecture: Structure and Reactivity of Clay Minerals and Its Environmental and Engineering Applications | 99 |

Session 1: General Session

| | |
|--|-----|
| Wed. 09:50-10:10, Room 2 (CONF 2265) - Nguyen: Synthesis of Smectite-Like Clays from Biotite in Mine Waste for Acid Mine Drainage Prevention | 32 |
| Wed. 10:10-10:30, Room 2 (CONF 2265) - Donahoe: Clay Minerals and Fe-Oxyhydroxides as Controls on Trace Metal Attenuation in an Acid Mine Drainage-Impacted Watershed, Alabama, USA | 35 |
| Wed. 10:50-11:10, Room 2 (CONF 2265) - Kang: Selective Microbial Iron Reduction in Nontronite-Maghemite Mixtures Under Repeated Freeze-Thaw Cycles | 38 |
| Wed. 11:10-11:30, Room 2 (CONF 2265) - Zeng [Remote]: Construction of Sepiolite-Supported Polyamidoxime Composite and Its Uranyl Ion Adsorption Performance | 41 |
| Wed. 11:30-11:50, Room 2 (CONF 2265) - Zhong [Remote]: Sepiolite-Supported Bimetallic Catalysts for the Oxidation of 5-Hydroxymethylfurfural to 2,5-Furandicarboxylic Acid | 43 |
| Fri. 10:30-12:40, Posters (CONF 2295) - Olorunfemi: Kaolin Membranes for Ethanol Steam Reforming and Gas Separation: Microstructural Evolution and Chemical Modification | 100 |
| Fri. 10:30-12:40, Posters (CONF 2295) - Matusik: Evaluating Zinc and Cobalt Doping of Layered Double Hydroxides on Their Efficiency of Lithium Extraction from Brines | 102 |
| Fri. 10:30-12:40, Posters (CONF 2295) - Agada [Remote]: Functional Evaluation of Clay Minerals and Carbon-Based Adsorbents for Antimicrobial and Cytoprotective Effects in a Poultry Disease Model | 104 |
| Fri. 10:30-12:40, Posters (CONF 2295) - Deng: Probing Structural Changes of Sepiolite and Zeolitic Water Dynamics with Temperature-Dependent Infrared Spectroscopy and Molecular Simulations | 105 |
| Fri. 10:30-12:40, Posters (CONF 2295) - Al-Laban [Remote]: Finite Element Analysis of Piled Raft Tunnel Interaction Under Changing Clay Conditions | 115 |
| Fri. 14:20-14:40, Room 2 (CONF 2265) - Wong [Remote]: Halloysite-Reinforced Nanocomposite Hydrogel as Multifunctional Injectable Wound Dressing | 117 |
| Fri. 14:40-15:00, Room 2 (CONF 2265) - Liu: Functionalization of Halloysite Nanotubes for Biomedical Application | 119 |
| Fri. 15:40-16:00, Room 2 (CONF 2265) - Bickmore: Evaluating and Correcting the Accuracy of the Full-Pattern Summation Method | 124 |
| Fri. 16:00-16:20, Room 2 (CONF 2265) - Wang: Interpretable Machine Learning for Predicting Brick Strength from Kaolinite and Illite | 124 |

Session 2: Clays as Paleoclimate Indicators

| | |
|---|----|
| Thu. 10:05-10:25, Room 3 (CONF 2267) - McIntosh: A Review of O-H Stable Isotope Methods for Improved Estimation of Temperature Using Phyllosilicates | 67 |
| Thu. 10:25-10:45, Room 3 (CONF 2267) - Smolen: Kinetic Controls on Clay Hydrogen Isotopes in Paleoclimate Archives | 70 |
| Thu. 10:45-11:05, Room 3 (CONF 2267) - Döbelin (Kanik): Recent Progress in the Understanding of Smectite-Stable Isotope Systematics: Methodological Considerations for Soil Science | 73 |
| Thu. 11:25-11:45, Room 3 (CONF 2267) - Andrzejewski: Assessing Paleoclimate Using Pedogenic Minerals from Cretaceous Paleosols of the Dakota Fm. in Kansas | 76 |
| Thu. 11:45-12:05, Room 3 (CONF 2267) - Burgener: Paleoclimate Reconstructions Using Paleosol Clay and Coarse Sediment Geochemistry: A Machine Learning Approach | 78 |

| | |
|--|-----|
| Fri. 10:30-12:40, Posters (CONF 2295) - Muhammad: Quaternary Reorganization of the Indonesian Throughflow and Its Influence on Regional Sea Level and Monsoon Dynamics | 107 |
|--|-----|

Session 3: Clays in the Computer

| | |
|---|----|
| Thu. 10:05-10:25, Room 2 (CONF 2265) - Holmboe [Remote]: Atomipy: A Python Framework and Topology Tool for Building Multicomponent Clay Systems for Molecular Simulations | 66 |
| Thu. 10:25-10:45, Room 2 (CONF 2265) - Swai [Remote]: MD Simulation on Ciprofloxacin-Montmorillonite Interaction: Interfacial Dynamics, Coordination Environment, and Adsorption Free Energy Landscapes | 69 |
| Thu. 10:45-11:05, Room 2 (CONF 2265) - Legg: The Energetics of Electrical Double Layers Over Heterogeneously Charged Surfaces | 75 |
| Thu. 11:25-11:45, Room 2 (CONF 2265) - Ho: Unraveling Long-Range Nanoconfinement Effects in Charged Layered Nanopores | 77 |
| Thu. 11:45-12:05, Room 2 (CONF 2265) - Underwood: When Pores Polarize: A Brownian Dynamics Examination of Membrane Polarization in Heterogeneously Charged Media | 80 |
| Thu. 12:05-12:25, Room 2 (CONF 2265) - Heinz [Remote]: Simulation of Alumina and Clay Minerals with pH Resolution to Study Electrolyte Interfaces and Organic Binding | 81 |

Session 4: Clay-hosted Critical Mineral Resources

| | |
|---|-----|
| Thu. 14:45-15:05, Room 2 (CONF 2265) - Meyer: Differentiating Lithium-Bearing Clays Using Orbital and Airborne Hyperspectral Data | 85 |
| Thu. 15:05-15:25, Room 2 (CONF 2265) - Day-Stirrat: Lithium-Bearing Clay Mineral Assemblages in the McDermitt Caldera, Oregon-Nevada, USA: An Exploration Framework | 87 |
| Thu. 15:25-15:45, Room 2 (CONF 2265) - Ogunsunlade: Mechanical Activation of Underclay for Enhanced Lithium Extraction and Amorphous Silica Production | 89 |
| Thu. 16:05-16:25, Room 2 (CONF 2265) - Molnar: The Effect of pH on the Interactions Between Rare Earth Element Ions and Gibbsite Nanoparticles | 92 |
| Thu. 16:25-16:45, Room 2 (CONF 2265) - Ellis: Clay Mineral Controls on REE Distribution and Recovery in Georgia Kaolin Mine Tailings | 94 |
| Thu. 16:45-17:05, Room 2 (CONF 2265) - Schroeder: History of Georgia and Cornwall Kaolin Production and New Insights for Co-Production of Critical Minerals | 96 |
| Thu. 17:05-17:25, Room 2 (CONF 2265) - Wei [Remote]: The Characteristics and Genesis of Secondary Minerals in the Granitic Rock Regolith in South China | 97 |
| Fri. 10:30-12:40, Posters (CONF 2295) - Gerratt: The Mineralogy, Geochemistry, and Genesis of the Silicon Ridge Clay Deposit, Utah County, Utah, USA | 109 |

Session 5: Software for Clays

| | |
|--|-----|
| Fri. 10:30-12:40, Posters (CONF 2295) - Kuligiewicz: LC-OD: A Portable R-Based Application for Smectite Layer Charge Calculation Using the OD Method | 110 |
| Fri. 10:30-12:40, Posters (CONF 2295) - Teeples: A Peak-Modeling Program for Thermogravimetric Analysis | 111 |
| Fri. 10:30-12:40, Posters (CONF 2295) - Evans: Machine Learning for Mineral Identification | 112 |
| Fri. 10:30-12:40, Posters (CONF 2295) - Bickmore: Emmalab: A Tool for Sediment Unmixing | 113 |
| Fri. 10:30-12:40, Posters (CONF 2295) - Burgener: The Terrestrial Paleoclimate Database: An Open-Access Resource for Sedimentologic and Geochemical Paleoclimate Studies | 114 |

Session 6: Clays, Organoclays, and Nanocomposites for Water Treatment

| | |
|--|----|
| Thu. 16:05-16:25, Room 1 (CONF 2254) - Rytwo: Application of Clay-Polymer Nanocomposites for the Removal of Toxic Cyanobacteria and Other Phytoplankton from Water | 91 |
|--|----|

Session 7: Science and Engineering of Bentonites and Other Clays for Nuclear Waste Disposal

| | |
|---|----|
| Wed. 09:50-10:10, Room 3 (CONF 2267) - Sanchez-Avellaneda [Remote]: A Miniature Device for Studying Swelling Pressure of Smectites | 33 |
| Wed. 10:10-10:30, Room 3 (CONF 2267) - Barbosa [Remote]: Coupled Thermo-Hydro-Mechanical Modeling of Mx-80 Bentonite Pellets Using a Double-Structure Framework | 36 |
| Wed. 10:50-11:10, Room 3 (CONF 2267) - Rybka: Is Humidity the Main Control of Hydration in Smectites? | 39 |
| Wed. 11:10-11:30, Room 3 (CONF 2267) - Xu: Immobilizing Radioactive Iodide and Iodate Using Chrysotile and Halloysite, Respectively | 42 |

| | |
|---|-----|
| Wed. 11:30-11:50, Room 3 (CONF 2267) - Morii: In Situ Observation of the Re-Oxidation Behavior of Structural Iron in Montmorillonite by X-Ray Absorption Fine Structure | 44 |
| Wed. 13:50-14:10, Room 3 (CONF 2267) - Kuligiewicz: The Apparent Layer Charge Changes in Dehydrated and Rehydrated Smectites and Bentonites | 47 |
| Wed. 14:30-14:50, Room 3 (CONF 2267) - Derkowski: Prospecting Raw Clay Materials for Nuclear Waste Repository Buffer Applications | 51 |
| Wed. 14:50-15:10, Room 3 (CONF 2267) - Skiba: Belchatów Bentonite Deposit: A Unique Case with Distinct Properties | 54 |
| Wed. 15:30-15:50, Room 3 (CONF 2267) - Chuang: Comparative Mineralogical Characterization of Asian Bentonites for Potential Engineered Clay Barrier Applications | 57 |
| Wed. 15:50-16:10, Room 3 (CONF 2267) - Bourg: Claycg: Towards a Coarse-Grained Model of Hydrated Clay Minerals | 60 |
| Fri. 10:30-12:40, Posters (CONF 2295) - Deng: In-Situ Monitoring of Micro-Morphology and Swelling Pressure of Na-Smectite at Elevated Temperatures | 101 |

Session 8: Investigating Clays on Planetary Bodies

| | |
|---|----|
| Thu. 10:05-10:25, Room 1 (CONF 2254) - Bose: An Overview of Clay-Rich Mudballs in Our Solar System | 65 |
| Thu. 10:25-10:45, Room 1 (CONF 2254) - Vierling: Alteration Histories of Asteroids Revealed by Clay Chemistry | 68 |
| Thu. 10:45-10:55, Room 1 (CONF 2254) - Bishop: Spectral Properties of NH₄⁺-Clays and Applications to Asteroids Ceres, Benu, and Ryugu | 71 |
| Thu. 10:55-11:05, Room 1 (CONF 2254) - Bishop: Clay Mineral Assemblages Provide Insights into Ancient Aqueous Alteration at Tyrrhena Terra, Mars | 72 |
| Thu. 11:25-11:45, Room 1 (CONF 2254) - Hendrickson: Evaluating Clay Mineral Ima Species in Gale Crater, Mars, and Maa Model Clay Predictions | 74 |
| Thu. 11:45-12:05, Room 1 (CONF 2254) - M. Elwood Madden: Clay Alteration in High Salinity Brines: Cation Exchange & Enhanced Aluminum Mobility | 79 |
| Thu. 14:45-15:05, Room 1 (CONF 2254) - A. Elwood Madden: Is There a Smectite Signature of Euxinic Chemical Weathering or Diagenesis? | 82 |
| Thu. 15:05-15:25, Room 1 (CONF 2254) - Sluder: Nano-Phases Formed at Redox Interfaces in a Sulfidic Spring | 84 |
| Thu. 15:25-15:45, Room 1 (CONF 2254) - Sahai: A Generalized Structure-Chemistry-Activity Relationship for Smectite-Catalyzed RNA Polymerization in Prebiotic Chemistry on Early Earth-Like Planetary Bodies | 86 |

Session 9: Sorption, Transport, and Remediation of Emerging Contaminants by Natural and Engineered Clays

| | |
|--|-----|
| Wed. 13:50-14:10, Room 1 (CONF 2254) - Ma: Incorporating Clay into Novel Nature-Based Solutions for Emerging Contaminants | 45 |
| Wed. 14:10-14:30, Room 1 (CONF 2254) - Dong: Tailoring Natural Clays for Selective and Sustainable PFAS Removal: Exploring Cation Exchange, Post-Grafting, and Fluorophilic Interactions | 48 |
| Wed. 14:30-14:50, Room 1 (CONF 2254) - Liang: The Use of Cationic Clay for Sorption of per- and Poly-Fluoroalkyl Substances and Destruction by Photoreduction | 52 |
| Wed. 15:30-15:50, Room 1 (CONF 2254) - Bouchelaghem [Remote]: Membrane Efficiency of Montmorillonite Suspensions | 55 |
| Wed. 15:50-16:10, Room 1 (CONF 2254) - Trung: Optimizing Bentonite Contents in Moraine for Low-Permeability Oxygen Barriers in Mine Waste Cover Systems | 58 |
| Fri. 10:30-12:40, Posters (CONF 2295) - Hsu: Chromium Oxidation on Ferrihydrite Under Atmospheric Conditions with Ultraviolet Irradiation: Trends and Mechanisms | 103 |

Session 10: Clay-Based Strategies for Mitigating Toxins

| | |
|---|-----|
| Fri. 10:30-12:40, Posters (CONF 2295) - Foysal: Develop a Clay-Based Platform as an Antibiotic Alternative to Disarm Pseudomonas Aeruginosa | 106 |
| Fri. 10:30-12:40, Posters (CONF 2295) - Oluseyifunmi: Protective Effects of a Bio-Clay Product on Growth, Jejunal Histomorphology, Bacteriome, and Metabolites in Aflatoxin-Challenged Broilers | 108 |
| Fri. 14:20-14:40, Room 1 (CONF 2254) - Foysal: A Clay-Based Platform to Sequester Virulence Factors Produced by Clostridium Perfringens to Regulate the Pathogen's Gene Expression | 116 |
| Fri. 14:40-15:00, Room 1 (CONF 2254) - Matusik: Surface and Interlayer Engineering of Smectites for Efficient Removal of Mycotoxins: Zearalenone, Alternariol and Enniatin B | 118 |
| Fri. 15:00-15:20, Room 1 (CONF 2254) - Phillips: Edible Clay for the Mitigation of Toxic Environmental Chemicals During Outbreaks, Emergencies and Disasters | 120 |

| | |
|---|-----|
| Fri. 15:40-16:00, Room 1 (CONF 2254) - Dziwiatka: From Mineral Surfaces to Mycotoxin Breakdown: UV-Activated Semiconductors Supported on Kaolin-Group Minerals | 121 |
| Fri. 16:00-16:20, Room 1 (CONF 2254) - Zolzaya: Results of the Study on Adsorption Quality of Zeolite by Artificially Increasing Rumen Cud Ammonia Concentration in Lambs | 123 |

Session 11: Clays and Zeolites in the Oil and Gas Industry

| | |
|---|----|
| Thu. 14:45-15:05, Room 3 (CONF 2267) - Smolen: Clay-Organic Interactions: Evolution of N-Alkanes During Early Maturation of Sedimentary Organic Matter | 83 |
| Thu. 15:05-15:25, Room 3 (CONF 2267) - Hudson: Elemental Geochemistry of the Mowry Shale as a Predictive Tool for Hydrocarbon Exploration | 88 |
| Thu. 15:25-15:45, Room 3 (CONF 2267) - Stokes: Evaluating the Effects of Smectite Species and Exchangeable Cations on Solid Bitumen Maturation in Hydrous Pyrolysis Experiments | 90 |
| Thu. 16:05-16:25, Room 3 (CONF 2267) - Fischer: Modeling the Geomechanical Effects of Layered Bentonites in Production of the Mowry Shale | 93 |
| Thu. 16:25-16:45, Room 3 (CONF 2267) - Cheshire: Smectite–Illite Transformation and Kaolinite Formation from Offshore Africa: Implications for Thermal Evolution and Fluid–Rock Interaction | 95 |

Session 12: Advanced Characterization of Clay Minerals

| | |
|---|----|
| Wed. 13:50-14:10, Room 2 (CONF 2265) - Legg: Imaging the Formation of Nanostructured Hydroxide Films on Mineral-Water Interfaces | 46 |
| Wed. 14:10-14:30, Room 2 (CONF 2265) - Cho: Iron Redox–Driven Arsenic Immobilization via Algal Biomineralization Revealed by Synchrotron Spectroscopy | 49 |
| Wed. 14:30-14:50, Room 2 (CONF 2265) - Oladele: Physicochemical Characterization and Surface Reactivity of Cookeite from Mineral Dissolution, Microscopic and Spectroscopic Studies | 50 |
| Wed. 14:50-15:10, Room 2 (CONF 2265) - Chipman: A Deep-Learning Approach for Phase Picking in X-Ray Powder Diffraction Analysis of Clay-Bearing Mixtures | 53 |
| Wed. 15:30-15:50, Room 2 (CONF 2265) - Xi [Remote]: Integrated Micro-To-Atomic Scale Characterization of Complex Phyllosilicates from the Long Valley Rhyolite: A Multi-Technique Approach | 56 |
| Wed. 15:50-16:10, Room 2 (CONF 2265) - Yang [Remote]: Three-Dimensional Electron Diffraction: A Revolutionary Technique for Rapid and Non-Destructive Identification of Clay Mineral Structures | 59 |
| Wed. 16:10-16:30, Room 2 (CONF 2265) - Zhang [Remote]: Accurate Identification of Element Occupancy Within Single Layers of Mg–Ni Saponite by Coupling FTIR and HAADF-STEM-EDXS | 61 |
| Wed. 16:30-16:50, Room 2 (CONF 2265) - Xu: Incommensurately Modulated Structure of Greenalite with Non-Stoichiometry: Z-Contrast Imaging and iDPC Imaging Study | 62 |

Session 14: Clay-sized Minerals in Soils

| | |
|---|----|
| Wed. 09:50-10:10, Room 1 (CONF 2254) - Ishimwe: Formation of Halloysite in Volcanic Soils: Insights for Podoconiosis | 30 |
| Wed. 10:10-10:30, Room 1 (CONF 2254) - Lam: Characterizing the Clay Mineralogy of the Pu‘u Ōhi‘a Andisol from O‘ahu, Hawai‘i | 34 |
| Wed. 10:50-11:10, Room 1 (CONF 2254) - Liu: Mg-Fe Layered Double Hydroxide as a Controlled-Release Phosphorus Fertilizer: Improving Plant P Uptake and Reducing Soil P Loss | 37 |
| Wed. 11:10-11:30, Room 1 (CONF 2254) - Ryan: Soil Heterogeneity and the Influence of Clay Minerals on Landslide Risk in Hilly Tropical Landscapes | 40 |

By Presenter Last Name

| | |
|--|-----|
| Agada [Remote] - S1 General Fri. 10:30-12:40 Posters (CONF 2295): Functional Evaluation of Clay Minerals and Carbon-Based Adsorbents for Antimicrobial and Cytoprotective Effects in a Poultry Disease Model | 104 |
| Al-Laban [Remote] - S1 General Fri. 10:30-12:40 Posters (CONF 2295): Finite Element Analysis of Piled Raft Tunnel Interaction Under Changing Clay Conditions | 115 |
| Andrzejewski - S2 Paleoclimate Thu. 11:25-11:45 Room 3 (CONF 2267): Assessing Paleoclimate Using Pedogenic Minerals from Cretaceous Paleosols of the Dakota Fm. in Kansas | 76 |
| Bickmore - S5 Software Fri. 10:30-12:40 Posters (CONF 2295): Emmalab: A Tool for Sediment Unmixing | 113 |
| Bickmore - S1 General Fri. 15:40-16:00 Room 2 (CONF 2265): Evaluating and Correcting the Accuracy of the Full-Pattern Summation Method | 122 |

| | |
|--|-----|
| Bishop - S8 Planetary Thu. 10:45-10:55 Room 1 (CONF 2254): Spectral Properties of NH₄⁺-Clays and Applications to Asteroids Ceres, Bennu, and Ryugu | 71 |
| Bishop - S8 Planetary Thu. 10:55-11:05 Room 1 (CONF 2254): Clay Mineral Assemblages Provide Insights into Ancient Aqueous Alteration at Tyrrhena Terra, Mars | 72 |
| Bose - S8 Planetary Thu. 10:05-10:25 Room 1 (CONF 2254): An Overview of Clay-Rich Mudballs in Our Solar System | 65 |
| Bouchelaghem [Remote] - S9 Contaminants Wed. 15:30-15:50 Room 1 (CONF 2254): Membrane Efficiency of Montmorillonite Suspensions | 55 |
| Bourg - S7 Nuclear Waste Wed. 15:50-16:10 Room 3 (CONF 2267): Claycg: Towards a Coarse-Grained Model of Hydrated Clay Minerals | 60 |
| Burgener - S5 Software Fri. 10:30-12:40 Posters (CONF 2295): The Terrestrial Paleoclimate Database: An Open-Access Resource for Sedimentologic and Geochemical Paleoclimate Studies | 114 |
| Burgener - S2 Paleoclimate Thu. 11:45-12:05 Room 3 (CONF 2267): Paleoclimate Reconstructions Using Paleosol Clay and Coarse Sediment Geochemistry: A Machine Learning Approach | 78 |
| Cheshire - S11 Oil & Gas Thu. 16:25-16:45 Room 3 (CONF 2267): Smectite–Illite Transformation and Kaolinite Formation from Offshore Africa: Implications for Thermal Evolution and Fluid–Rock Interaction | 95 |
| Chipman - S12 Characterization Wed. 14:50-15:10 Room 2 (CONF 2265): A Deep-Learning Approach for Phase Picking in X-Ray Powder Diffraction Analysis of Clay-Bearing Mixtures | 53 |
| Cho - S12 Characterization Wed. 14:10-14:30 Room 2 (CONF 2265): Iron Redox–Driven Arsenic Immobilization via Algal Biomineralization Revealed by Synchrotron Spectroscopy | 49 |
| Chuang - S7 Nuclear Waste Wed. 15:30-15:50 Room 3 (CONF 2267): Comparative Mineralogical Characterization of Asian Bentonites for Potential Engineered Clay Barrier Applications | 57 |
| Day-Stirrat - S4 Critical Minerals Thu. 15:05-15:25 Room 2 (CONF 2265): Lithium-Bearing Clay Mineral Assemblages in the McDermitt Caldera, Oregon-Nevada, USA: An Exploration Framework | 87 |
| Deng - S7 Nuclear Waste Fri. 10:30-12:40 Posters (CONF 2295): In-Situ Monitoring of Micro-Morphology and Swelling Pressure of Na-Smectite at Elevated Temperatures | 101 |
| Deng - S1 General Fri. 10:30-12:40 Posters (CONF 2295): Probing Structural Changes of Sepiolite and Zeolitic Water Dynamics with Temperature-Dependent Infrared Spectroscopy and Molecular Simulations | 105 |
| Derkowski - S7 Nuclear Waste Wed. 14:30-14:50 Room 3 (CONF 2267): Prospecting Raw Clay Materials for Nuclear Waste Repository Buffer Applications | 51 |
| Döbelin (Kanik) - S2 Paleoclimate Thu. 10:45-11:05 Room 3 (CONF 2267): Recent Progress in the Understanding of Smectite-Stable Isotope Systematics: Methodological Considerations for Soil Science | 73 |
| Donahoe - S1 General Wed. 10:10-10:30 Room 2 (CONF 2265): Clay Minerals and Fe-Oxyhydroxides as Controls on Trace Metal Attenuation in an Acid Mine Drainage-Impacted Watershed, Alabama, USA | 35 |
| Dong - S9 Contaminants Wed. 14:10-14:30 Room 1 (CONF 2254): Tailoring Natural Clays for Selective and Sustainable PFAS Removal: Exploring Cation Exchange, Post-Grafting, and Fluorophilic Interactions | 48 |
| Dziewiatka - S10 Toxins Fri. 15:40-16:00 Room 1 (CONF 2254): From Mineral Surfaces to Mycotoxin Breakdown: UV-Activated Semiconductors Supported on Kaolin-Group Minerals | 121 |
| Eberl - Plenary Wed. 09:05-09:45 Room 1 (CONF 2254): My Half Century as a Clay Scientist | 29 |
| Elliott - Plenary Thu. 09:20-10:00 Room 1 (CONF 2254): Brindley Lecture: Occurrences and Distributions of the Rare-Earth Elements in the Georgia Kaolins and Enclosing Sands, Upper Coastal Plain, Georgia | 64 |
| Ellis - S4 Critical Minerals Thu. 16:25-16:45 Room 2 (CONF 2265): Clay Mineral Controls on REE Distribution and Recovery in Georgia Kaolin Mine Tailings | 94 |
| A. Elwood Madden - S8 Planetary Thu. 14:45-15:05 Room 1 (CONF 2254): Is There a Smectite Signature of Euxinic Chemical Weathering or Diagenesis? | 82 |
| M. Elwood Madden - S8 Planetary Thu. 11:45-12:05 Room 1 (CONF 2254): Clay Alteration in High Salinity Brines: Cation Exchange & Enhanced Aluminum Mobility | 79 |
| Evans - S5 Software Fri. 10:30-12:40 Posters (CONF 2295): Machine Learning for Mineral Identification | 112 |
| Fischer - S11 Oil & Gas Thu. 16:05-16:25 Room 3 (CONF 2267): Modeling the Geomechanical Effects of Layered Bentonites in Production of the Mowry Shale | 93 |
| Foyzal - S10 Toxins Fri. 10:30-12:40 Posters (CONF 2295): Develop a Clay-Based Platform as an Antibiotic Alternative to Disarm Pseudomonas Aeruginosa | 106 |
| Foyzal - S10 Toxins Fri. 14:20-14:40 Room 1 (CONF 2254): A Clay-Based Platform to Sequester Virulence Factors Produced by Clostridium Perfringens to Regulate the Pathogen’s Gene Expression | 116 |
| Gerratt - S4 Critical Minerals Fri. 10:30-12:40 Posters (CONF 2295): The Mineralogy, Geochemistry, and Genesis of the Silicon Ridge Clay Deposit, Utah County, Utah, USA | 109 |
| Barbosa [Remote] - S7 Nuclear Waste Wed. 10:10-10:30 Room 3 (CONF 2267): Coupled Thermo-Hydro-Mechanical Modeling of Mx-80 Bentonite Pellets Using a Double-Structure Framework | 36 |
| Heinz [Remote] - S3 Computer Thu. 12:05-12:25 Room 2 (CONF 2265): Simulation of Alumina and Clay Minerals with pH Resolution to Study Electrolyte Interfaces and Organic Binding | 81 |

| | |
|---|-----|
| Hendrickson - S8 Planetary Thu. 11:25-11:45 Room 1 (CONF 2254): Evaluating Clay Mineral Ima Species in Gale Crater, Mars, and Maa Model Clay Predictions | 74 |
| Ho - S3 Computer Thu. 11:25-11:45 Room 2 (CONF 2265): Unraveling Long-Range Nanoconfinement Effects in Charged Layered Nanopores | 77 |
| Holmboe [Remote] - S3 Computer Thu. 10:05-10:25 Room 2 (CONF 2265): Atomipy: A Python Framework and Topology Tool for Building Multicomponent Clay Systems for Molecular Simulations | 66 |
| Hsu - S9 Contaminants Fri. 10:30-12:40 Posters (CONF 2295): Chromium Oxidation on Ferrihydrite Under Atmospheric Conditions with Ultraviolet Irradiation: Trends and Mechanisms | 103 |
| Hudson - S11 Oil & Gas Thu. 15:05-15:25 Room 3 (CONF 2267): Elemental Geochemistry of the Mowry Shale as a Predictive Tool for Hydrocarbon Exploration | 88 |
| Ishimwe - S14 Soils Wed. 09:50-10:10 Room 1 (CONF 2254): Formation of Halloysite in Volcanic Soils: Insights for Podoconiosis | 30 |
| Kang - S1 General Wed. 10:50-11:10 Room 2 (CONF 2265): Selective Microbial Iron Reduction in Nontronite-Maghemite Mixtures Under Repeated Freeze-Thaw Cycles | 38 |
| Kuligiewicz - S5 Software Fri. 10:30-12:40 Posters (CONF 2295): LC-OD: A Portable R-Based Application for Smectite Layer Charge Calculation Using the OD Method | 110 |
| Kuligiewicz - S7 Nuclear Waste Wed. 13:50-14:10 Room 3 (CONF 2267): The Apparent Layer Charge Changes in Dehydrated and Rehydrated Smectites and Bentonites | 47 |
| Lam - S14 Soils Wed. 10:10-10:30 Room 1 (CONF 2254): Characterizing the Clay Mineralogy of the Pu'u 'Ōhi'a Andisol from O'ahu, Hawai'i | 34 |
| Legg - S3 Computer Thu. 10:45-11:05 Room 2 (CONF 2265): The Energetics of Electrical Double Layers Over Heterogeneously Charged Surfaces | 75 |
| Legg - S12 Characterization Wed. 13:50-14:10 Room 2 (CONF 2265): Imaging the Formation of Nanostructured Hydroxide Films on Mineral-Water Interfaces | 46 |
| Liang - S9 Contaminants Wed. 14:30-14:50 Room 1 (CONF 2254): The Use of Cationic Clay for Sorption of per- and Poly-Fluoroalkyl Substances and Destruction by Photoreduction | 52 |
| Liu - S1 General Fri. 14:40-15:00 Room 2 (CONF 2265): Functionalization of Halloysite Nanotubes for Biomedical Application | 119 |
| Liu - S14 Soils Wed. 10:50-11:10 Room 1 (CONF 2254): Mg-Fe Layered Double Hydroxide as a Controlled-Release Phosphorus Fertilizer: Improving Plant P Uptake and Reducing Soil P Loss | 37 |
| Ma - S9 Contaminants Wed. 13:50-14:10 Room 1 (CONF 2254): Incorporating Clay into Novel Nature-Based Solutions for Emerging Contaminants | 45 |
| Matusik - S1 General Fri. 10:30-12:40 Posters (CONF 2295): Evaluating Zinc and Cobalt Doping of Layered Double Hydroxides on Their Efficiency of Lithium Extraction from Brines | 102 |
| Matusik - S10 Toxins Fri. 14:40-15:00 Room 1 (CONF 2254): Surface and Interlayer Engineering of Smectites for Efficient Removal of Mycotoxins: Zearalenone, Alternariol and Enniatin B | 118 |
| McIntosh - S2 Paleoclimate Thu. 10:05-10:25 Room 3 (CONF 2267): A Review of O-H Stable Isotope Methods for Improved Estimation of Temperature Using Phyllosilicates | 67 |
| Meyer - S4 Critical Minerals Thu. 14:45-15:05 Room 2 (CONF 2265): Differentiating Lithium-Bearing Clays Using Orbital and Airborne Hyperspectral Data | 85 |
| Molnar - S4 Critical Minerals Thu. 16:05-16:25 Room 2 (CONF 2265): The Effect of pH on the Interactions Between Rare Earth Element Ions and Gibbsite Nanoparticles | 92 |
| Morii - S7 Nuclear Waste Wed. 11:30-11:50 Room 3 (CONF 2267): In Situ Observation of the Re-Oxidation Behavior of Structural Iron in Montmorillonite by X-Ray Absorption Fine Structure | 44 |
| Muhammad - S2 Paleoclimate Fri. 10:30-12:40 Posters (CONF 2295): Quaternary Reorganization of the Indonesian Throughflow and Its Influence on Regional Sea Level and Monsoon Dynamics | 107 |
| Nguyen - S1 General Wed. 09:50-10:10 Room 2 (CONF 2265): Synthesis of Smectite-Like Clays from Biotite in Mine Waste for Acid Mine Drainages Prevention | 32 |
| Trung - S9 Contaminants Wed. 15:50-16:10 Room 1 (CONF 2254): Optimizing Bentonite Contents in Moraine for Low-Permeability Oxygen Barriers in Mine Waste Cover Systems | 58 |
| Ogunsunlade - S4 Critical Minerals Thu. 15:25-15:45 Room 2 (CONF 2265): Mechanical Activation of Underclay for Enhanced Lithium Extraction and Amorphous Silica Production | 89 |
| Oladele - S12 Characterization Wed. 14:30-14:50 Room 2 (CONF 2265): Physicochemical Characterization and Surface Reactivity of Cookeite from Mineral Dissolution, Microscopic and Spectroscopic Studies | 50 |
| Olorunfemi - S1 General Fri. 10:30-12:40 Posters (CONF 2295): Kaolin Membranes for Ethanol Steam Reforming and Gas Separation: Microstructural Evolution and Chemical Modification | 100 |
| Oluseyifunmi - S10 Toxins Fri. 10:30-12:40 Posters (CONF 2295): Protective Effects of a Bio-Clay Product on Growth, Jejunal Histomorphology, Bacteriome, and Metabolites in Aflatoxin-Challenged Broilers | 108 |
| Phillips - S10 Toxins Fri. 15:00-15:20 Room 1 (CONF 2254): Edible Clay for the Mitigation of Toxic Environmental Chemicals During Outbreaks, Emergencies and Disasters | 120 |

| | |
|---|-----|
| Ryan - S14 Soils Wed. 11:10-11:30 Room 1 (CONF 2254): Soil Heterogeneity and the Influence of Clay Minerals on Landslide Risk in Hilly Tropical Landscapes | 40 |
| Rybka - Plenary Fri. 09:00-09:40 Room 1 (CONF 2254): Huff Lecture: Rehydration Behaviour of Smectites and Bentonites | 98 |
| Rybka - S7 Nuclear Waste Wed. 10:50-11:10 Room 3 (CONF 2267): Is Humidity the Main Control of Hydration in Smectites? | 39 |
| Rytwo - S6 Water Treatment Thu. 16:05-16:25 Room 1 (CONF 2254): Application of Clay-Polymer Nanocomposites for the Removal of Toxic Cyanobacteria and Other Phytoplankton from Water | 91 |
| Sahai - S8 Planetary Thu. 15:25-15:45 Room 1 (CONF 2254): A Generalized Structure-Chemistry-Activity Relationship for Smectite-Catalyzed RNA Polymerization in Prebiotic Chemistry on Early Earth-Like Planetary Bodies | 86 |
| Sanchez-Avellaneda [Remote] - S7 Nuclear Waste Wed. 09:50-10:10 Room 3 (CONF 2267): A Miniature Device for Studying Swelling Pressure of Smectites | 33 |
| Schroeder - S4 Critical Minerals Thu. 16:45-17:05 Room 2 (CONF 2265): History of Georgia and Cornwall Kaolin Production and New Insights for Co-Production of Critical Minerals | 96 |
| Skiba - S7 Nuclear Waste Wed. 14:50-15:10 Room 3 (CONF 2267): Belchatów Bentonite Deposit: A Unique Case with Distinct Properties | 54 |
| Sluder - S8 Planetary Thu. 15:05-15:25 Room 1 (CONF 2254): Nano-Phases Formed at Redox Interfaces in a Sulfidic Spring | 84 |
| Smolen - S2 Paleoclimate Thu. 10:25-10:45 Room 3 (CONF 2267): Kinetic Controls on Clay Hydrogen Isotopes in Paleoclimate Archives | 70 |
| Smolen - S11 Oil & Gas Thu. 14:45-15:05 Room 3 (CONF 2267): Clay-Organic Interactions: Evolution of N-Alkanes During Early Maturation of Sedimentary Organic Matter | 83 |
| Stokes - S11 Oil & Gas Thu. 15:25-15:45 Room 3 (CONF 2267): Evaluating the Effects of Smectite Species and Exchangeable Cations on Solid Bitumen Maturation in Hydrous Pyrolysis Experiments | 90 |
| Swai [Remote] - S3 Computer Thu. 10:25-10:45 Room 2 (CONF 2265): MD Simulation on Ciprofloxacin-Montmorillonite Interaction: Interfacial Dynamics, Coordination Environment, and Adsorption Free Energy Landscapes | 69 |
| Wei [Remote] - S4 Critical Minerals Thu. 17:05-17:25 Room 2 (CONF 2265): The Characteristics and Genesis of Secondary Minerals in the Granitic Rock Regolith in South China | 97 |
| Teeples - S5 Software Fri. 10:30-12:40 Posters (CONF 2295): A Peak-Modeling Program for Thermogravimetric Analysis | 111 |
| Underwood - S3 Computer Thu. 11:45-12:05 Room 2 (CONF 2265): When Pores Polarize: A Brownian Dynamics Examination of Membrane Polarization in Heterogeneously Charged Media | 80 |
| Velbel - Plenary Thu. 08:35-09:15 Room 1 (CONF 2254): Bailey Lecture: From Earth to Mars: A Framework for Interpreting Martian Clay Minerals and Ancient Mars | 63 |
| Vierling - S8 Planetary Thu. 10:25-10:45 Room 1 (CONF 2254): Alteration Histories of Asteroids Revealed by Clay Chemistry | 68 |
| Wang - S1 General Fri. 16:00-16:20 Room 2 (CONF 2265): Interpretable Machine Learning for Predicting Brick Strength from Kaolinite and Illite | 124 |
| Wong [Remote] - S1 General Fri. 14:20-14:40 Room 2 (CONF 2265): Halloysite-Reinforced Nanocomposite Hydrogel as Multifunctional Injectable Wound Dressing | 117 |
| Xi [Remote] - S12 Characterization Wed. 15:30-15:50 Room 2 (CONF 2265): Integrated Micro-To-Atomic Scale Characterization of Complex Phyllosilicates from the Long Valley Rhyolite: A Multi-Technique Approach | 56 |
| Yunfei Xi - Plenary Fri. 09:45-10:25 Room 1 (CONF 2254): Jackson Award Lecture: Structure and Reactivity of Clay Minerals and Its Environmental and Engineering Applications | 99 |
| Xu - S7 Nuclear Waste Wed. 11:10-11:30 Room 3 (CONF 2267): Immobilizing Radioactive Iodide and Iodate Using Chrysotile and Halloysite, Respectively | 42 |
| Xu - S12 Characterization Wed. 16:30-16:50 Room 2 (CONF 2265): Incommensurately Modulated Structure of Greenalite with Non-Stoichiometry: Z-Contrast Imaging and iDPC Imaging Study | 62 |
| Yang [Remote] - S12 Characterization Wed. 15:50-16:10 Room 2 (CONF 2265): Three-Dimensional Electron Diffraction: A Revolutionary Technique for Rapid and Non-Destructive Identification of Clay Mineral Structures | 59 |
| Zeng [Remote] - S1 General Wed. 11:10-11:30 Room 2 (CONF 2265): Construction of Sepiolite-Supported Polyamidoxime Composite and Its Uranyl Ion Adsorption Performance | 41 |
| Zhang [Remote] - S12 Characterization Wed. 16:10-16:30 Room 2 (CONF 2265): Accurate Identification of Element Occupancy Within Single Layers of Mg-Ni Saponite by Coupling FTIR and HAADF-STEM-EDXS | 61 |
| Zhong [Remote] - S1 General Wed. 11:30-11:50 Room 2 (CONF 2265): Sepiolite-Supported Bimetallic Catalysts for the Oxidation of 5-Hydroxymethylfurfural to 2,5-Furandicarboxylic Acid | 43 |
| Zolzaya - S10 Toxins Fri. 16:00-16:20 Room 1 (CONF 2254): Results of the Study on Adsorption Quality of Zeolite by Artificially Increasing Rumen Cud Ammonia Concentration in Lambs | 123 |

PIONEER LECTURE: MY HALF CENTURY AS A CLAY MINERALOGIST

Eberl, Dennis *¹

¹U.S. Geological Survey (retired)

My career as a clay scientist started in the late 1960's when I began synthesizing clays at Case Western Reserve University in Cleveland. At that time I attended my first Clay Mineral Society meeting with my thesis advisor, John Hower. I was introduced to John by Dartmouth professor Bob Reynolds during a climb of Bear Hat Mountain in Glacier National Park. I spent that summer as Bob's field assistant, climbing and collecting rocks in the Montana and Canadian Rockies as a part of Bob's study of Precambrian paleosalinity. My PhD thesis measured the kinetics of the smectite to illite reaction that occurs naturally with depth in the Gulf of Mexico basin, a reaction that I duplicated in hydrothermal experiments. Later, I joined the geology department faculty at the University of Illinois where I continued to synthesize clays. I knew that crystals of clay grew in my hydrothermal bombs, but I could not apply crystal growth theories to the experiments. The mathematics of these theories, such as BCF theory, were beyond me. Luckily, I did not invest time in learning these theories because I found a much simpler, non-thermodynamic approach to the phenomenon after I joined the USGS in 1981.

My talk describes this non-classical approach to crystal growth, as well as some other research done at the USGS before my retirement in 2011. During my time at the Survey I wrote a series of computer programs in Excel macros, which were then applied to geological studies. The crystal growth program is named GALOPER, an acronym for Growth According to the Law Of Proportionate Effect and by Ripening. It calculates the shapes of crystal size distributions for a variety of crystal growth mechanisms. Other programs include RockJock for quantitative X-ray mineral analysis, MudMaster to calculate crystallite size distributions from the shapes of X-ray peaks, SedUnMix for determining quantitative sediment provenance from quantitative mineral analyses, HandLens for calculating the chemistry of minerals in mixtures, Stackman for calculating mixed-layer clay X-ray patterns from MudMaster measurements of crystallite thickness distributions, as well as other programs. Unfortunately, these programs no longer work because newer versions of Excel were not completely downward compatible. So now these programs exist as proof of concepts. Fortunately, Barry Bickmore and his students are rewriting several of them in a more sophisticated manner using a better computer language.

The Clay Minerals Society was home throughout my scientific career. I even served as its president for one unremarkable year. My former wife, Jo, was the office manager for many years and helped to publish the now defunct CMS newsletter. I hope that you are having as much fun with science as I did in my nearly 60 years as a clay mineralogist, and that you will meet as many fine and interesting fellow scientists.

FORMATION OF HALLOYSITE IN VOLCANIC SOILS: INSIGHTS FOR PODOCONIOSIS

Benite Ishimwe*

beniteishimwe@berkeley.edu

Arahan Lim¹, Sam W Song¹, Guillaume Nyagatara², Hamoud Rukangantambara², Alida Perez-Fódich⁴, Jean de Dieu Nsenganeza³, Kazi Tani Sarra Latifa³, Penny Elaine Wieser¹, Laurent Charlet³, Benjamin Gilbert¹

¹*University of California, Berkeley, CA, United States*

²*University of Rwanda, Kigali, Rwanda*

³*University of Grenoble, Grenoble, France*

⁴*University of Chile, Santiago, Chile*

Nanotubular aluminosilicate minerals formed through the chemical weathering of volcanic materials are hypothesized to cause podoconiosis, a neglected tropical disease affecting approximately four million agricultural workers in 27 countries. Halloysite, a rigid nanotubular mineral morphologically similar to pathogenic asbestiform fibers, is a strong candidate as the causative agent because it can translocate across tissues and cells and induce oxidative stress. However, the geochemical conditions governing halloysite formation in tropical volcanic soils remain poorly constrained, limiting our ability to predict which soils pose the greatest disease risk. In this work, we investigate the geochemical and climatic factors controlling halloysite formation in volcanic soils in Rwanda, within the East African Rift.

We collected rock, ash, and soil samples from volcanic sites with known podoconiosis prevalence. We analyzed mineral phases using synchrotron X-ray diffraction, transmission and scanning electron microscopy, and low-voltage energy-dispersive spectroscopy. To examine how halloysite formation differs across basaltic volcanic parent materials with varying Al³⁺/Si ratios in volcanic glass, we are developing CrunchFlow reactive transport models. These models will compare the weathering of basaltic columns from Rwanda and Hawaii, accounting for their distinct climates and topographies. We are incorporating key weathering drivers, including leaching conditions, soil CO₂ concentrations from microbial respiration, and the complexation of Al³⁺ and Fe^{3+/2+} by low-molecular-weight organic acids from rhizodeposits. Additionally, we are constructing country-scale spatial predictions of halloysite distribution using machine-learning approaches trained on climate, topography, geology, lithologic age, and soil-property attributes.

Field samples confirm that halloysite nanotubes are present in the soil clay fraction of Rwandan volcanic soils, with variations in width and length (Figure 1). Initial reactive transport simulations show moderate halloysite accumulation in Hawaii, peaking at only 5 wt% below 1.5m depth. In contrast, in Rwanda, the halloysite concentration reaches up to 10 wt% after a 20,000-year simulation period. Additionally, in Rwanda, the maximum buildup occurs at shallower depths, between 0.5 and 1m, which is directly relevant to podoconiosis risk because higher halloysite levels nearer the surface increase human exposure through barefoot contact. This difference indicates that Rwanda's climate and hydrologic conditions result in slower infiltration rates, reducing silica leaching and maintaining silica concentration within the halloysite formation window longer than in Hawaii.

Together, the reactive transport modeling and spatial predictions provide a geochemical and predictive framework for mapping podoconiosis risk and guiding public health interventions in affected agricultural communities.

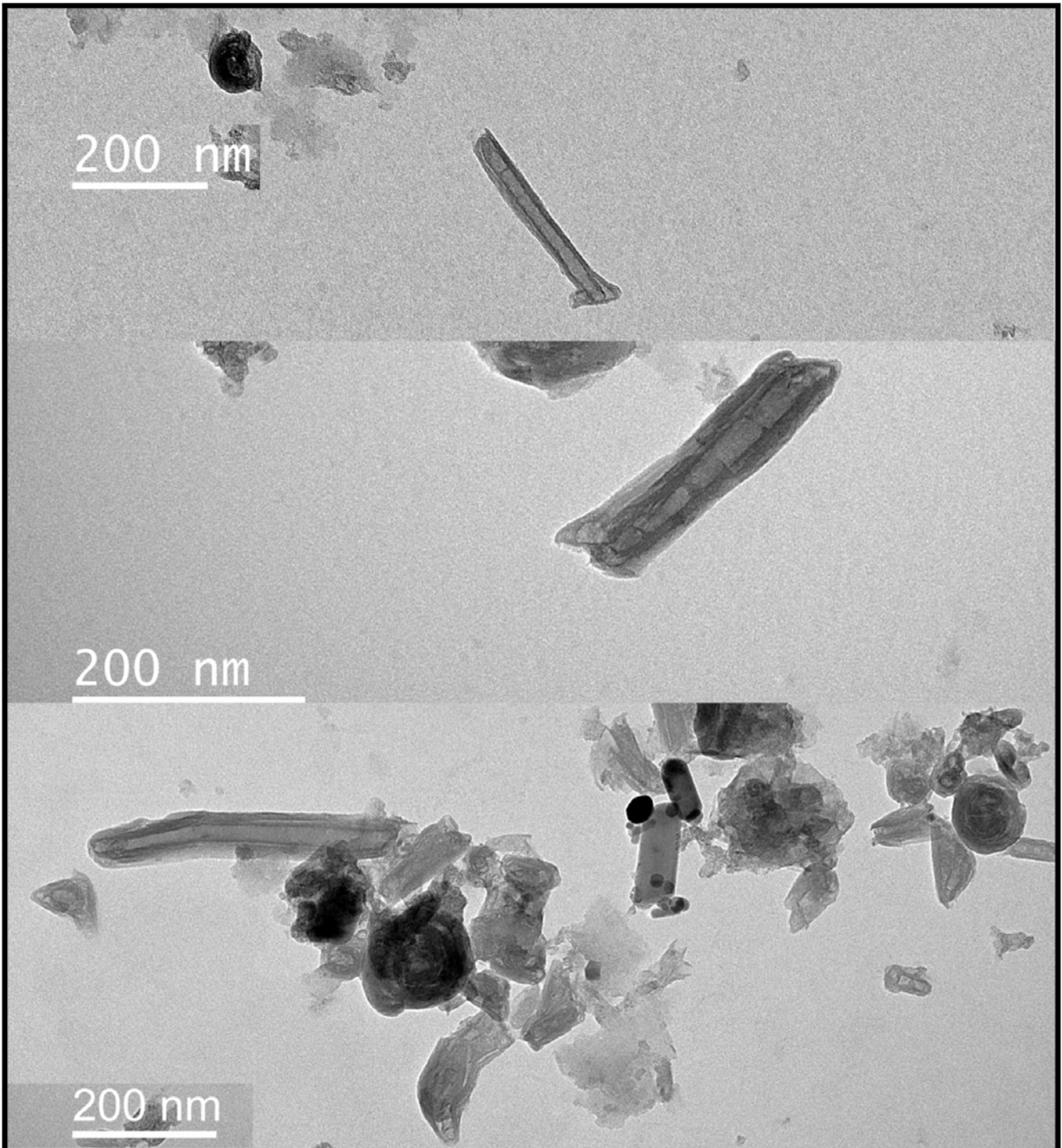


Figure 1. Transmission electron microscopy of Halloysite nanotube of varying lengths found in volcanic soil samples weathered from basalt ash from a cinder cone in Rwanda, Virunga volcanic province.

SYNTHESIS OF SMECTITE-LIKE CLAYS FROM BIOTITE IN MINE WASTE FOR ACID MINE DRAINAGE PREVENTION

Nguyen, Trung*¹, Duong, Chau-Anh¹, and Holmboe, Michael¹

¹Department of Chemistry, Umeå University, 901 87, Umeå, Sweden.

* trung.nguyen@umu.se

Aitik mine (Sweden), Europe's largest Cu mine, generates vast volumes of tailings dominated by feldspars and micas (biotite, muscovite) [1], as well as approx. 1.5 % sulfides capable of producing acid mine drainage (AMD). Upon mine closure, the potential acid-generating tailings are separated and require engineered covers with low hydraulic conductivity ($k = 10^{-9}$ m/s) to limit oxygen ingress, typically by using bentonite-amended moraine. However, this bentonite demand represents a substantial economic and material burden. Therefore, reprocessing the locally biotite-rich tailings into swellable clay-like materials offers a potential in-situ low-cost alternative for sustainable mine waste control.

We investigated alteration of biotite driven by Fe^{2+} oxidation coupled with K^+ - Na^+ interlayer exchange, aiming to reduce layer charge, promote K^+ release, and transform biotite towards oxybiotite with preferentially smectite-like properties. Experiments were conducted on well-characterized biotite [2] and Aitik mine tailings using H_2O_2 as oxidants in Na^+ -bearing solutions. Elemental release was quantified by ICP-OES and $\text{Fe}^{2+}/\text{Fe}^{3+}$ ratios by UV-Vis spectroscopy [3], while structural expansion and evolution (oxidation states, coordination environments) were revealed by XRD and XAS, respectively. Additional characterization included XRF, SEM-EDS, FTIR, Raman, TGA, dynamic vapor sorption, cation exchange capacity, and hydraulic permeability measurements to bridge structural transformation with barrier performance.

After an oxidative treatment of the Aitik tailing material, up to 20 % of Fe^{2+} was converted to Fe^{3+} , leading interlayer expansion of biotite from 10 to 15 Å under dry conditions, and 18.8 Å upon full hydration. ICP-OES confirmed significant but incomplete release of interlayer K^+ and mobilization of structural cations, indicating partial cation exchange and structural reorganization.

These results show that oxidative reprocessing of biotite-rich tailings can potentially induce smectite-like swelling behavior, particularly in fine-grained fractions. This study outlines a mechanistically grounded pathway for transforming mine waste into an engineered oxygen barrier, advancing sustainable AMD mitigation and responsible mine closure strategies.

[1] Forsberg, L., Reclamation of copper mine tailings using sewage sludge. 2008.

[2] Malmström, M., et al., The dissolution of biotite and chlorite at 25°C in the near-neutral pH region. *Journal of Contaminant Hydrology*, 1996. 21(1): p. 201-213.

[3] Amonette, J.E. and J. Charles Templeton, Improvements to the Quantitative Assay of Nonrefractory Minerals for Fe(II) and Total Fe Using 1,10-Phenanthroline. *Clays and Clay Minerals*, 1998. 46(1): p. 51-62.

A MINIATURE DEVICE FOR STUDYING SWELLING PRESSURE OF SMECTITES

Sanchez-Avellaneda, Camilo*¹ AL-Masri, Roa'a¹, Sanchez¹ Marcelo, and Deng, Youjun²

¹Zachry Department of Civil and Environmental Engineering, Texas A&M University, College Station 77840, TX, USA.

²Department of Soil and Crop Sciences, Texas A&M University, College Station, TX 77843, USA.

*cjsancheza@tamu.edu

The current concept for isolating high-level nuclear waste uses compacted bentonite as a buffer material in deep geological repositories. Smectite clay in bentonite is the major clay mineral responsible for the high swelling capacity and low permeability of the buffer. Recent investigations have reported a decrease in layer charge density of smectite specimens exposed to temperatures between 90-110 °C¹ and above 200 °C². Investigating mineral alterations in bentonite exposed to high temperature is challenging due to the long time (months and even years) and large quantities of materials required to perform each experiment. It is nearly impossible to systematically address the effects of many mineralogy factors, such as variations of accessory minerals, type of smectite, different charge densities of the smectites, and multiple types of exchangeable cations and the large variations in counterions' relative abundances in the interlayer of the clay. This work aimed to develop a miniature device to perform swelling pressure experiments on the clay fraction from bentonites with minimal amount of material. This study evaluated potential changes in smectite's swelling pressures caused by heat exposure from like that from nuclear waste repositories. This miniature device enabled the investigation of mono-ionic saturated smectites. The Results of Na-, K-, Li-, and Cs-saturated smectites are reported here.

The clay fractions (<2 µm) of a Texas bentonite were harvested and saturated with Na⁺, K⁺, Li²⁺, and Cs²⁺ ions, respectively. These samples were heated to 200 °C to 250 °C for ten days to mimic the heat from nuclear waste. X-ray diffraction (XRD), cation exchange capacity (CEC), SEM-EDS, and infrared spectroscopy (IR) were employed to characterize the smectite before and after the heating periods. A miniature swelling pressure device is developed to accommodate pellet shape specimens of ~15 mm in diameter and ~2 mm in thickness. The raw bentonite was used to validate the miniature device by conducting swelling pressure tests. This setup required less than 0.5 g of samples and duration time of less than 1 day, whereas the conventional swelling pressure test requires tens to hundreds of grams of material and nearly weeks or a month of duration.

The SEM-EDS results confirmed a complete cation exchange after ion-saturation. Preliminary results on the sample exposed to 200 °C and 250 °C showed none to minimal effects on the basal spacing (d₀₀₁), IR pattern, and apparent CEC of the Na, K, and Cs clays. The miniature device tested on the raw bentonite showed a comparable swelling pressure result obtained from literature and our in-house experiments, also, the swelling pressure reached equilibrium within few hours.

¹Villar, M. V., et al. (2025). Five-year thermo-hydro-mechanical and chemical evolution of compacted bentonite: Physical and mineralogical analysis. *Applied Clay Science*, 276, 107931.

² Kaufhold, S., Dohrmann, R. and Ufer, K. (2016). Interaction of magnesium cations with dioctahedral smectites under HLRW repository conditions. *Clays and Clay Minerals*, 64(6), 743-752.

CHARACTERIZING THE CLAY MINERALOGY OF THE PU‘U ‘ŌHI‘A ANDISOL FROM O‘AHU, HAWAI‘I.

Lam, Kristy ^{*1}, Skiba, Michał ², Błachowski, Arthur ³, Cieslak, Jakub ⁴, Stucki, Joseph ⁵, Hodges, Ryan ⁶, Rowland, Scott ⁷, McClellan Maaz, Tai ^{8,1}, Crow, Susan E. ⁹

¹Department of Natural Resources & Environmental Management, University of Hawai‘i at Mānoa, Honolulu, HI 96822, USA.

²Institute of Geological Sciences, Jagiellonian University, Krakow, Poland.

³Faculty of Geology, Geophysics, & Environmental Protection, AGH University, Krakow, Poland.

⁴Faculty of Physics & Applied Computer Science, AGH University, Krakow, Poland.

⁵Department of Natural Resources and Environmental Sciences, University of Illinois at Urbana-Champaign, Urbana, IL 61801 USA.

⁶Research Branch, National Soil Survey Center, USDA-NRCS, Lincoln, NE, 68508, USA.

⁷Department of Earth Sciences, University of Hawai‘i at Mānoa, Honolulu, HI 96822, USA.

⁸Department of Tropical Plant & Soil Sciences, University of Hawai‘i at Mānoa, Honolulu, HI 96822, USA.

⁹Soil, Water, and Ecosystem Sciences Department, University of Florida, Gainesville, FL 32607, USA.

[*klam3@hawaii.edu](mailto:kklam3@hawaii.edu)

In Andisols, nanocrystalline clays (i.e. allophane, imogolite, and ferrihydrite) actively influence chemical reactivity, resulting in unique soil behaviors such as phosphorus sorption, irreversible drying, and thixotropy. Andisols are difficult to study using traditional methods, such as x-ray diffractometry (XRD), because they irreversibly dry and contain a large portion of x-ray amorphous phases in their XRD patterns. This is particularly the case with highly weathered Andisols of Hawai‘i, thus, a combination approach is required because it utilizes various techniques to confirm the identification of nanocrystalline clays. The aim of this research was to characterize the clay mineralogy of the Pu‘u ‘Ōhi‘a Andisol (*Medial over pumiceous or cindery, ferrihydritic, isothermic Typic Hapludands*) from O‘ahu, Hawai‘i using XRD, x-ray fluorescence (XRF), Fourier-transform infrared spectroscopy (FTIR), and Mössbauer spectroscopy (MS). The data will be the basis for understanding the soil genesis story of Pu‘u ‘Ōhi‘a by identifying the potential mineral origin, transformation, dissolution, and formation pathways. This study focused on a ~3 m deep ferrihydritic Andisol profile at Lyon Arboretum. Parent cinders, bulk soil samples, and the separated clay (i.e. <2 μm and <0.2 μm) fractions were analysed. XRD showed that the parent cinder is composed of halloysite, magnetite/maghemite, and some gibbsite. Bulk soil samples were composed of 57-68% x-ray amorphous phases, 10-21% coarse-crystalline gibbsite, 6-9% halloysite, and up to 10% magnetite/maghemite. An increase in gibbsite relative to halloysite in the upper horizons indicates desilication. In the surface horizon, traces of quartz suggest minor aeolian input. MS showed the presence of Fe²⁺ in the silicate structure and an abundance of nanocrystalline Fe oxides. The clay fractions across all horizons contain 10 Å halloysite, gibbsite, and most likely abundant x-ray amorphous phase(s). In the upper horizons, 7 Å halloysite and dioctahedral vermiculite. The 7 Å phase may have formed at the expense of 10 Å halloysite due to wetting-drying cycles. The dioctahedral vermiculite is likely of aeolian and weathering origin.

CLAY MINERALS AND FE-OXYHYDROXIDES AS CONTROLS ON TRACE METAL ATTENUATION IN AN ACID MINE DRAINAGE IMPACTED WATERSHED, ALABAMA, USA

Sunday, Godwin^{1,3}, Donahoe, Rona*¹, and Bearden, Rebecca²

¹Department of Geological Sciences, University of Alabama, 201 7th Ave, Tuscaloosa, AL 35487, USA.

²Geological Survey of Alabama, 420 Hackberry Lane, Tuscaloosa, AL 35401, USA.

³Department of Civil and Environmental Engineering, University of Massachusetts Dartmouth, 285 Old Westport Rd, Dartmouth, MA 02747, USA.

*rdonahoe@ua.edu

This study evaluated the roles of stream and retention pond sediment grain size and secondary clay mineral and Fe-oxyhydroxide contents in controlling aqueous metal mobility within an abandoned mine lands (AML) site in the Hurricane Creek watershed, Alabama. Sediment samples were collected quarterly and water samples were collected monthly over a 2-year period and characterized by multiple analytical techniques (PSA, X-ray fluorescence, X-ray diffraction, partial digestion, ICP-OES, ion chromatography). The data produced were analyzed using principal component analysis (PCA) and PHREEQC modeling to resolve grain size and mineralogical controls on trace metal partitioning between water and sediments.

Silt-rich retention pond sediments (SS9–SS10) exhibited the highest total metal concentrations (Fe >200,000 mg/kg; Al >133,000 mg/kg), reflecting sustained accumulation under low-flow, acidic pond conditions that promote metal deposition and retention. In contrast, sand-dominated stream sediments showed lower total metal concentrations but higher percent extractability of Fe, Mn, and Ni, indicating weaker sorption and limited incorporation of these metals into stable secondary mineral phases. Aluminum exhibited consistently low extractability (<37%), attributable to its structural incorporation within kaolinite (0–61.7%) and gibbsite (0–12.5%).

Statistical analysis helped further resolve mineralogical controls on metal mobility within this AMD-impacted site. PC1 (32.7%) linked high extractable metal concentrations and goethite contents to AMD-driven accumulation of metals in fine-grained sediments. PC2 (30.1%) reflected lithogenic silicate metal inputs distinct from AMD-derived metal enrichment. PC3 (11%) was interpreted to represent sorption-controlled trace metal retention by Fe oxyhydroxides. Principle component analysis successfully distinguished AMD control of metal enrichment from primary mineral inputs and surface-complexation processes governing metal partitioning. Geochemical modeling supported these conclusions, showing that circumneutral waters are supersaturated with respect to ferrihydrite and goethite, promoting Fe-oxyhydroxide formation and metal scavenging, while acidic pond waters remain undersaturated, indicating that Fe minerals in retention pond sediments represent accumulated rather than actively precipitating phases.

The results of this study demonstrated that trace metal attenuation by sediments within the study site is primarily controlled by secondary clay and Fe-oxyhydroxide mineral phases and grain size, with Fe-oxyhydroxides governing transition metal retention through sorption and co-precipitation, and clay mineral precipitation limiting Al mobility.

COUPLED THERMO-HYDRO-MECHANICAL MODELING OF MX-80 BENTONITE PELLETS USING A DOUBLE-STRUCTURE FRAMEWORK

Barbosa, Lucas G.*¹, Greathouse, Jeffery A.², Deng, Youjun¹, Sanchez, Marcelo¹

¹Zachry Department of Civil and Environmental Engineering, Texas A&M University, College Station, TX 77840, USA.

²Nuclear Waste Disposal Research & Analysis, Sandia National Laboratories, Albuquerque, NM, 87185, USA.

*guarnierilucas@tamu.edu

Geological disposal facilities (GDF) rely on a multi-barrier concept to ensure the long-term isolation of high-level nuclear waste (HLW) and spent nuclear fuel (SNF). A key component of this strategy is the Engineered Barrier System (EBS), where clay-based materials, primarily bentonite, are used as a protective buffer. In this context, this study investigates the complex thermo-hydro-mechanical (THM) response of an EBS composed of a mixture of MX-80 bentonite pellets and powder, using a numerical modeling approach to analyze its evolution of the barrier under hydration and heating processes.

The modeling framework is developed to reproduce a laboratory infiltration experiment designed to simulate in-situ thermal and hydraulic conditions. A two-dimensional representation of a confined column system is adopted, incorporating bottom heating and controlled hydration through axial and radial injection. This configuration enables the investigation of coupled THM processes within a heterogeneous pellet-powder mixture under high-temperature conditions. To capture the system response, a coordinated instrumentation system was utilized.

To capture the complex behavior of expansive bentonite, the Double-Structure Model proposed by Sánchez et al. [1, 2] is employed. This constitutive framework distinguishes between microstructural (intra-aggregate) and macrostructural (inter-aggregate) levels, allowing explicit representation of their mechanical coupling. In this approach, microstructural swelling driven by hydration leads to progressive macro-pore occlusion, which is essential for describing the behavior of pelletized bentonite systems.

The integration of experimental data with the double-structure simulations enables the analysis of hydration and thermal gradients and their influence on the evolution of dry density and stress states within the barrier. These results provide insights into the long-term stability and sealing efficiency of pelletized clay barriers, contributing to better decisions and refinement of the performance of geological repositories.

Sandia National Laboratories is managed and operated by NTESS under DOE NNSA contract DE-NA0003525.

[1] Sánchez, M., Gens, A., Guimarães, L. J. N., & Olivella, S. (2005). A double structure generalized plasticity model for expansive materials. *International Journal for Numerical and Analytical Methods in Geomechanics*, 29 (8), 751-787. [2] Sánchez, M., Gens, A., Villar, M. V., & Olivella, S. (2016). Fully Coupled Thermo-Hydro-Mechanical Double-Porosity Formulation for Unsaturated Soils. *International Journal of Geomechanics*, 16 (6), 04016082.

MG-FE LAYERED DOUBLE HYDROXIDE AS A CONTROLLED-RELEASE PHOSPHORUS FERTILIZER: IMPROVING PLANT P UPTAKE AND REDUCING SOIL P LOSS

Liu, Yu-Ting ^{*1,2}, Li, Wen-Hui¹, Hsu, Liang-Ching¹

¹Department of Soil and Environmental Sciences, National Chung Hsing University, Taichung, 40227, Taiwan.

²Innovation and Development Center of Sustainable Agriculture, National Chung Hsing University, Taichung, 40227, Taiwan.

*yliu@nchu.edu.tw

Phosphorus (P) management remains a major challenge in agriculture due to low fertilizer use efficiency and high risks of P loss to aquatic environments. To address these limitations, this study evaluated a synthesized Mg–Fe layered double hydroxide (LDH) as a controlled-release phosphorus fertilizer, compared with a conventional commercial fertilizer, triple superphosphate (TSP). Fertilizers were applied at two rates (65 and 130 mg P kg⁻¹ soil), with an unfertilized control (BK), and their impacts on P partitioning and chemical speciation were assessed.

Phosphorus distribution results demonstrated clear differences in P fate between LDH and TSP treatments. Across application rates, LDH promoted a larger fraction of P accumulation in plant tissues while maintaining a greater proportion of soil available P compared with TSP. In contrast, TSP treatments showed greater P loss to water bodies, indicating reduced P use efficiency and elevated environmental risk. These findings suggest that LDH can better synchronize P availability with plant demand while mitigating undesirable P runoff/leaching pathways.

To further clarify the mechanism, soil P speciation was determined using P K-edge XANES spectroscopy with linear combination fitting. The analysis identified two dominant P pools: labile-P represented by KH₂PO₄, and Fe(III)-bound phosphate represented by phosphate adsorbed on ferrihydrite. LDH treatments exhibited a higher proportion of labile-P and a lower proportion of Fe(III)-P relative to TSP, supporting the hypothesis that LDH reduces transformation into strongly sorbed Fe-associated forms. This mechanistic evidence aligns with the observed improvements in plant P uptake and reductions in P fixation and loss.

Overall, the LDH fertilizer shows strong potential as an environmentally responsive, controlled-release phosphorus strategy to enhance agronomic performance and mitigate the environmental impacts of P fertilization.

SELECTIVE MICROBIAL IRON REDUCTION IN NONTRONITE-MAGHEMITE MIXTURES UNDER REPEATED FREEZE-THAW CYCLES

Selective Microbial Iron Reduction in Nontronite–Maghemite Mixtures under Repeated Freeze–Thaw Cycles

Insung Kang ^{*1}, Young Kyu Park^{1,2}, and Jinwook Kim¹

¹Department of Earth System Sciences, Yonsei University, Seoul, Republic of Korea

²Korea Polar Research Institute, Incheon, Republic of Korea

*21insung@yonsei.ac.kr

Understanding the microbial reduction and dissolution of iron-bearing minerals provides insights into the sources and behavior of dissolved iron entering the ocean. In environments such as polar regions, repeated freeze-thaw cycles represent an environmental condition that can influence these biogeochemical processes. This study investigated the microbial iron reduction of nontronite (NAu-2) and maghemite mixtures by *Shewanella vesiculosa* under repeated freeze-thaw cycles ranging from 15°C to -10°C. The mixed system exhibited a total Fe reduction extent of approximately 5% in bulk solution, as measured by the 1,10-phenanthroline assay. This stands in contrast to results from single-mineral systems, where microbial reduction typically exceeded 20%. XRD analysis showed no detectable mineralogical changes or the neoformation of secondary minerals. However, TEM-EELS analysis revealed higher localized reduction extents in the immediate vicinity of microorganisms. Specifically, nontronite particles in close proximity to bacteria exhibited high levels of reduction, whereas maghemite particles in similar proximity showed relatively lower reduction. This preferential reduction of nontronite, which possesses a lower iron content compared to the iron-rich maghemite, likely contributes to the limited overall iron reduction observed in the bulk system. These results suggest that the observed mineral selectivity may be associated with hetero-aggregation between the two mineral phases. Such aggregation could potentially alter the effective grain size and spatial morphology of the mineral aggregates, thereby modifying microbial access to iron-bearing sites and leading to the differences in reduction extent between nontronite and maghemite.

IS HUMIDITY THE MAIN CONTROL OF HYDRATION IN SMECTITES?

Rybka, Karolina*¹, Derkowski, Arkadiusz¹, Skiba, Michał², Stępak, Magdalena³, and Nowicka, Beata³

¹Institute of Geological Sciences, Polish Academy of Sciences, Senacka 1, 31002, Kraków, Poland.

²Institute of Geological Sciences, Faculty of Geography and Geology, Jagiellonian University in Krakow, Gronostajowa 3a, 30387 Kraków, Poland.

³Faculty of Chemistry, Jagiellonian University in Kraków, Gronostajowa 2, 30387 Kraków, Poland.

*ndrybka@cyf-kr.edu.pl

Water retention in smectites reflects the interplay between interlayer hydration states, adsorption on external surfaces, and interparticle water. Interlayer hydration is generally considered to increase stepwise and non-linearly with relative humidity (RH), whereas the role of temperature (T) is typically discussed only in the context of dehydration and is rarely evaluated together with RH. Quantifying the distribution of water between interlayer and non-interlayer sites and understanding the combined effects of T and RH remain challenging, yet essential for predicting swelling, transport, and reactivity of smectite-rich materials.

Dynamic Vapor Sorption (DVS) measured water uptake over T = 5–65 °C and RH = 0–97%, while X-ray powder diffraction (XRD) tracked basal spacing (d00l series) at RH = 30 and 50% and T = 10–80 °C. Na- and Ca-exchanged S_{Ca}-3 (“Otay”) smectites were investigated to assess the influence of interlayer cations with contrasting hydration enthalpies.

DVS confirmed the expected trends: water content increases with RH, decreases with T, and is higher for Ca²⁺- than Na⁺-exchanged samples. Notably, hysteresis loops observed typically in DVS analyses at room temperature, disappeared above 35°C for Ca-S_{Ca}-3, indicating removal of kinetic or thermodynamic barriers. Comparison of total water content with d00l changes indicated that interlayer thickness expands linearly with water content, regardless of T. The non-interlayer water (external and interparticle) remained substantial. The XRD data revealed temperature-driven changes between hydration states typical for smectites, including 2W → 1W → 0W transitions with increasing T even at constant RH. It demonstrated, that temperature directly controls layer hydration and exerts the effect of RH; for example, Na-S_{Ca}-3 remains in the 0W state at RH 30% for T > 60 °C despite the presence of water vapor. While current reactive transport models for clay-rich formations use RH as the main controlling factor of water content, using T as correction on diffusion coefficients, the present results demonstrate that T independently may drive interlayer collapse by one full hydration step, reducing swelling pressure in ways not captured by RH-based isotherms alone.

Acknowledgements: The project is financed by the Ministry of Science and Higher Education (Poland) under the "Science for Society II" Program.

SOIL HETEROGENEITY AND THE INFLUENCE OF CLAY MINERALS ON LANDSLIDE RISK IN HILLY TROPICAL LANDSCAPES

Ryan, Peter C.*¹, Parkinson, Theodora J.¹, Pérez-Martín, Isabel L.¹, and Reyes Collovati, M. Jorgelina¹

¹Earth and Climate Sciences Dept., Middlebury College, Middlebury Vermont 05753, USA.

*pryan@middlebury.edu

The high degree of soil heterogeneity in hilly tropical landscapes like those of Puerto Rico leads to a wide range in landslide susceptibility over small spatial scales. The heterogeneity is driven by the action of landslides themselves, which locally remove much of the soil mantle, typically exposing soil C-horizons or saprolite; this reduces landslide probability relative to adjacent parts of the hillslope where landslides have not recently occurred. In the wake of hurricanes, landslide prevalence tends to be highest where soil parent material is granodiorite, and also where volcanoclastic rocks are soil parent material. Slip surfaces tend to be shallow (typically < 100 cm) with soils mobilized rapidly into long runout distances. To assess the mineralogy and composition of soils and landslide slip surfaces, pits were located adjacent to scarps from previous landslides, facilitating sampling of soils downward through extrapolated slip surfaces. Documenting local-scale soil diversity and the role of clay-rich subsoil horizons is contributing to a landslide alert program currently under development by a team of researchers from University of Puerto Rico at Mayaguez (<https://derrumbe.net/>).

XRD, XRF, TGA and SEM-EDS indicate that soils are laterally and vertically heterogeneous, often with C-horizons or B-horizons enriched in clay minerals and immobile elements (Al, Fe, Ti) relative to overlying soil horizons. In particular, Inceptisols on steep slopes often contain smectite-rich horizons at 30-60 cm depth that contain 15-25% more smectite than overlying more-granular horizons, making these clay-rich horizons potential slip surfaces. In other cases, clay-rich horizons in Ultisols are observed to contain 25-35% more halloysite or kaolinite than overlying coarser horizons, also creating potential slip surfaces. Understanding factors that lead to the presence of deeply-weathered clay-rich horizons at depth is relevant to understanding landslide risk, and field observations and mineralogical-chemical analysis indicate that clay-rich subsoils situated below more-permeable shallow horizons can form by (1) higher chemical weathering rates along joints or bedding planes that accelerate clay formation along planar features in the subsurface, (2) prior landslides that bury a smectite-rich AB-horizon under permeable colluvium, (3) fluctuating perched water tables that cause intense weathering at this wetting-drying front (e.g. 70-100 cm deep), and (4) inherited clay-rich horizons from volcanoclastic sediment. Where clay-rich soil horizons occur beneath more-permeable overlying horizons, rainfall infiltration through OA-horizons and upper B-horizons can rapidly load moisture downward where it is absorbed by clay-rich subsoil horizons, causing decreased shear strength and increased landslide susceptibility. The fact that these mass movements are triggered in the upper 100 cm of soil makes understanding soil mineralogy especially important.

CONSTRUCTION OF SEPIOLITE-SUPPORTED POLYAMIDOXIME COMPOSITE AND ITS URANYL ION ADSORPTION PERFORMANCE

Zeng Jiamin*¹, Zhang Qingcheng¹, Yuan Peng¹

¹School of Environmental Science and Engineering, Guangdong University of Technology, Guangzhou, 510006, China. *zengjiaminn@163.com

Keywords: Sepiolite; Polyamidoxime; Uranyl ion; Adsorption.

Abstract: The efficient extraction of uranium resources from aqueous environments is of great significance for the sustainable development of nuclear energy and the remediation of radioactive pollution. Amidoxime-functionalized materials exhibit excellent selective adsorption capacity due to the strong coordination interactions formed with UO_2^{2+} . However, the experimental capacity of polyamidoxime (PAO) adsorbents is often far lower than their theoretical capacity due to issues such as easy agglomeration, poor structural stability, and low utilization rates of active sites.

To address this issue, this study utilizes natural fibrous sepiolite (Sep) as an inorganic carrier to construct an in-situ fiber-supported organic-inorganic composite, designated as PAO@Sep, through in-situ polymerization followed by an amidoximation reaction. The unique fibrous structure of sepiolite, along with the abundant Mg-OH and Si-OH active sites on its surface, provides excellent interfacial conditions for the growth and anchoring of the polymer. This facilitates improved polymer dispersion and promotes uniform loading onto the carrier surface. Unlike amidoxime-functionalized composites prepared via simple physical blending or surface coating, the PAO in this study is interfacially anchored onto the sepiolite surface via in-situ polymerization, forming a continuous distribution along the fiber structure. Consequently, a core-shell structure with the sepiolite skeleton as the core is constructed, significantly enhancing the exposure and accessibility of the amidoxime groups (C=N-OH) in PAO. Furthermore, the N and O atoms within the amidoxime groups act as electron donors to form stable coordination bonds (U-O/U-N) with UO_2^{2+} , and enhancing their electron-donating ability is highly beneficial for strengthening this coordination interaction. The Mg-OH active sites on the sepiolite surface can regulate the electron distribution of the amidoxime groups in PAO, thereby enhancing the electron-donating ability of the N and O atoms and promoting electron transfer to the uranyl ions. This fundamentally improves the uranyl ion adsorption performance of PAO@Sep. Adsorption performance tests demonstrate that PAO@Sep achieves a U(VI) adsorption capacity of 857.20 mg/g, representing a 75.6% increase compared to pure PAO. This natural mineral-based composite strategy not only improves polymer dispersion and active site utilization efficiency but also offers the advantages of abundant raw material sources and relatively low costs, providing a valuable reference for the design and optimization of amidoxime-functionalized uranium adsorbents.

IMMOBILIZING RADIOACTIVE IODIDE AND IODATE USING CHRYSOTILE AND HALLOYSITE, RESPECTIVELY

Xu, Huifang *¹

¹Department of Geoscience, University of Wisconsin-Madison, Madison, Wisconsin 53706, USA

*hfxu@geology.wisc.edu

Radioactive iodines are the by-products of uranium fission, and they are abundant in nuclear wastes. Radioiodines have been released into soils and the atmosphere during the course of nuclear weapon tests, nuclear power plant operations, and nuclear accidents such as those occurred at Three Mile Island in the USA in 1979, at Chernobyl in Russia in 1986, and at Fukushima in Japan in 2011. In aqueous environments, iodine exists primarily as the anions iodide (I^-) and iodate (IO_3^-) depending on redox conditions and pH. Of these two species, the reduced form, I^- , is more common in suboxic to reducing conditions with pH values around 4–10 in natural environment.

Chrysotile bundles (Chry-B) with wedged-shaped nanopores exhibited very strong adsorption to I^- , with a distribution coefficient (K_d) of 179.24 mL/g, which is two orders of magnitude higher than those for previously reported clay minerals. The adsorption isotherm of I^- fitted well with Langmuir isotherm and the Langmuir adsorption capacity of Chry-B was 4.13 mg/g, which is three orders of magnitude higher than those of natural soil samples and one order of magnitude higher than that of ferrihydrite. The wedge-shaped nanopores among the neighboring nanotubes in Chry-B proved to be the primary adsorption sites for I^- by comparing the adsorption of Chry-B with those of dispersed chrysotile single nanotubes, lizardite and brucite. The severe superposition of electric potential from the narrowing charged walls of the wedges constituted a key mechanism in I^- adsorption process, which significantly strengthened the electrostatic interaction between I^- and wedge surface $>Mg-OH$. These results demonstrated

that the shape of nanopore geometry was crucial in I^- adsorption, and that chrysotile with significant reserves worldwide had the potential to be an inexpensive and efficient adsorbent for the radioactive iodide removal.

The nanosized tubular halloysite exhibited higher adsorption capacity and stronger adsorption to IO_3^- than the platy kaolinite. The specific surface area normalized K_d values of halloysite are 13.5 times higher than that of kaolinite. About <23% of pre-adsorbed IO_3^- was released from halloysite after 48 h desorption. In contrast, > 90% of pre-adsorbed IO_3^- was removed from kaolinite after 1 h desorption. What is more, halloysite had high selectivity to IO_3^- , and the adsorption capacity on halloysite is slightly affected by the concurrent anions. These results are attributed to the curved octahedral sheet in the inner surface of halloysite nanotubes. It is proposed that the curved octahedral sheet caused geometry match between three oxygen atoms in the iodate and three OH above the vacant site of the octahedral sheet. With the excellent IO_3^- adsorption performance and low cost, halloysite is a potential adsorbent for immobilizing radioactive iodate in natural and engineered environments. Future

SEPIOLITE-SUPPORTED BIMETALLIC CATALYSTS FOR THE OXIDATION OF 5-HYDROXYMETHYLFURFURAL TO 2,5-FURANDICARBOXYLIC ACID

Zhong Xuemin^{*1}, Yuan Peng², Wang Xiuping³, and Wu Honghai³

¹College of Resources and Environment, Yangtze University, Wuhan 430100, China.

²School of Environmental Science and Engineering, Guangdong University of Technology, Guangzhou 510006, China.

³School of Environment, South China Normal University, Guangzhou 510006, China.

[*zhongxuemin@yangtzeu.edu.cn](mailto:zhongxuemin@yangtzeu.edu.cn)

Sepiolite is a typical one-dimensional clay mineral widely used in catalysis due to its fibrous morphology, porous structure, large specific surface area, high surface activity, low cost, and environmental friendliness. The synthesis of chemicals derived from biomass has attracted considerable attention, among which the oxidation of 5-hydroxymethylfurfural (HMF) to 2,5-furandicarboxylic acid (FDCA) represents an important reaction in biomass conversion. However, efficient and stable catalysts for this reaction remain to be developed. In this work, sepiolite was used as a support to load PdAu bimetallic catalysts, and the as-prepared catalysts were applied to the oxidation of HMF to FDCA. The results show that PdAu bimetallic nanoparticles were uniformly dispersed on the sepiolite surface, forming an alloyed structure with a fine particle size. Among the catalysts tested, 1Pd₁Au₄/Sep exhibited the highest catalytic activity, achieving an FDCA yield of 97% within 10 minutes under optimal conditions, corresponding to an FDCA formation rate of 2560.72 mmol·g⁻¹·h⁻¹. After 30 minutes, the FDCA yield reached 99.9%. Furthermore, 1Pd₁Au₄/Sep demonstrated high stability and reusability. The dispersing effect of sepiolite on metal nanoparticles significantly enhanced catalytic activity. In addition, sepiolite exhibited an adsorption effect toward HMF, facilitating its conversion. Oxygen vacancies in sepiolite also promoted the adsorption and activation of O₂. Meanwhile, the alloying effect between Pd and Au improved catalytic activity and promoted the activation and dehydrogenation of both reactants and intermediates, thereby accelerating the conversion of 5-hydroxymethyl-2-furancarboxylic acid (the rate-limiting step) and further increasing the FDCA yield. Therefore, this study develops high-performance catalysts for HMF oxidation and expands the application of sepiolite in biomass catalytic conversion.

***In situ* observation of the re-oxidation behavior of structural iron in montmorillonite by X-ray absorption fine structure**

Morii, Shiori*^{1,2}, Yamaguchi, Akiko^{1,2}, Derkowski, Arkadiusz³, and Takahashi, Yoshio²

¹Japan Atomic Energy Agency, Ibaraki 319-1184, Japan.

²Graduate School of Science, The University of Tokyo, Tokyo 113-0033, Japan.

³Institute of Geological Sciences, Polish Academy of Sciences, Krakow 31-002, Poland.

*morii.shiori@jaea.go.jp

The redox processes of structural iron (Fe) in clay minerals can alter their structure, layer charge, cation exchange capacity, and swelling properties. Structural Fe(III), common in smectite, can be reduced under various natural and anthropogenic conditions, and then re-oxidized when transferred to higher Eh conditions. In this study, Fe K-edge X-ray absorption fine structure (XAFS) was applied for *in situ* observation of the re-oxidation of reduced structural Fe in montmorillonite. We analyzed short-term time-dependent changes in the oxidation state and coordination environment of structural Fe.

The reduced montmorillonite (SWy-3; Fe content: 2 wt%) was prepared by dithionite reduction of a size-fractionated suspension in an anaerobic glovebox, resulting in the reduction of 75 % of structural Fe. Immediately before the XAFS measurement, the initially sealed sample was exposed to air. The XAFS spectra obtained immediately after exposure and after 30 minutes and 5 hours were compared with those of SWy-3 before and after dithionite reduction. Additional experiments were conducted under high-humidity conditions and in oxygen-saturated water to evaluate the effect of water on the re-oxidation behavior.

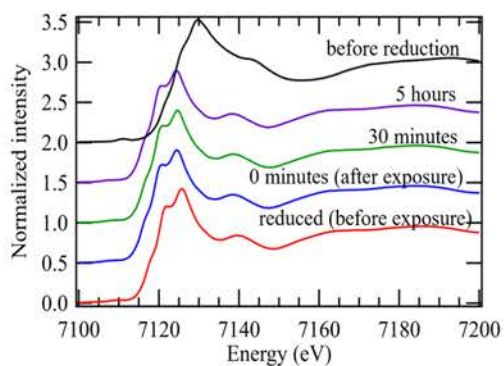


Figure 1. Time-dependent re-oxidation behavior of structural iron in dithionite-reduced SWy-3 observed *in situ* with XAFS.

According to Figure 1, even after 5 hours of exposure to air, the spectra showed almost no change compared to that before exposure. Similar trends were observed under high-humidity conditions and in oxygen-saturated water. These results indicate that the re-oxidation of structural Fe(II) in clay minerals proceeds slowly. One possible explanation is that SWy-3 contains a relatively low amount of structural Fe, which may limit electron transfer within the structure. The longer-term re-oxidation behavior and associated changes in coordination environment will be discussed along with the kinetics of the process.

Acknowledgements: This study was performed with the approval of SPring-8 (2025A1991) and Photon Factory (2024G123), and was partly supported by JSPS KAKENHI Grant-in-Aid for Scientific Research (C) (25K00227).

INCORPORATING CLAY INTO NOVEL NATURE-BASED SOLUTIONS FOR EMERGING CONTAMINANTS

Ma, Xingmao*¹, Deng, Youjun², Dong, Qiangqiang²

¹Department of Civil and Environmental Engineering, Texas A&M University, College Station, TX 77843, USA.

²Department of Soil and Crop Sciences, Texas A&M University, College Station, TX 77843, USA.

*samuelma@tamu.edu

Emerging contaminants such as per- and polyfluoroalkyl substances (PFAS) are widespread in our environment and pose serious health risks to the public and our ecosystem. Even though energy intensive technologies have displayed great performance for concentrated contaminants in small volumes of polluted media, they are prohibitive for the vast amount of moderately contaminated soil and water. Therefore, there is a critical need to develop nature-based solutions to effectively address the concerns from emerging contaminants at relatively moderate but still hazardous levels.

Clays are ubiquitous in the natural environment and exhibit many desirable features for contaminant control, making it a strong candidate for nature-based solutions to address the rising concerns of emerging contaminants. These features include large specific surface area, permanent or variable surface charge, abundant structural defects and tunable surface properties. These properties allow clays to function as natural adsorbents, supporting material for nanocomposite catalysts and activators of oxidants to generate highly reactive species. This presentation aims to assess the opportunities and potential challenges of applying clay as a major component of nature-based solutions for the growing concerns of emerging contaminants.

IMAGING THE FORMATION OF NANOSTRUCTURED HYDROXIDE FILMS ON MINERAL-WATER INTERFACES

Legg, Benjamin A*¹, Song, Shuhong¹, Molnár, Zsombor¹, De Yoreo, James J.¹, Zhang, Mingyi².

¹Pacific Northwest National Laboratory, Richland, WA 99354, USA

²University of Oklahoma, Norman, OK 73019, USA. *benjamin.legg@pnnl.gov

Mineral-water interfaces host critical adsorption and precipitation phenomena that dictate the distribution of elements throughout the environment. Liquid-cell atomic force microscopy can now provide atomic-scale imaging of sorbed ions on phyllosilicate minerals such as clays and micas and thus provides unprecedented insights into the molecular-scale modes of sorption and precipitation.

In one recent study, we have studied the sorption of divalent and trivalent cations onto muscovite mica, using a combination of in situ AFM and streaming potential measurements. These studies have revealed complex modes of ion adsorption and interfacial precipitation.

Divalent cations (i.e. Mg^{2+} , Co^{2+} , and Ni^{2+}) showed relatively simple behavior, with modest adsorption at lower pH values, and generating continuous hydroxide monolayers via a classical ‘birth and spread’ process as the pH was raised toward the saturation point. However, trivalent cations (i.e. Al^{3+} , Fe^{3+} , Cr^{3+}) showed much more complex behavior. At lower pH, the trivalent ions form ordered ion networks (OINs), with nanometer-scale correlations between ions. As the pH was increased, the ions formed hydroxide films, but instead of forming continuous films, they created a 2D network of islands and gaps. The formation of nanostructured films was accompanied by abrupt reversals in the interfacial potential, indicating that electrostatic forces play a key role in the nanostructure generation. Monte Carlo models indicate that the complex modes of sorption arise from a ‘charge frustrated’ competition between hydroxyl bridges that drive ion clustering, and long-range electrostatic forces that limit cluster size.

In related studies on the sorption of trivalent rare earth element ions (e.g. La^{+3} and Yb^{+3}) on micas, clays, and oxides we see similar complexities. These include charge reversals, and the concurrent formation of nm-thick amorphous hydroxide films. To better understand these behaviors, we employ advanced 3D AFM imaging techniques, which allow us to map out short-range hydration structures and long-range electrostatic forces. These provide interface-specific insights into interfacial forces and charge distributions that control ion adsorption, and allow us to observe preferential sorption onto specific crystallographic features such as step edges and facets.

THE APPARENT LAYER CHARGE CHANGES IN DEHYDRATED AND REHYDRATED SMECTITES AND BENTONITES

Kuligiewicz, Artur. ^{*1}, Rybka, Karolina¹, and Derkowski, Arkadiusz¹

¹Institute of Geological Sciences, Polish Academy of Sciences, Krakow, Poland.
^{*}ndkuligi@cyf-kr.edu.pl

Bentonites are one of the engineered barriers in most radioactive waste repository designs. Many of the desirable bentonite qualities in such an environment are the result of layer charge (LC) residing in 2:1 layers of smectite, which is the main constituent of a bentonite rock. A detailed understanding of all factors that lead to changes in the smectite LC is therefore, crucial for developing reliable models of the long-term performance of bentonite buffers.

This contribution summarizes the results of multiple smectite dehydration and rehydration experiments performed at the IGS PAS over the last 5 years. Smectite reference samples (SAz-2, SCA-3, and SBId-1), as well as bentonite rock samples in various cationic forms, were dried in a laboratory oven at temperatures ranging from 60 to 250°C. After drying, samples were stored in a powder form or subjected to hydrothermal rehydration to examine the impact of storage or the hydrothermal treatment on the LC. The LC of the samples was measured by the spectroscopic OD method immediately after drying and subsequently periodically checked over extended periods to assess the impact of rehydration on the LC.

Measurable shifts in the ν O-D stretching mode used as the LC proxy in the OD method were noted for all smectites, however, their magnitude was dependent on the heating temperature and the interlayer cation type. For the Li-exchanged SAz-2 sample, the position of ν O-D could be shifted by drying at a temperature as low as 90°C under a dry N₂ purge. Considerable ν O-D shifts were observed for Li-exchanged SBId-1 beidellite heated > 100°C. A gradual shift of ν O-D towards higher LC (i.e., apparent LC regeneration) was observed for Li⁺ and Mg²⁺-exchanged SAz-2 sample stored for 3 years in a powder form. The apparent LC regeneration was also observable in the hydrothermal conditions for Mg²⁺ and Fe²⁺-exchanged samples, with the extent depending on the initial dry-heating temperature. The observed shifts in ν O-D are in many cases the result of the formation and subsequent desorption of the inner-sphere complexes in the smectite's interlayer, therefore, a term "apparent LC change" is recommended for the description of this phenomenon.

Acknowledgments

The project is financed by the Ministry of Science and Higher Education (Poland) under the "Science for Society II" Program.

TAILORING NATURAL CLAYS FOR SELECTIVE AND SUSTAINABLE PFAS REMOVAL: EXPLORING CATION EXCHANGE, POST-GRAFTING, AND FLUOROPHILIC INTERACTIONS

Qianqian Dong, Department of Soil and Crop Sciences, Texas A&M University, College Station, TX

Yin Wang, Department of Civil and Environmental Engineering, University of Wisconsin-Milwaukee, Milwaukee, WI

Per- and polyfluoroalkyl substances (PFAS) are a large group of toxic chemicals widely detected in water and soil, stemming from both domestic release and long-distance environmental translocation. The development of cost-effective methods for reducing PFAS concentrations in water is urgently needed. Functionalized clay materials represent a promising approach, yet the structural diversity and hydrophobicity of PFAS pose distinct challenges for optimizing sorption performance.

In this work, we present a series of clay-based sorbents developed via cation exchange and post-grafting strategies, to enhance PFAS removal from water. By maximizing hydrophobic, electrostatic, and fluorophilic interactions between PFAS molecules and tailored clay substrates, we established an effective design strategy for selective and sustainable PFAS remediation. Our results demonstrated that these engineered clay sorbents not only achieve improved adsorption capacity and affinity for diverse PFAS but also exhibit enhanced selectivity and reusability. This work provides new insights into the rational design of clay-based sorbents for practical PFAS removal, paving the way for sustainable water treatment technologies.

IRON REDOX–DRIVEN ARSENIC IMMOBILIZATION VIA ALGAL BIOMINERALIZATION REVEALED BY SYNCHROTRON SPECTROSCOPY

Cho Yen-Lin ^{*1,2}, Than Nhu Anh Thi ³, Liu Yu-Ting ^{3,4}

¹ Department of Marine Environment and Engineering, National Sun Yat-sen University, 70 Lien-hai Road, Kaohsiung, 40704, Taiwan (R.O.C.)

² The Center for Water Resources Studies, National Sun Yat-sen University, 70 Lien-hai Road, Kaohsiung, 40704, Taiwan (R.O.C.)

³ Department of Soil and Environmental Sciences, National Chung-Hsing University, 145 Xingda Road, Taichung, 40227, Taiwan (R.O.C.)

⁴ Innovation and Development Center of Sustainable Agriculture, National Chung Hsing University, 145 Xingda Road, Taichung, 40227, Taiwan (R.O.C.)

*ylcho@mail.nsysu.edu.tw

Arsenic mobility in groundwater is strongly regulated by iron redox cycling in soils and sediments. Under anaerobic conditions, reductive dissolution of ferric iron [Fe(III)] phases could enhance arsenic release. This study investigated Fe-mediated arsenic immobilization in microalga (*Cyanidium caldarium*) under aerobic and anaerobic conditions. Under anoxic conditions, the algae oxidized more than 97% of Fe(II) and promoted the formation of reactive Fe(III) hydroxide phases. These phases enhanced arsenic retention. Under aerobic conditions, arsenic was also effectively associated with cellular components and Fe-rich surface phases. Synchrotron-based X-ray fluorescence mapping and X-ray absorption spectroscopy revealed the distribution and speciation of arsenic as intracellular As(III)-cysteine complexes and as surface-bound species associated with Fe phases and polysaccharides. The results suggest that arsenic immobilization was controlled by Fe redox transformation, biomineralization, and organic-mineral interactions. This study provides new insight into arsenic retention in Fe-rich soil, sediment, and groundwater systems.

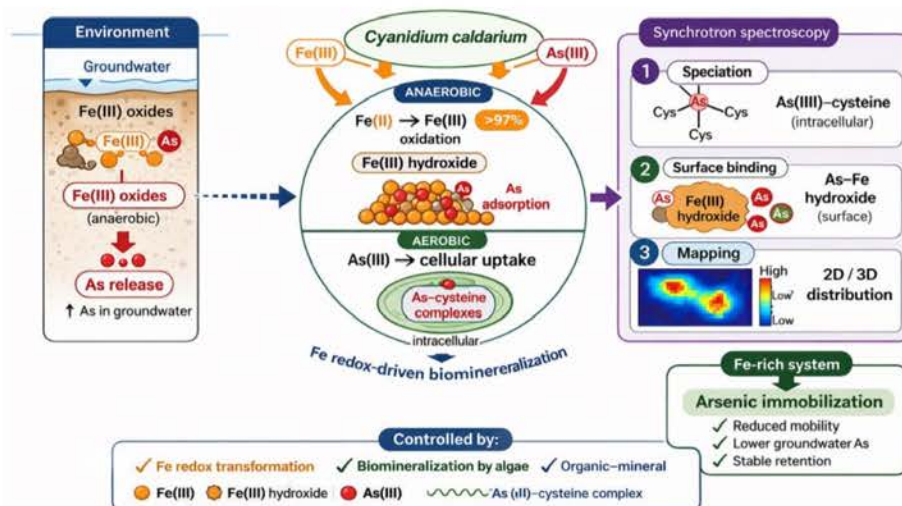


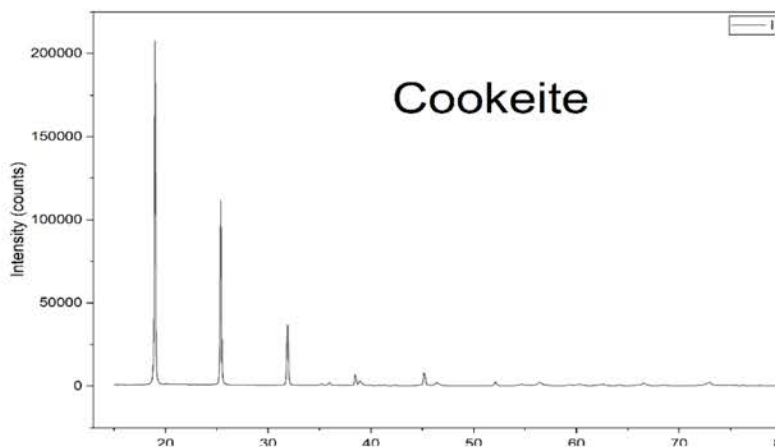
Figure 1. Mechanistic framework of Fe redox–driven arsenic immobilization by *Cyanidium caldarium*.

PHYSICOCHEMICAL CHARACTERIZATION AND SURFACE REACTIVITY OF COOKEITE FROM MINERAL DISSOLUTION, MICROSCOPIC AND SPECTROSCOPIC STUDIES

Oladele, Segun O. ^{*1}, Kumar, Ashish R. ¹, and Ogunmodimu, Samuel O. ¹

¹John and Willie Leone Family Department of Energy and Mineral Engineering, The Pennsylvania State University, University Park, PA 16803, USA.

[*soo5254@psu.edu](mailto:soo5254@psu.edu)



Cookeite is a lithiumbearing dioctahedral chlorite that occurs in pegmatites and hydrothermal systems and has recently gained attention as a potential lithium host in clayrich deposits. Despite its economic and geochemical relevance, the physicochemical properties governing its surface reactivity and processing behavior remain poorly constrained. In this study, a comprehensive characterization of researchgrade cookeite sourced from Minas Gerais, Brazil, was conducted using a combination of mineralogical, spectroscopic, thermal, and surface analytical techniques. Phase identification by powder Xray diffraction confirmed the presence of cookeite polytypes with slight structural variations, consistent with previously reported lattice parameters. Transmission electron microscopy revealed a layered platelet morphology typical of chloritegroup minerals. Vibrational spectroscopic analyses using FTIR and Raman spectroscopy identified characteristic OH stretching and Si–O lattice modes, with distinct changes observed upon hydration and vacuum drying. Surface chemical states and hydrationinduced speciation effects were evaluated by Xray photoelectron spectroscopy, showing systematic shifts in O 1s and Si 2p environments. Physicochemical measurements indicate that cookeite exhibits moderate wettability, with a contact angle of approximately 50°, and a negatively charged surface across a wide pH range, as revealed by zeta potential analysis. BET surface area measurements and atomic force microscopy demonstrate that vacuuminduced dehydration promotes platelet delamination and increased surface area, while subsequent aqueous exposure results in partial restacking and edgefocused dissolution. These observations suggest that cookeite reactivity is dominated by edgeplane processes rather than basalplane interactions. The integrated results provide new insights into the surface chemistry, hydration behavior, and dissolution mechanisms of cookeite, with direct implications for lithium recovery from clayhosted deposits.

PROSPECTING RAW CLAY MATERIALS FOR NUCLEAR WASTE REPOSITORY BUFFER APPLICATIONS

Derkowski, Arkadiusz *¹, Skiba, Michał², Kuligiewicz, Artur¹, Ciesielska, Zuzanna¹, Kowalik-Hyla, Mariola¹, Zięba, Adam¹, Rybka, Karolina¹, and Szczerba, Marek¹

¹ Institute of Geological Sciences, Polish Academy of Sciences, Krakow, Poland

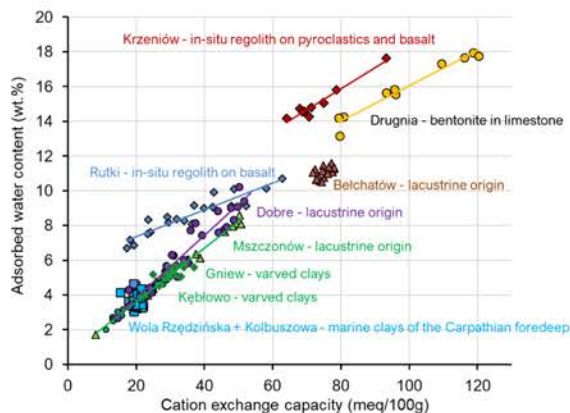
² Institute of Geological Sciences, Jagiellonian University, Krakow, Poland

*ndderkow@cyf-kr.edu.pl

Bentonites and other smectite-rich clay materials are planned for use as buffer materials in various designs of deep geological repository (DGR) for nuclear waste disposal allowing the wastes isolation for at least 10,000 years. The Polish nuclear energy program is a key element of Poland's energy independence and an important contribution to reducing industrial emissions. The aim of this project is to study deposits of potential buffer materials in Poland and to determine their material properties according to internationally accepted DGR criteria.

Here, we present the results of a geological survey of ten major Polish clay material deposits, assessing material quality and deposit heterogeneity in terms of mineral and chemical composition, adsorbed water content (H_2O_{ads}), cation exchange capacity (CEC), and the smectite layer charge (LC). The study matches various properties and compositions, presenting a reliable prediction of the clay quality, a deposit geological origin, and economic value.

Regardless the location, the origin of a deposit is clearly reflected by its mineral composition: in-situ clays developed on basaltic and pyroclastic regolith are rich in magnetite, nontronite, halloysite, and vermiculite. Marine-origin and varved clays are rich in carbonate minerals and kaolinite, whereas the non-varved lacustrine clays show abundance of goethite and kaolinite. Micaceous minerals contribute significantly to marine clays composition. H_2O_{ads} and CEC form linear relationships controlled primarily by smectite content, which serves as a diagnostic tool. The LC of smectitic minerals remains at 0.39-0.44 e^-/pfu for varved and marine clays, 0.49-0.53 e^-/pfu in other lacustrine clays, and $>0.55 e^-/pfu$ (including vermiculitic LC) in the regolith.



Only one clay deposit studied was a true bentonite formed by a distal sedimentation of fine rhyolitic ash on a limestone platform. The most likely the purest bentonite in the world, containing up to 99% of montmorillonite shows CEC nearly 120 meq/100g and with LC 0.53-0.56 e^-/pfu . The montmorillonite is contaminated by traces of mica, quartz, and rutile, which is indicated in trace elements trends. This material is proposed to serve as a new CMS reference material.

Acknowledgements: The project is financed by the Ministry of Science and Higher Education (Poland) under the "Science for Society II" Program

THE USE OF CATIONIC CLAY FOR SORPTION OF PER- AND POLY-FLUOROALKYL SUBSTANCES AND DESTRUCTION BY PHOTOREDUCTION

Liang Yanna*, Jiang Tao, Pervez Md. Nahid, Ilango Aswin Kumar

Department of Environmental and Sustainable Engineering, University at Albany, State University of New York, Albany, New York 12222, United States

*yliang3@albany.edu

Per- and polyfluoroalkyl substances (PFAS) are a class of synthetic compounds characterized by strong carbon-fluorine bonds that confer extreme chemical stability and resistance to degradation. To remove PFAS from water, a wide range of adsorptive materials have been reported, many of which, however, suffer from drawbacks, such as high cost, insufficiency to remove mixtures of PFAS, and unsuitability to be used in flow through systems, etc.

In this talk, we will introduce a suite of clay-based materials for capturing PFAS in water. Starting from Montmorillonite K10, we synthesized modified clay (MC) using cetyltrimethyl ammonium chloride (CTAC). The MC demonstrated nearly 100% of removal of short and long chain PFAS and a few PFAS precursors¹. Based on detailed characterizations, the mechanisms underlying the sorption were found to be a combined effect of hydrophobic and electroactive interactions. To enhance separation of MC from treated water, we fabricated magnetic MC (MMC), which showed much higher and faster PFAS removal compared to granular activated carbon (GAC) and powdered activated carbon (PAC)². The MMC also had complete removal of PFAS in river water regardless of impurities in that water. To regenerate PFAS-laden MMC, UV irradiation with reducing reagents led to >65% of defluorination³. The regenerated MMC was able to be reused for at least three cycles. In order to use MC in flow through systems, we further synthesized MC beads (MCB). When MCB were operated side by side with GAC in column tests, the MCB had higher bed volumes and reached breakthrough later than the GAC. In summary, the clay-based sorbents having different compositions are suitable for PFAS removal in batch and flow through systems. Their low cost, high efficiency, regenerability and reusability warrant their use in industry scales.

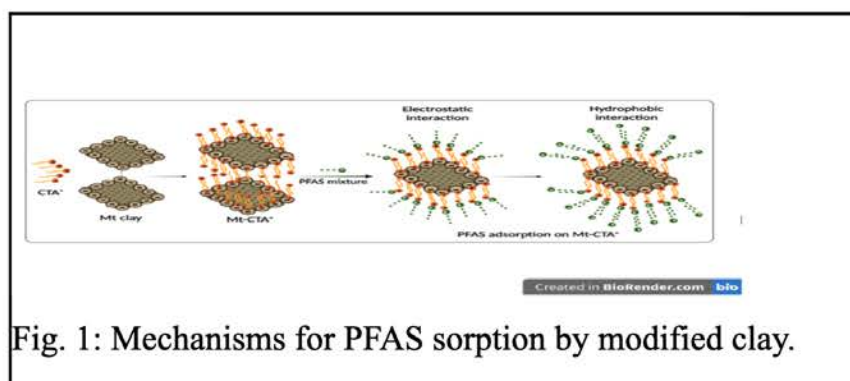


Fig. 1: Mechanisms for PFAS sorption by modified clay.

References cited:

- Jiang, T, Zhang, W, Ilango, A, Feldblyum, J, Wei Z, Efstathiadis, H, Yigit M, Liang. Y-N. 2023. ACS Advanced Engineering Materials. 1, 1, 394–407.
- Jiang, T., Pervez, N., Ilango, A., Ravi Y., Zhang, W., Feldblyum. J., Yigit, M., Efstathiadis, H., Liang. Y-N. 2024. Journal of Hazardous

Materials. 471, 134390.

3. Jiang, T., Pervez, N., Ilango, A., Liang, Y.-N., 2024. Journal of Water Process Engineering. 69, 106733.

A DEEP-LEARNING APPROACH FOR PHASE PICKING IN X-RAY POWDER DIFFRACTION ANALYSIS OF CLAY-BEARING MIXTURES

Chipman, Aaron J.^{*1}, Bickmore, Barry R.¹, Evans, Emily J.², Campbell, Branton J.³

¹Department of Geological Sciences, Brigham Young University, Provo, UT 84606, USA.

²Department of Mathematics, Brigham Young University, Provo, UT 84606, USA.

³Department of Physics and Astronomy, Brigham Young University, Provo, UT 84606, USA.

[*achip13@byu.edu](mailto:achip13@byu.edu)

When performing a quantitative mineralogical analysis on a complex sample, picking the phases to include in the analysis for quantification (Rietveld method, Reference Intensity Ratio (RIR) method) is the major source of error, and it depends largely on the experience (e.g., familiarity with X-Ray Powder Diffraction (XRPD) analysis, and geological background knowledge of things such as mineral prevalence and co-occurrence) of the analyst rather than the specific method or software used. This is not always straightforward for complex geological mixtures, especially when they include clay minerals. Clay XRPD patterns are strongly affected by things like particle size, solid solution, layer-rotational disorder, and stacking disorder among layers of different types. We have successfully tested a deep learning architecture for phase picking based on a database of simulated XRPD patterns for mixtures involving geologically plausible combinations of 2-15 phases selected from a set of 66 minerals, which did not include disordered clays. Now we are creating software to generate another database that does include disordered clays while running an open-source Rietveld refinement program, BGMN, in the background. We will generate peak shape and disorder parameters based on probability distributions obtained by fitting empirical XRPD patterns, taking into account correlation between the parameters, randomly vary the instrumental geometry (since BGMN does first-principles Rietveld calculations), and add random noise. We will also be using a large database of minerals occurring at different locations to guide the selection of geologically relevant phase combinations and will be randomly choosing the proportions of the phases chosen. Once the database has been constructed, we will begin testing various machine-learning and deep-learning strategies for predicting the presence of different phases based on XRPD patterns.

BELCHATÓW BENTONITE DEPOSIT: A UNIQUE CASE WITH DISTINCT PROPERTIES

Skiba, Michał*¹, Derkowski, Arkadiusz ², Kuligiewicz, Artur², Ciesielska, Zuzanna², Kowalik-Hyla, Mariola², Zięba, Adam², Rybka, Karolina², and Szczerba, Marek²

¹ Institute of Geological Sciences, Jagiellonian University, Krakow, Poland

² Institute of Geological Sciences, Polish Academy of Sciences, Krakow, Poland

*michal.skiba@uj.edu.pl

The Bełchatow bentonite deposit is one of the few yet the largest economic accumulations of smectitic clays in Poland. Its mineralogy has been studied since the 70s; however, detailed data on the deposit's heterogeneity and properties are lacking in the available studies. The present study aimed to perform detailed mineralogical and geochemical analyses of the bentonite in terms of its potential use as a buffering material for long-term radioactive waste storage, as well as to evaluate the heterogeneity of the deposit available for exploitation. Another objective of the study was to assess the origin of the deposit.

The collected bulk samples were analyzed for mineral composition (using XRD), chemical composition (using XRF, ICP-OES, and ICP-MS methods), cation exchange capacity (using the Co-hexammine method), adsorbed water content, and layer charge (using the OD method). Clay fractions separated from selected samples were also analyzed for mineral and chemical composition. The location of the layer charge in smectites was estimated based on the Greene-Kelly (1952) test.

The studied bulk samples showed a quite uniform mineral composition, dominated by smectite, quartz, and kaolinite, with traces of anatase and illite. Also, all other chemical properties of the studied samples turned out to be uniform within the deposit. Smectite present in the studied samples showed at least partly its Fe-beidellitic character, having the layer charge between 0.47 and 0.52 per T_4O_{10} .

The mineral composition, the nature of the smectite, and the homogeneity of the studied samples suggested that the deposit was formed through the accumulation of fine soil-derived products of weathering within an aquatic (likely fresh-water) environment.

Literature

Greene-Kelly, R (1952) A Test for Montmorillonite. *Nature* 170, 1130 – 1131.

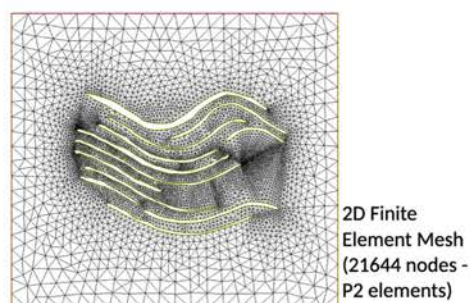
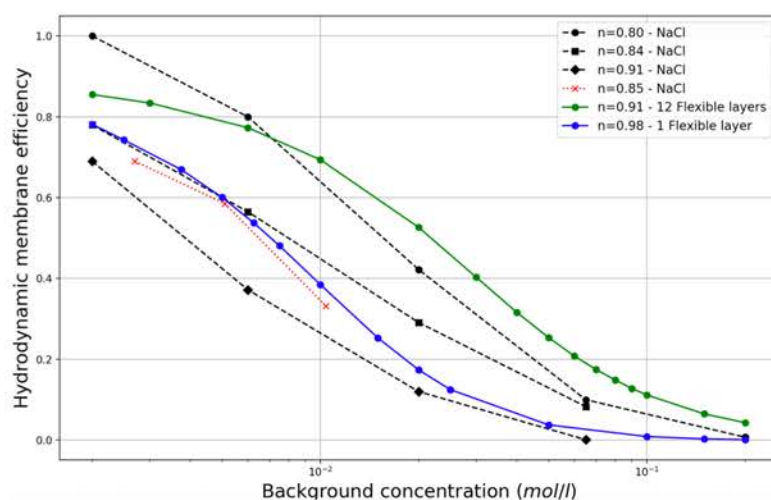
MEMBRANE EFFICIENCY OF MONTMORILLONITE SUSPENSIONS

Bouchelaghem, Fatiha *¹

¹Institut Jean le Rond d'Alembert CNRS UMR 7190, Sorbonne Université, Paris, 75005, France.

*fatiha.bouchelaghem@sorbonne-universite.fr

Smectite suspensions consist in a variable number of elongated and flexible montmorillonite layers with a permanent negative surface charge, surrounded by an electrolyte solution. In complementarity with existing approaches at the molecular or macroscopic scales, we use real microstructures to investigate the role of the bending and stacking of montmorillonite layers in stationary ionic transport when a moderate concentration gradient is applied at the boundaries of the clay membrane. The emphasis is laid on anisotropy effects, anion exclusion resulting from electrostatic repulsion, and overall membrane efficiency at an intermediate scale of description (i.e. for pore diameters greater than 3-5 nm). The coupled solute transport and electrostatic phenomena at the scale of the interlayer pores are classically described by the Poisson-Boltzmann equation for the electric potential ψ , the Nernst-Planck equation for the ionic species concentrations c^+ and c^- . Stokes equations with coupling terms depending on the ionic concentrations and electric potential are employed to describe the fluid motion. The local problem is then rigorously upscaled using the Homogenization of Porous Media approach in order to characterize the overall membrane behavior. This approach leads to a series of uncoupled and weakly coupled problems, which allows cost-effective numerical computations. We obtain three series of problems, solved using the Finite Element Method: the first series allows to determine the electric potential gradient in the vicinity of the montmorillonite layers' surface and the induced or external electric potential related to the imposed concentration gradient. The second series allows to compute the ionic concentrations and the effective diffusion tensors. Finally, the third series of problems leads to the determination of the fluid velocity field \mathbf{v} , the hydrostatic pressure gradient, the membrane potential and the membrane efficiency. To assess the capabilities of the model, quantitative comparisons are made with existing electro-osmosis experiments in electrochemical cells, and a particular attention is given to the anisotropy of the membrane efficiency at the mesoscopic scale.



Hydrodynamic membrane efficiency vs background electrolyte concentration. Confrontation with experimental data from (Kemper and Rollins, 1966) and (Dominijanni et al., 2011).

INTEGRATED MICRO-TO-ATOMIC SCALE CHARACTERIZATION OF COMPLEX PHYLLOSILICATES FROM THE LONG VALLEY RHYOLITE: A MULTI-TECHNIQUE APPROACH

Jiaxin XI^{*1}, Yiping YANG¹, and Huifang XU²

¹ State Key Laboratory of Deep Earth Processes and Resources, Guangzhou Institute of Geochemistry, Chinese Academy of Sciences, Guangzhou 510640, P.R. China

² Department of Geoscience, University of Wisconsin-Madison, Madison, Wisconsin 53706, USA

*xijiaxin@gig.ac.cn

Biotite is a common rock-forming mineral in igneous rocks and its polytypism has been widely utilized to discern crystallization conditions. However, accurately deciphering these records requires advanced techniques capable of revealing the atomic arrangement and equilibrium or metastable nature of various mica structures, especially long-period/complex polytypes. Here we investigate biotite phenocrysts and their alteration products in rhyolite from the Long Valley Caldera, California, via integrated, multi-technique approaches. By combining micro X-ray diffraction (μ XRD) and in-situ Raman spectroscopy on thin sections, we mapped polytype distribution and structural order, revealing distinct core-rim zoning with ordered $2M_1$ cores and disordered rims. Major and trace element profiles obtained by electron probe microanalysis (EPMA) and laser ablation inductively coupled plasma mass spectrometry (LA-ICP-MS) link these structural variations to changes in crystallization environments. At the (sub-)atomic scale, high-angle annular dark-field (HAADF)-STEM imaging resolves complex and long-period polytypes and reveals a previously unreported twin structure in berthierine. Electron energy loss spectroscopy (EELS) measurements of $\text{Fe}^{3+}/\Sigma\text{Fe}$ ratios help distinguish different redox conditions during crystallization and subsequent alteration. The coexistence of multiple polytypes suggests nucleation under non-equilibrium conditions, while screw dislocations observed throughout the biotite domains indicate that spiral growth may play a key role in forming long-period polytypes. These multiscale observations point to a complex crystallization history and suggest that non-classical, particle-attachment-dominated growth mechanisms may be involved in forming complex polytypes. Those integrated analytical approaches provide a framework for investigating phyllosilicate crystallization, mineral-fluid reactions, and non-equilibrium processes in magmatic systems.

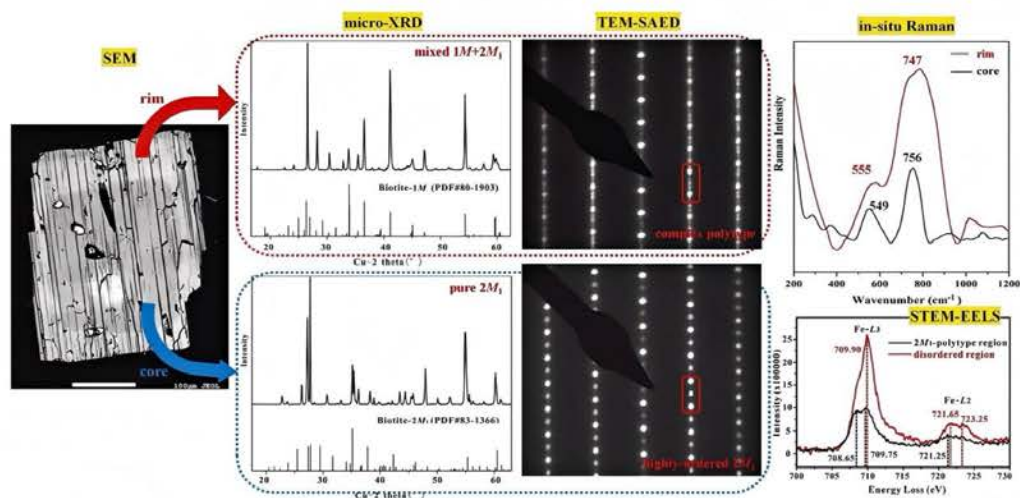


Figure 1. The combination of SEM, micro-XRD, in-situ Raman spectra, TEM-SAED, and STEM-EELS to reveal the structural and Fe-valence state zoning of biotite in Long valley.

COMPARATIVE MINERALOGICAL CHARACTERIZATION OF ASIAN BENTONITES FOR POTENTIAL ENGINEERED CLAY BARRIER APPLICATIONS

Chuang, Yi-Fang* and Ya-Ting, Chang

¹Department of Chemical Engineering, National Atomic Research Institute, Taoyuan, Taiwan.

*yifang@nari.org.tw

The geological disposal of high-level radioactive waste requires robust engineered barrier systems, in which compacted bentonite is widely used as the primary buffer and sealing material. Among various bentonites, MX-80 from the United States has commonly been adopted as a reference material due to its high montmorillonite content and favorable swelling properties. In recent years, several repository programs have increasingly explored the use of locally available clay resources in order to improve material availability and long-term supply reliability.

Given the limited domestic bentonite resources in Taiwan, this study evaluates five Asian bentonites—Kunigel V1 (Japan), WRK (Republic of Korea), GTC4 (India), API (Indonesia), and THR (Indonesia)—as potential alternative materials for future repository construction. MX-80 bentonite was included as a reference material for comparison.

Mineralogical compositions were determined using X-ray diffraction (XRD) with semi-quantitative analysis of montmorillonite and accessory minerals. The results indicate that the montmorillonite content of the investigated Asian bentonites ranges from approximately 55% to 81%. The Indonesian API bentonite shows a relatively high montmorillonite content (75–81%), exceeding that of the MX-80 reference material (65–72%). Distinct mineralogical characteristics were observed for each bentonite source. Kunigel V1 is characterized by relatively high quartz (19–26%) and zeolite (8–16%) contents, while the Korean WRK bentonite contains a significant fraction of cristobalite (15–20%).

Additional variations in accessory minerals were observed among the Indian and Indonesian bentonites. THR contains notable kaolinite (15–20%), whereas GTC4 is characterized by the presence of iron-bearing minerals including goethite, hematite, and maghemite, together with anatase. In contrast, MX-80 contains mica (7–12%) and gypsum (1–3%), which are less prominent in the investigated Asian bentonites. These mineralogical differences, particularly the presence of zeolites, cristobalite, and various iron oxides, may influence the hydro-mechanical and geochemical behavior of bentonite barriers. This study provides mineralogical data useful for screening potential alternative bentonite sources for engineered barrier applications in the Asian region.

OPTIMIZING BENTONITE CONTENTS IN MORAINE FOR LOW-PERMEABILITY OXYGEN BARRIERS IN MINE WASTE COVER SYSTEMS

Nguyen, Trung*¹, Duong, Chau-Anh¹, and Holmboe, Michael¹

¹Department of Chemistry, Umeå University, 901 87, Umeå, Sweden.

* trung.nguyen@umu.se

Most ore extracted during mining ultimately end up as waste rocks and mine tailings, which may contain acid-generating sulfides (*e.g.*, pyrite) capable of producing acid mine drainage (AMD). Europe's largest Cu mine (Aitik, northern Sweden) covers 12 km², the majority of which is occupied by extensive tailings deposits containing up to 1.5 wt.% sulfides [1]. After separation from inert waste, the potential acid-generating fraction (PAG) can be enriched to 35 wt.% sulfur [2]. Upon mine closure, these PAG wastes require engineered covers with low hydraulic conductivity ($k = 10^{-9}$ m/s) to limit oxygen ingress by using bentonite-amended moraine. However, the bentonite demand for the closure of this mine represents a substantial economic and material burden, consuming 20-30 % of its global annual production and costing approx. \$250M. Therefore, optimizing bentonite used in cover systems is necessary to reduce mine closure costs and enable sustainable mine waste management.

Here, we evaluated how bentonite contents (0 to 5 wt.%) and mixing strategy control the hydraulic performance of natural moraine-based oxygen barriers. Two preparation methods were compared: (i) conventional dry mixing and (ii) pre-wetted-clay mixing, where bentonite is overhydrated prior to blending. By doing this, we target to the lowest permeability reaching $k = 10^{-9}$ m/s with lowest bentonite contents. Hydraulic conductivity was measured by a KSAT permeability meter, and mineralogical and surface properties were characterized by X-ray diffraction and Nitrogen cryosorption according to Brunauer-Emmett-Teller (BET) to link physicochemical properties with barrier performance.

The results show hydraulic conductivity decreases systematically with increasing bentonite contents. In dry-mixed systems, permeability decreased exponentially from 10^{-4} m/s to $\sim 2 \times 10^{-7}$ m/s across 0-5 wt.% bentonite. In contrast, pre-wetted-clay mixing enhanced barrier performance, reducing hydraulic conductivity to $\sim 7 \times 10^{-6}$ m/s at only 2 wt.% of bentonite, with minimal variation at higher contents. This behavior indicates that pre-hydration promotes osmotic swelling and completed clay layer separation prior mixing, enabling more effective pore sealing within the moraine matrix.

These results showed that mixing strategy is a key control on barrier efficiency. Pre-wetted-clay mixing method provides a simple and scalable approach to achieve low permeability with reduced bentonite demand, offering a more sustainable design for oxygen barriers in mine closure systems.

[1] Forsberg, L., Reclamation of copper mine tailings using sewage sludge. 2008.

[2] Lindvall M. 2005. Strategies for remediation of very large deposits of mine waste; the Aitik mine, Northern Sweden. Licentiate Thesis. Department of Chemical Engineering and Geosciences, Division of Applied Geology, Luleå University of Technology.

THREE-DIMENSIONAL ELECTRON DIFFRACTION: A REVOLUTIONARY TECHNIQUE FOR RAPID AND NON-DESTRUCTIVE IDENTIFICATION OF CLAY MINERAL STRUCTURES

Yiping Yang^{*1}, Yuhuan Yuan¹, Jiaxin Xi¹, Haiyang Xian¹, Hongping He¹ and Huifang Xu²

¹ State Key Laboratory of Deep Earth Processes and Resources, Guangzhou Institute of Geochemistry, Chinese Academy of Sciences, Guangzhou 510640, P.R. China;

² Department of Geoscience, University of Wisconsin-Madison, Madison, Wisconsin 53706, USA.

*yangyiping@gig.ac.cn

Clay minerals, as fine-grained components widely distributed on the Earth's surface, typically occur as nanoscale particles intimately associated with multiple mineral phases. The complex crystal structure analysis of these minerals has long relied on tedious purification and oriented sample preparation processes. However, traditional single-crystal X-ray diffraction techniques have stringent requirements regarding sample size and crystal perfection, making direct application to such finely intergrown mineral assemblages difficult. Meanwhile, powder diffraction faces challenges such as peak overlap in multiphase mixtures and ambiguities in phase identification, and the purification process is both time-consuming and labor-intensive, potentially disrupting the original interlayer structural information of the minerals.

The emergence of three-dimensional electron diffraction (3DED) technology has fundamentally broken through this bottleneck. It utilizes a nanometer-sized electron beam, focused within a transmission electron microscope, to directly target individual clay particles embedded within a sample for data collection. This technique enables rapid, non-destructive acquisition of accurate unit cell parameters in minutes without requiring special sample preparation, achieving "in-situ" and precise identification of complex mineral assemblages, and even allowing differentiation between structurally similar mineral polytypes. This technological advantage is particularly critical for special research tasks involving extremely limited and scientifically interesting samples.

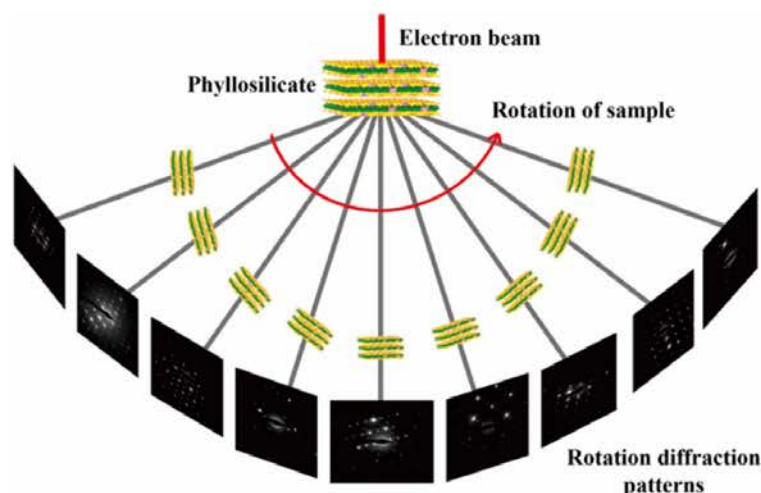


Figure 1: Schematic of the data collection process of 3DED.

CLAYCG: TOWARDS A COARSE-GRAINED MODEL OF HYDRATED CLAY MINERALS

Bourg, Ian C. *¹, Shen, Xinyi¹, and Zheng, Xiaojin¹

¹Department of Civil and Environmental Engineering, Princeton University, Princeton, NJ 08544, USA.

*bourg@princeton.edu

Several key properties of engineered clay barriers used in the isolation of high-level radioactive waste (including swelling pressure, rheology, and permeability) emerge from *nanoscale* interactions between primary clay particles, counterions, and water molecules but are strongly modulated by the *mesoscale* structure and energetics of clay assemblages containing thousands of clay particles. This simultaneous importance of a wide range of lengths scales (from Angstroms to tens of micrometers) presents a significant challenge in efforts to use atomistic simulations (e.g., molecular dynamics or density functional theory simulations) to predict the fundamental properties of compacted clay. Here, we present our recent progress towards the development of a coarse-grained model parameterized to reproduce the structure and energetics of smectite clay assemblages predicted using the well-known ClayFF all-atom molecular dynamics simulation model. This new coarse-grained model enables the simulation of hydrated clay assemblages with accuracy approaching that of MD simulation predictions, at a fraction of the computational cost.

ACCURATE IDENTIFICATION OF ELEMENT OCCUPANCY WITHIN SINGLE LAYERS OF MG–NI SAPONITE BY COUPLING FTIR AND HAADF-STEM-EDXS

Chaoqun ZHANG*¹, Fabien BARON², Alain DECARREAU¹, Hongping HE³ and Sabine PETIT²

¹Key Laboratory of Earth and Planetary Physics, Institute of Geology and Geophysics, Chinese Academy of Sciences, Beijing, China.

²CNRS, Université de Poitiers, Institut de Chimie des Milieux et Matériaux de Poitiers-IC2MP, 86022 Poitiers.

³CAS Key Laboratory of Mineralogy and Metallogeny/Guangdong Provincial Key Laboratory of Mineral Physics and Materials, Guangzhou Institute of Geochemistry, Chinese Academy of Sciences, 510640 Guangzhou, China.

*zhangchaoqun@mail.iggcas.ac.cn

Accurate identification of cation occupancy within individual clay mineral layers remains a major challenge because most conventional characterization techniques provide only bulk-averaged structural information, while nanoscale imaging alone is often insufficient to resolve local crystal-chemical environments. In this study, we propose a correlative analytical approach combining Fourier-transform infrared spectroscopy (FTIR) and high-angle annular dark-field scanning transmission electron microscopy coupled with energy-dispersive X-ray spectroscopy (HAADF-STEM-EDXS) to investigate element occupancy in synthetic Mg–Ni saponite. Mg–Ni saponite provides an ideal model system because Mg and Ni can substitute within the trioctahedral octahedral sheet, while their distribution at the single-layer scale is difficult to constrain using a single technique. FTIR is sensitive to the local OH vibrational environments and therefore provides statistical information on short-range octahedral cation configurations, whereas HAADF-STEM-EDXS offers direct nanoscale observation of elemental distribution within individual particles and layers. By integrating these two approaches, it becomes possible to bridge bulk-average crystal-chemical signatures with spatially resolved compositional information, thereby improving the reliability of cation occupancy identification in clay minerals. This combined strategy provides a powerful methodological framework for studying cation distribution, local structural heterogeneity, and crystal-chemical organization in phyllosilicates, and may be broadly applicable to other complex clay mineral systems.

References

Zhang, C. Q., He, H. P., Petit, S., Baron, F., Tao, Q., Grégoire, B., Zhu, J. X., Yang, Y. P., Ji, S. C., & Li, S. Y. (2021). The evolution of saponite: An experimental study based on crystal chemistry and crystal growth. *American Mineralogist*, 106, 909–921.

Zhang, C., Decarreau, A., Blanc, P., Baron, F., Yuan, Y., Tao, Q., Grégoire, B., Zhu, J., He, H., & Petit, S. (2024). Kinetics of Mg–Ni saponite crystallization from precursor mixtures. *Clays and Clay Minerals*, 72, e16, 1–10.

INCOMMENSURATELY MODULATED STRUCTURE OF GREENALITE WITH NON-STOICHIOMETRY: Z-CONTRAST IMAGING AND iDPC IMAGING STUDY

Xu, Huifang ^{*1}, and Yiping Yang ²

¹Department of Geoscience, University of Wisconsin-Madison, Madison, Wisconsin 53706, USA

² Guangzhou Institute of Geochemistry, Chinese Academy of Sciences, Guangzhou, Guangdong, 510640, PRC

*hfxu@geology.wisc.edu

Greenalite was first discovered and described by C. K. Leith when he studied the Biwabik Iron Formation in the Mesabi Range, Northeastern Minnesota. Greenalite commonly occurs as granules, ooids, laminated layers, and disseminated aggregates in chert / jasper bands in Precambrian iron formations. Greenalite contains a significant number of vacancies in the octahedral sites and additional oxygen (~ 9.5 oxygen per 2Si) compared to serpentine (9 oxygen per 2 Si). This additional oxygen is associated with non-connected tetrahedra of the tetrahedral sheet in the disordered inter-island regions. The general formula for greenalite for comparison to serpentine can be written as $\text{Fe}^{2+}_{(3-x-y-z)}\text{Fe}^{3+}_x\text{Mg}_y\text{Si}_z\text{O}_{(3.5+x-2z)}(\text{OH})_{(6-x+2z)}$. In-plane disorder in the tetrahedral sheet results in an average modulation period and diffuse satellite reflections around ($hk0$) reflections with $k \neq 3n$. By contrast, long-range periodicity in the octahedral sheet through vacancy ordering produces sharp satellite spots around ($hk0$) with $k = 3n$.

Z-contrast imaging shows ordered modulation in the octahedral sheet, which produce sharp satellite spots around ($hk0$) with $k = 3n$. However, the features in the tetrahedral sheets are very weak and fuzzy, which indicates that the tetrahedra along [100] zone-axis (the beam direction) are not aligned / ordered. However, iDPC (integrated differential phase contrast) images provide good contrast of oxygen atoms and changing / curving of the tetrahedral sheet. The non-periodic packing of the tetrahedra resulted in very diffuse satellite reflections around ($hk0$) reflections with $k \neq 3n$. A new structure model for greenalite can be obtained based iDPC images.

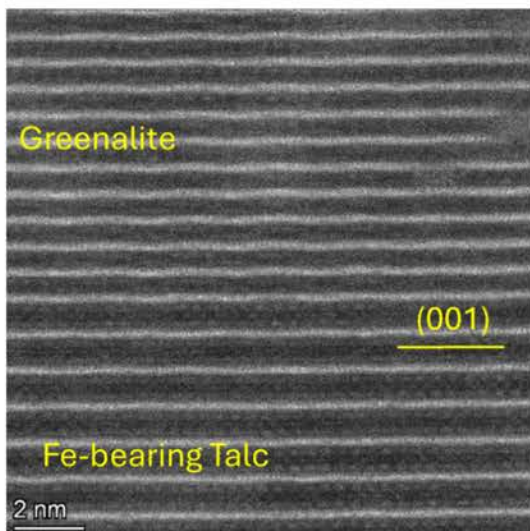


Figure 1: Z-contrast image along [100] zone-axis showing modulated greenalite layers with 7.3 Å periodicity (up part) and Fe-bearing talc layers with 9.3 Å periodicity (lower part). They keep the same orientation. Bright layers are octahedral sheet (Fe).

FROM EARTH TO MARS: A FRAMEWORK FOR INTERPRETING MARTIAN CLAY MINERALS AND ANCIENT MARS

Velbel, Michael A.*¹

¹Department of Earth and Environmental Sciences, Michigan State University, East Lansing, MI 48824-1115, USA.

*velbel@msu.edu

Over the past 50 years, Mars landers and rovers from *Viking* through *Perseverance* have carried increasingly capable instruments for imaging and imaging spectroscopy, and elemental analysis, and *Curiosity* carries an X-ray diffractometer. Orbiter and lander/rover studies of Mars' surface [1] and studies of Mars meteorites [2,3] indicate that abundant and widespread clay and other phyllosilicate minerals formed early in the geologic history of Mars. On Earth, these minerals commonly form by mineral-water interactions. The origin and distribution of clay minerals in surface materials is studied in the context of regolith and Critical Zone geoscience [4-7]. Such research investigates the geological, mineralogical, geochemical, and geomorphic factors that control mineral alterations at the Earth's surface and the migration of chemical elements through the landscape, including the rates, mechanisms, and timescales of mineral-water interactions during rock and mineral weathering in natural systems. Studies of active weathering processes include aqueous geochemistry data (solute concentration and flux) from small watersheds [7-9].

On Mars, the aqueous solutions left the regolith and near-surface rock long ago, and – as in many situations of interest on Earth – it is from the surviving solids that the former processes must be inferred [4-6]. Although reactant and product solutions and volatiles may no longer exist, considerable insight into their nature, abundance, and properties can be achieved by examining the reactant and product minerals.

Carefully selected and well-studied naturally weathered regolith occurrences on Earth can serve as analogs for specific weathered materials on Mars. This contribution reviews several examples of approaches to terrestrial weathering that have been and are being used by Mars mission scientists to support inferences about low-temperature surface and near-surface weathering on Mars from the study of the clay-mineral products of mineral-water interactions and their host materials, as characterized by Mars mission analyses.

- [1] Cuadros J. (ed.) (2025) *Clay on Mars*, Developments in Clay Science no. 12, Elsevier, 527 p.
- [2] Velbel M. A. (2012) In Grotzinger, J., and Milliken, R. (eds.) *Sedimentary Geology of Mars*, SEPM – Society for Sedimentary Geology Special Publication 102, p. 97-117.
- [3] Velbel M. A. (2025) *Clays in Martian meteorites*. In Cuadros J. (ed.) *Clays on Mars*, p. 359-398
- [4] Taylor G. and Eggleton R. A. (2001) *Regolith Geology and Geomorphology*, Wiley, 375 p.
- [5] Nahon D. B. (1991) *Introduction to the Petrology of Soils and Chemical Weathering*, Wiley 313 p
- [6] Delvigne J. (1998) *Canadian Mineralogist Special Publication 3*, 495 p.
- [7] Schroeder P. A. (2018) *Clays in the Critical Zone*, Cambridge Univ. Press, 246 p.
- [8] Velbel M. A. (1985) *American Journal of Science*, v. 285, p. 904-930.
- [9] Berner E. K. and Berner R. A. (2012) *Global Environment: Water, Air, and Geochemical Cycles* (2nd ed.), Princeton Univ. Press, 376 p.

OCCURRENCES AND DISTRIBUTIONS OF THE RARE-EARTH ELEMENTS IN THE GEORGIA KAOLINS AND ENCLOSING SANDS, UPPER COASTAL PLAIN, GEORGIA.

Elliott, W. Crawford*

Department of Geosciences, Georgia State University, Atlanta, GA 30302-3965, USA.

[*wcelliott@gsu.edu](mailto:wcelliott@gsu.edu)

The rare earth elements (REE: Sc, Y, La-Lu) are critical metals needed for our modern technologies. The Georgia Kaolin ore deposits comprise relatively novel REE resources given the highly weathered kaolin ore and the insolubility of the REE. Significant concentrations of the REE have been found in the clay fractions, the discarded mine waste (grit) of the mined kaolin ore, Piedmont regolith adjacent to the Coastal Plain, and the sand formations enclosing the mined kaolins.^{1,2} The REE are present as sorbed species on kaolinite.³ The REE are also present within phosphate minerals (monazite, xenotime), zircon, and hematite found in trace amounts in the kaolin ore, mine waste, and enclosing sands. The whole rock total REE concentrations (< 100 ppm - < 600 ppm) and the presence of ion-sorbed REE (< 25% of the total REE) vary considerably in kaolin rocks in the Georgia Coastal Plain. The highest total REE concentrations were found at specific horizons in these sections (e.g. contact between bauxite and kaolin, lignitic kaolin) and attributed to the presence of REE minerals such as monazite, xenotime, and zircon. Higher percentages of leaching efficiencies (ion-sorbed REE) were found at base of bauxite layer within the larger kaolin lens, lignite-rich kaolin, a kaolin layer above the bauxite, and at the contact between kaolin and an Fe-oxide rich basal kaolin in these sections.⁴⁻⁶ Differences in porosity, permeability, and overall mineralogy hypothetically cause REE ions to aggregate at these contacts.

Heavy mineral subfractions of kaolin mine waste are enriched in the heavy rare earth elements (Y, Tb-Lu) by 50-150 times relative to their concentrations in Upper Continental Crust (UCC).⁷ Heavy mineral stringers in sand units contain considerable concentrations of REE (46,000 ppm) that are enriched in the Light REE (LREE: La-Eu).² Heavy mineral subfractions of sand mine tailings from Cretaceous-Paleocene sands enclosing kaolin ore in places contain high REE concentrations (9 wt.% REO). These heavy subfractions are enriched in both LREE and HREE 400 times compared to UCC.⁸ All told, the occurrences of the novel REE resources are amenable to being coproduced from existing kaolin and sand mining operations in the Georgia Upper Coastal Plain. Several knowledge gaps need to be overcome to coproduce these REE and bring them to market. The gaps include separation of clay from mine waste, and the development of new extractive techniques.

1. Cheshire, M.C. *et al.* 2018, *ACS Earth Space* **2**.
2. Boxleiter, A., Elliott, W.C., 2023, *Clays Clay Min.*, **71**, 274-308.
3. Boxleiter A., *et al.*, 2026, *Chem Geol.*, **707**, 123312.
4. Boxleiter A., *et al.*, 2024, *Chem Geol.*, **660**, 212551.
5. Ashcraft, J., *et al.*, 2025, *Geol. Soc Am Abstract, Programs*, **57** (2).
6. Hooper, G. *et al.*, 2026, *Geol. Soc Am Abstract, Programs*, **58**.
7. Elliott, W.C., *et al.*, 2018, *Clays Clay Min*, **66**, 245-260.
8. Al-Zehhawi, M., 2023, *Thesis*, Georgia State University.

AN OVERVIEW OF CLAY-RICH MUDBALLS IN OUR SOLAR SYSTEM

Bose, Maitrayee*¹, Williams, L.¹, and Castillo-Rogez, J.²

¹School of Earth and Space Exploration, Arizona State University, Tempe, AZ, USA.

²Jet Propulsion Laboratory, California Institute of Technology, CA, 91109.

*Maitrayee.Bose@asu.edu

Clay formation across Mars, asteroids like Ryugu and Bennu, and the dwarf planet Ceres reveal a shared history of aqueous alteration, where liquid water reacted with primary silicates to create new mineralogical records. While these bodies share fundamental similarities, their differing sizes, volatile inventories, and geological histories have produced distinct clay assemblages.

The Uniqueness of Ceres. Ceres' primary distinction is the ubiquitous presence of ammoniated phyllosilicates (NH₄-clays), which has been found on several other large asteroids but not on Mars. The presence of ammonia in Ceres' clays suggests the dwarf planet either formed in the outer solar system or accreted material that drifted inward¹. Ceres' large size facilitated internal hydrothermal alteration and partial differentiation, leading to a globally homogeneous surface of Mg-serpentine and NH₄-clays, occasionally punctuated by localized "bright spots" of sodium carbonates, ammonium chloride, and Al-rich clays.

Distinctive Features of Mars. Mars is unique for its widespread Fe/Mg smectites found in ancient Noachian terrains, occurring in over 75% of clay-bearing sites. A key difference on Mars is a distinctive stratigraphic sequence where Al-rich clays (like kaolinite) consistently overlie Fe/Mg clays². This suggests a "top-down" alteration process where transient surface water leached mobile ions from the upper layers, a process more akin to terrestrial soil formation than the closed-system alteration seen on smaller asteroids. Additionally, Mars features high-temperature phases like prehnite and chlorite excavated from depth, indicating a complex subsurface hydrothermal history.

Asteroids Bennu and Ryugu. Clays on asteroids Bennu and Ryugu are dominated by Mg-rich serpentine and saponite³. Unlike Mars, these bodies represent relatively low-temperature hydrothermal systems (~25–37 °C) where fluids evolved from neutral to highly alkaline (pH 9–10). The lack of primary anhydrous silicates (like chondrules) in certain samples indicates that the water-rock reaction was nearly complete.

Similarities in Clay Composition and Different Origins. The most significant similarity is that all these bodies host smectite-group minerals, particularly Fe- and Mg-rich varieties like nontronite and saponite. These clays formed early in solar system history (within the first billion years) through the interaction of liquid water with basaltic or anhydrous minerals. On asteroids and Ceres, this water was sourced from the melting of accreted primordial ice, while on Mars, it involved surface weathering and subsurface hydrothermal systems. Both Mars and Ceres show evidence of clays formed or exposed by impact-induced heating, which created transient melt reservoirs. Ceres and asteroids experienced internal hydrothermal circulation driven by radiogenic heat. Mars likely hosts extensive subsurface hydrothermal systems that remained active during its early history.

[1] Kurokawa et al. (2021) <https://doi.org/10.1029/2021AV000568>. [2] Ehlmann et al. (2011) <https://doi.org/10.1038/nature10582>. [3] Viennet et al. (2022) <https://doi.org/10.7185/geochemlet.2307>.

ATOMIPY: A PYTHON FRAMEWORK AND TOPOLOGY TOOL FOR BUILDING MULTICOMPONENT CLAY SYSTEMS FOR MOLECULAR SIMULATIONS

Holmboe, Michael*¹, Lavauzelle, Nathan¹, Rogers, E. Swai¹

¹Department of Chemistry, Umeå University, 901 87, Umeå, Sweden.

*michael.holmboe@umu.se

Atomistic molecular dynamics (Monte-Carlo and MD) simulations are increasingly used to study the structure and behavior of clay minerals and geochemical systems. However, constructing physically sound multicomponent models and generating consistent input and topology files has historically been challenging, particularly for newcomers in this field. As a result, atomistic simulations in the clay community have often remained limited to specialists developing their own tools, contributing to a perception of the field as complex and inaccessible.

Recent years advances in general purpose and/or domain specific tools such as CHARMM-GUI, ClayCode, and the MATLAB-based atom library,¹⁻³ combined with AI-assisted vibe coding, are lowering these barriers. Here, we present *atomipy*,⁴ a Python-based framework that modernizes and extends the original MATLAB atom library, with the goal of making simulation setup more accessible and reproducible, even for users and undergraduate students with limited programming experience.

Overall, *atomipy* provides both a flexible programmatic and GUI environment for constructing, and manipulating atomistic systems, with emphasis on layered and anisotropic geochemical materials. Users can build mineral slabs, replicate systems, introduce interlayer species, add ions, and solvate structures while maintaining periodic boundary conditions and topological consistency. The framework supports handling of XYZ, PDB, GRO and CIF files, and automated generation of topology files for GROMACS, LAMMPS, NAMD2, and CP2K, and is compatible with established forcefields such as CLAYFF,⁵ as well as the newer MINFF forcefield.⁶

Apart from the Python programmatic library, a key component is the *atomipy* topology server (www.atomipy.io), which offers a browser-based interface for generating simulation-ready systems, including a visual Multicomponent System Builder, enabling users to assemble workflows through an intuitive interface and export directly to multiple formats.

Compared to existing topology tools, *atomipy* emphasizes a general, nearest-neighbor-based and extensible approach, supporting both curated unit cell libraries and user-defined structures for building complex multicomponent systems. Integration with the MINFF forcefield, which introduces angular constraints for improved structural fidelity, further enhances the platform.

References:

- [1] Choi, Y.K., et al., J. Chem. Theory Comput. 2022, 18, 479–493.
- [2] Pollak, H., Degiacomi, M.T., Erastova, V. Chem. Theory Comput. 2024, 20, 9606–9617.
- [3] Holmboe, M., Clays and Clay Minerals., 67(5), 419–426, 2019.
- [4] Holmboe, ATOMIPY repository, web: github.com/mholmboe/atomipy
- [5] Cygan, Liang and Kalinichev. J. Phys. Chem. B 2004, 108, 1255–1266.
- [6] Holmboe, MINFF repository, web: github.com/mholmboe/minff

A REVIEW OF O-H STABLE ISOTOPE METHODS FOR IMPROVED ESTIMATION OF TEMPERATURE USING PHYLLOSILICATES

McIntosh, Julia A. ^{1*}, Andrzejewski, Kate ², Gulbranson, Erik L. ³, Ibarra, Daniel ^{4,5}

¹ U.S. Geological Survey, Denver, CO 80225, USA

² Kansas Geological Survey, Lawrence, KS 66047, USA

³ Environment, Geography, and Earth Sciences, Gustavus Adolphus College, Saint Peter, MN 56082, USA

⁴ Earth, Environmental and Planetary Sciences, Brown University, Providence, RI 02912, USA

⁵ Institute at Brown for Environment and Society, Brown University, Providence, RI 02912, USA

*jmcintosh@usgs.gov

Fossilized soils, or paleosols, contain soil-formed phyllosilicates whose stable isotopic compositions may be used to calculate paleotemperature and thus reconstruct ancient terrestrial environments. Though paleosols are common in the geologic record, the use of phyllosilicates as paleotemperature proxies is limited in the literature owing to difficulties with selecting optimal paleosols, isolation from non-clay minerals and organic materials, mixtures of phyllosilicates in natural samples, wide variations of chemical compositions for phyllosilicates, and limited to undefined equilibrium fractionation factors between phyllosilicates and water. Here, we address some of these challenges by examining and comparing methods used for sample selection, conventional and developing methods for O and H isotopic analyses, and determination of phyllosilicate and water equilibrium fractionation factors.

We find that careful consideration must first be given to sample selection by targeting mature paleosols; sampling >30 cm from the top of the paleosol; sampling multiple times from each horizon; and preferentially selecting samples with less complex clay mixtures. Once selected, samples must be screened and pretreated to remove non-clay minerals while also ensuring the preservation of the original isotopic composition. By reviewing the traditional and modern stable isotope collection methods we recognize that O and H isotope analyses may be optimized using laser fluorination and thermal conversion elemental analyzers, while new advancements in coupled thermogravimetric analyses and laser spectroscopy methods provide promising results for analyzing O-H bond specific isotope compositions. Additionally, we highlight and discourage the inappropriate use of previously determined mineral specific phyllosilicate-water equilibrium fractionation factors for paleotemperature calculations of multi-mineral clay mixtures and instead encourage calculating unique fractionation factors using elemental chemistry, mineral abundances, and O-H stable isotope compositions to provide more accurate paleotemperature estimations.

With ongoing efforts to refine this multi-faceted paleotemperature approach, the stable isotope geochemistry of soil formed phyllosilicates continues to be an invaluable proxy system, enhancing our understanding of terrestrial paleoenvironments and paleoclimate. Moreover, these findings are widely applicable to any geothermometry study of authigenic clay minerals in argillaceous rocks.

ALTERATION HISTORIES OF ASTEROIDS REVEALED BY CLAY CHEMISTRY

Vierling, Sarah A.*¹, Williams, Lynda B.¹, and Bose, Maitrayee¹

¹School of Earth and Space Exploration, Arizona State University, Tempe, AZ 85287, USA.

*svierlin@asu.edu

Introduction: Aqueous alteration in CI- and CM-type carbonaceous chondrites transforms high-temperature silicates into clays that incorporate Li cations into their structures during hydrothermal alteration. Clay interlayers also host exchangeable cations and possibly organics¹ derived from the last fluids in contact with the mineral. We characterize the primary clays in meteorites, employ a cation-exchange protocol to isolate interlayer Li and associated organics, and characterize the organic-rich fluid to reconstruct fluid chemical evolution and controls on organic synthesis in asteroidal environments.

Methods: Clay-bearing carbonaceous chondrite meteorites MIL 07700 and Murchison were gently crushed, and <1 μm particles were separated by Stokes's law into <0.02, 0.2 to 0.5 μm , and 0.5 to 1.0 μm size fractions. Mineralogy will be determined using a Rigaku SmartLab XRD. Samples will be saturated with 1 M CaCl_2 to remove interlayer Li and associated organics. Liquids collected afterward will be evaluated by LECO GCxGC TOF-MS and JEOL LCmate LC-MS to characterize organic composition and fluid chemistry.

Method efficacy is supported by clay analogs². Analogs saponite and montmorillonite were rinsed with Ambersep-filtered deionized water and treated overnight in 1 M NH_4Cl to establish baseline interlayer Li content. Samples were then exposed to 1 M LiCl . A second NH_4Cl treatment allowed NH_4^+ ions to exchange with newly adsorbed Li^+ on clay interlayers. Centrifugation separated solids and solutions between each step. Subsamples collected after each treatment were examined with the Nanoscale Secondary Ion Mass Spectrometer (NanoSIMS) 50L to track Li adsorption and removal.

Results and discussion: NanoSIMS measurements of the analogs indicate LiCl exposure leads to Li enrichment in saponite and montmorillonite, increasing $^7\text{Li}/^{29}\text{Si}$ by ~ 2.91 and ~ 5.55 , respectively. Subsequent NH_4Cl treatment removes 100% of adsorbed Li introduced by LiCl , confirming the protocol effectively exchanges interlayer Li. XRD analysis of a saponite standard shows d -spacings (14.53 \AA , 9.95 \AA , and 2.89 \AA) characteristic of saponite, dehydrated saponite, and a high-order basal reflection, ensuring reliable instrument conditions for meteorite samples.

Conclusion: Combining clay identification with extraction and characterization of interlayer species can provide key insights into links between clay mineralogy and organic products, generated during aqueous alteration. This approach offers new constraints on the mineralogy in the solar system that may be responsible for the formation of the building blocks of life.

¹Williams LB, Ferrell RE. Ammonium Substitution in Illite During Maturation of Organic Matter. *Clays and Clay Minerals*. 1991;39(4):400-408. doi:10.1346/CCMN.1991.0390409

²Williams, Lynda B., Vierling, Sarah A., & Bose, Maitrayee (In Revision), Mannitol extraction of adsorbed-lithium from clay minerals: a tool for probing fluid Li-isotopic changes from past to present, *Clays and Clay Minerals*.

MD SIMULATION ON CIPROFLOXACIN-MONTMORILLONITE INTERACTION : INTERFACIAL DYNAMICS, COORDINATION ENVIRONMENT, AND ADSORPTION FREE ENERGY LANDSCAPES

Swai*¹, Rogers E. and Holmboe¹, Michael

¹Umeå University, Chemistry Department, Umeå, Sweden

*rogers.evarist@umu.se

Ciprofloxacin (CIP) mobility and retention in soils hinge on its interactions with clay minerals, which are governed by surface charge, hydration, and the pH-dependent speciation of CIP (CIP⁺, CIP^{+/-}, and CIP⁻).

Our study employed advanced molecular dynamics simulation and spatial mapping approaches to qualitatively and quantitatively investigate the surface distribution and adsorption free-energy pathways, providing mechanistic insight into how surface charge heterogeneity, interlayer cation identity, and concentration govern the energetic landscape for CIP adsorption to the montmorillonite (MMT) surface. The interlayer cation strongly associates with the Mg²⁺/Al³⁺ substitution sites and pulls coordination water along with them, leaving patches with slightly lower water densities on the surface, offsetting the energy cost of displacing the water for the CIP adsorption (Fig 1a). While the CIP⁺ competes with the cations for the negative sites, the CIP^{+/-} and CIP⁻ accommodate the left-out, less negatively charged patches. Here we also show that the negative charge density and its location within the MMT structure affect the properties of the clay–water interface. Strong water polarization around the basal oxygen, with more isotropic behavior in the ditrigoal cavities. This water polarization is generally attenuated in patches with fewer cations and fewer Mg²⁺/Al³⁺ substitutions.

Umbrella sampling free energy of adsorptions revealed CIP⁺ to have the strongest energy, followed by CIP^{+/-} and CIP⁻. Despite its negative charge, CIP⁻ showed a significant propensity to adsorb on the MMT surface. Overall, the standard adsorption free energies follow the sequence CIP⁻ ($\Delta G^\circ \approx -2.1 \text{ kJ mol}^{-1}$) < CIP^{+/-} ($-11.8 \text{ kJ mol}^{-1}$) < CIP⁺ ($-30.0 \text{ kJ mol}^{-1}$)¹. Investigating Mg²⁺, Ca²⁺, K⁺, and Na⁺ additions in the Na-MMT system, Mg²⁺ strongly influenced the adsorption of the less energetically favored CIP⁻, followed by Ca²⁺, Na⁺, and K⁺. Statistical Boltzman distribution for the cations, showed low energy regions where there is high density of Mg²⁺/Al³⁺ substitutions (Fig 1b).

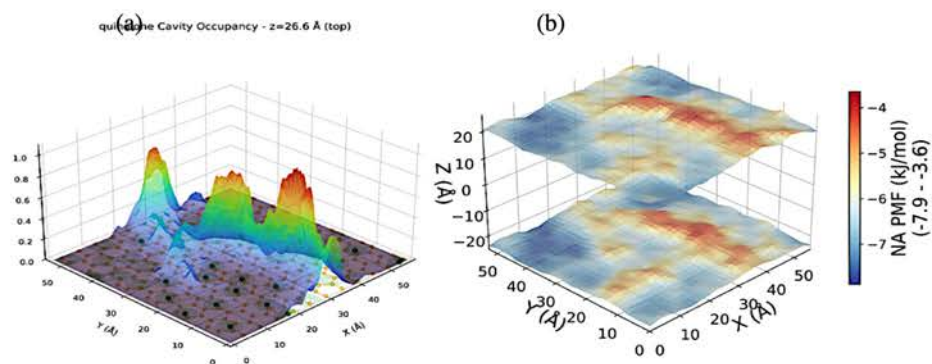


Fig 1. Local charge density heterogeneity influence to CIP⁻ (a), and cation surface adsorption (b)

1. Swai RE, Holmboe M. Molecular dynamics simulations of pH-dependent ciprofloxacin adsorption to Na-montmorillonite. *Phys Chem Chem Phys*. 2026;18–23.

KINETIC CONTROLS ON CLAY HYDROGEN ISOTOPES IN PALEOCLIMATE ARCHIVES

Smolen, Jonathan D.^{1,2,3*}, Derkowski, Arkadiusz⁴, Sparacio, Christopher A.¹, Hren, Michael T.¹

¹Department of Earth Sciences, University of Connecticut, Storrs, CT 06268, USA.

²Department of Earth and Planetary Sciences, Harvard University, Cambridge, MA 02138, USA.

³Department of Human Evolutionary Biology, Harvard University, Cambridge, MA 02138, USA.

⁴Institute of Geological Science, Polish Academy of Sciences, Krakow, Poland.

*jonathansmolen@fas.harvard.edu

Hydrogen isotopic compositions of clay minerals have long been used to reconstruct the climate, environment, and hydrology of Earth's past – even recently seeing extension to Mars. Despite the requisite assumption of primary signal preservation used in these studies, rates and mechanisms of post-formational isotopic exchange with secondary waters are not well understood nor accounted for. Here, we consider both atomistic mechanisms and environmental variables that place kinetic controls on the isotopic compositions in clay minerals – with a focus on the fidelity of paleoclimatic reconstructions.

We demonstrate mineral-fluid hydrogen exchange within kaolinite and montmorillonite structures in the absence of mineralogical alteration, suggesting hydrogen hopping as the mechanism. We designed an improved “moving r ” model to accurately capture exchange kinetics deviating from simple first order kinetics typically assumed, a necessity for realistic extrapolations of experimental studies to geological timescales. Moreover, we pair the results of this approach with empirical forward modelling that can be used to extend results to relevant planetary surface temperatures.

Applying these models to the experimental data, we find that some amount of hydrogen exchange for both clay minerals is inevitable over geological timescales – potentially less so for montmorillonite than kaolinite (Fig. 1). Though some amount of hydrogen exchange for both clay minerals is inevitable over geological timescales, this may be analytically indistinguishable and insignificant within paleo-reconstructions depending on system specifics. This allows us to quantitatively assess ramifications of exchange in paleoclimate contexts.

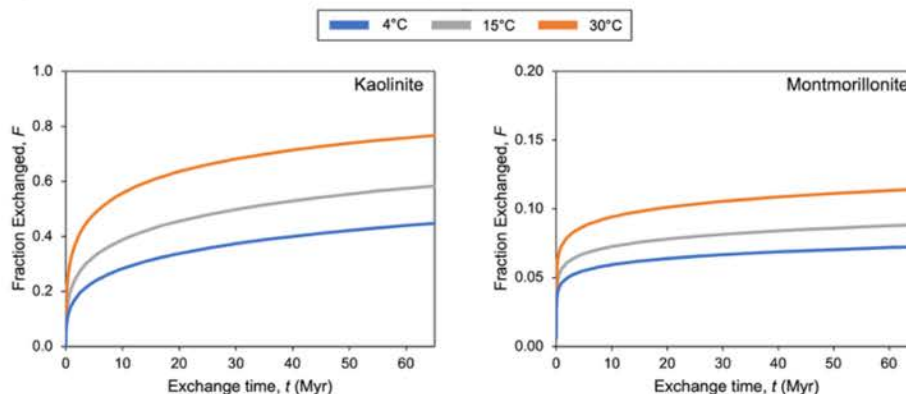


Fig 1. Predicted hydrogen exchange behavior through the Pleistocene for kaolinite-water and montmorillonite-water systems at Earth surface T (4, 15, and 30°C in the absence of mineralogical alteration).

SPECTRAL PROPERTIES OF NH_4^+ -CLAYS AND APPLICATIONS TO ASTEROIDS CERES, BENNU, AND RYUGU

Bishop, Janice L.*¹, Andrejkovičová, Slavka², Elwood Madden, Megan E.³, Fakhreshafaei, Kyle A.⁴, Geyer, Christopher⁴, Rebelo, Rafael², Pálková, Helena⁵,

¹SETI Institute, Mountain View, CA, 94043, USA. ²GeoBioTec, University of Aveiro, Aveiro, Portugal. ³Michigan State University, East Lansing MI 48824 USA. ⁴University of Oklahoma, Norman OK 73019 USA. ⁵Institute of Inorganic Chemistry, Slovak Academy of Sciences, Bratislava, Slovakia.

*jbishop@seti.org

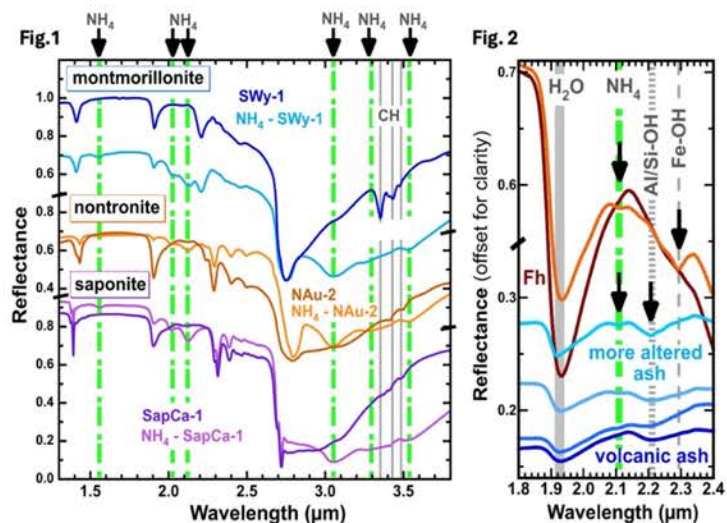
Asteroids Ceres, Bennu, and Ryugu all include NH_4^+ associated with phyllosilicates. This lab study focuses on NH_4^+ treatments of multiple clay minerals, clay-bearing rocks, and additional materials to constrain how ammonium could be connected to clays or other materials in these asteroids. Reflectance spectroscopy is used to identify NH_4^+ vibrational bands in remote sensing spectra of Ceres and in lab studies of returned samples of Bennu and Ryugu.

Our NH_4^+ cation exchange procedures and NH_4Cl brine treatments were highly successful in binding NH_4^+ to smectites in the interlayer cation sites (Fig. 1), were partially effective in binding NH_4^+ to other clays and some poorly crystalline phases (Fig. 2), and not successful for many other samples.

Infrared reflectance spectra of the NH_4^+ -smectite samples include features at 1.55, 2.00-2.02, 2.11-2.13, 3.05-3.06, 3.29-3.30, and 3.52-3.54 μm (Fig. 1) that are covered by spectra of asteroids. The NH_4^+ bands near 2.12 and 3.06 μm are the strongest and are the best candidates for detection in asteroid spectra. The band near 3.06 μm is observed in remote sensing spectra of Ceres and shifts slightly in our lab experiments, depending on the sample type and reaction conditions. Serpentine, carbonates, and hydrocarbons are also observed on Ceres, but lab studies indicate that NH_4^+ is more likely connected to the smectite than serpentine or carbonate.

Figure 1. Reflectance spectra measured under dry air conditions from 1.3-3.8 μm of montmorillonite, nontronite, and saponite with and without NH_4^+ in interlayer sites. Spectral bands due to NH_4^+ are marked with green lines and black arrows.

Figure 2. Reflectance spectra 1.8-2.4 μm of NH_4^+ -treated altered volcanic ash and ferrihydrite (Fh), where clay-like OH bands are associated with a weak NH_4^+ band at $\sim 2.11 \mu\text{m}$. Lines and arrows mark key features.



CLAY MINERAL ASSEMBLAGES PROVIDE INSIGHTS INTO ANCIENT AQUEOUS ALTERATION AT TYRRHENA TERRA, MARS

Bishop, Janice L.*¹, Tirsch, Daniela², Viviano, Christina E.³, Lane, Melissa D.⁴, Tornabene, Livio L.⁵, Voigt, Joana R.C.⁶, Ojha, Lujendra⁷, Sacks, Leah E.⁷, Loizeau, Damien⁸, Seelos, Kimberly D.³, Grant, Fiona H.¹, Seelos, Frank P.³

¹SETI Institute, Mountain View, CA, USA. ²German Aerospace Center (DLR), Berlin, Germany. ³Johns Hopkins University Applied Physics Laboratory, Laurel, MD, USA. ⁴Fibernetics LLC, Lititz, PA, USA. ⁵Western University, London, ON, Canada. ⁶University of California, Riverside, CA, USA. ⁷Rutgers University, Piscataway, NJ, USA. ⁸Institut d'Astrophysique Spatiale (IAS), Orsay, France.

*jbishop@seti.org

Tyrrhena Terra is a phyllosilicate-bearing region on Mars located between two large impact basins (Isidis Planitia and Hellas Planitia) and contains abundant altered minerals including Fe/Mg-smectites, smectite/chlorite mixtures, chlorites, zeolites, hydrated sulfates, and carbonates. We are correlating these phyllosilicate assemblages with mafic outcrops, geologic units, and regional trends in chemistry, thermal properties, and magnetic anomalies to uncover the geologic history. Orbital mineral detections from the Compact Reconnaissance Imaging Spectrometer for Mars (CRISM) are coordinated with 3D views from the High Resolution Stereo Camera (HRSC) and High Resolution Imaging Science Experiment (HiRISE) to characterize the stratigraphy of the mafic and alteration units.

Smectite is common throughout the Isidis/Tyrrhena Terra/Hellas region and is thought to have formed ~4 Ga through alteration of ancient pyroxene-rich basalt. In contrast, chlorites are significantly more common in central Tyrrhena Terra compared to the regions bordering Isidis and Hellas.

These high-temperature clays appear to be a result of geothermal flux rather than impacts and may be associated with ancient volcanism at the Syrtis Major volcano. Olivine-bearing volcanic material from a subsequent eruption partially covers the pyroxene and phyllosilicate-bearing units, which were excavated by impacts and fluvial processes. Two ~20-km diameter complex craters in the central eastern part of Tyrrhena Terra expose ample outcrops of phyllosilicates and associated alteration minerals in CRISM images (Figure 1).

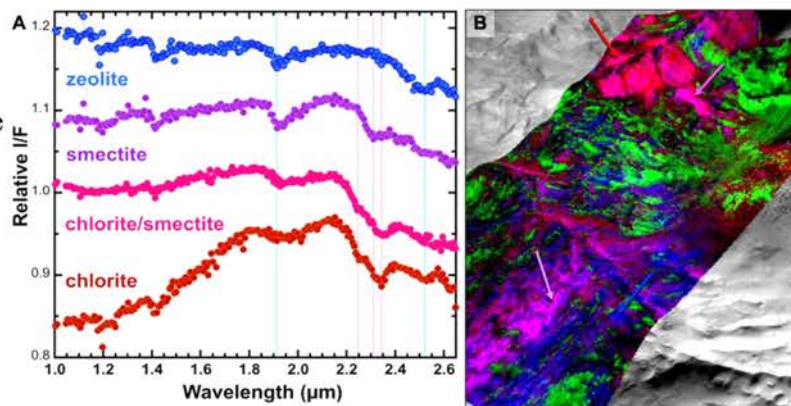


Figure 1. A) CRISM spectra at Enns-Steyr crater region contain chlorite (red), chlorite/smectite (pink), Fe/Mg-smectite (purple), and zeolite (blue). B) CRISM/HRSC perspective view showing mafic materials (green), clays and zeolite (red-blue) and locations of spectra in A.

RECENT PROGRESS IN THE UNDERSTANDING OF SMECTITE-STABLE ISOTOPE SYSTEMATICS: METHODOLOGICAL CONSIDERATIONS FOR SOIL SCIENCE

Döbelin (Kanik), Nadine *¹

¹ Natural Building Materials and Applied Clay Mineralogy, Karlsruhe Institute of Technology, Karlsruhe, Germany. nadine.kanik@kit.edu

Smectites are a common component of natural soil materials and host structurally bound hydrogen (H) and oxygen (O), making them attractive materials for H- and O-stable isotope-based paleoclimate reconstructions. However, over the past ~70 years, fundamental uncertainties have persisted regarding: (1) whether smectite isotopic compositions are fixed during formation or subject to post-formational exchange; (2) the temperatures and conditions under which such exchange occurs, and whether H and O behave similarly; (3) how to reliably account for adsorbed atmospheric water during H-isotope analysis; and (4) whether routine chemical pre-treatments, used to isolate clay fractions from organics and other mineral phases, introduce isotopic artefacts.

This presentation addresses these questions through recent experimental work by Kanik et al. (2022, 2024, 2025), integrating controlled pre-treatment experiments and smectite–water interaction studies across thermal gradients. Results demonstrate that both laboratory procedures and environmentally relevant conditions can induce isotope exchange in smectites, with implications for analytical accuracy and data interpretation. Emphasis will be placed on practical methodological considerations, providing guidance for the soil scientist who is seeking to apply clay isotope systematics in studies of pedogenesis, smectite–water interactions, and paleoenvironments.

EVALUATING CLAY MINERAL IMA SPECIES IN GALE CRATER, MARS, AND MAA MODEL CLAY PREDICTIONS

Hendrickson, Kate¹, Yee, Forest², Prabhu, Anirudh³, Sheppard, Rachel^{4,5}, Rampe, Elizabeth B.⁶, Jibrin, Zakaria¹, Thorpe, Michael T.⁷, Morrison, Shaunna M.¹

¹Rutgers University, Department of Earth and Planetary Sciences, New Brunswick, NJ 08854, USA. (kate.hendrickson@rutgers.edu)

²Trinity School, New York, NY 10024, USA.

³Carnegie Institution for Science, Earth and Planets Laboratory, Washington DC 20015, USA.

⁴Planetary Science Institute, Tucson, AZ 85719, USA.

⁵Institut d'Astrophysique Spatiale, Université Paris-Saclay, CNRS, Orsay, France.

⁶NASA Johnson Space Center, Houston, TX 77058, USA.

⁷NASA Goddard Space Flight Center, Greenbelt, MD 20771, USA.

Minerals on Mars have recorded the planet's geologic history, environmental change, and aqueous activity. Recently, Morrison et al. (2023) used Mineral Association Analysis (MAA) to predict previously unknown localities of several economic mineral species and at Mars analog sites by analyzing patterns in the Mineral Evolution Database, many of which were later ground truthed (MED: ruff.info/evolution). Here, we apply the earth-trained MED MAA model to Mars by predicting minerals in Gale crater with data from the NASA Mars Science Laboratory (MSL) CheMin (Chemistry and Mineralogy) X-ray diffraction instrument.

In this study, we apply the MED MAA model to mineral species at CheMin sample locations. The model successfully generated statistically strong mineral predictions for Mars, including igneous minerals, hydrothermal minerals, and secondary alteration minerals. Notably, the MAA analysis yielded repeated high-confidence predictions of opal; phyllosilicates; sulfates including gypsum, baryte, alunite; carbonates including calcite, dolomite, siderite; and sulfides including pyrite, galena, sphalerite, chalcopyrite. These results demonstrate that mineral association rules generate statistically robust and geologically plausible predictions and indicate that mineral diversity at Gale Crater localities is likely greater than currently recognized.

In order to run MAA, all inputs must be valid IMA mineral species. We present one interpretation of clay mineral species sourced from various literature (Blake et al. 2024; Tu et al. 2021; Rampe, Blake, et al. 2020; Rampe, Bristow, et al. 2020, Haber et al. 2022; Rudolph et al. 2022, Rampe et al. 2025). This interpretation of mineral species classifies trioctahedral smectites as saponite, the majority of dioctahedral smectites are classified as nontronite, until Nontron at the clay-sulfate transition, where the rest of the samples are more consistent with montmorillonite. Certain 9.6 Å basal spacing samples are interpreted to be ferripyrophyllite. Some of these collapsed smectites show a 9.22 Å spacing interpreted as a mixture of talc and greenalite (the more Fe-rich serpentine phase on Mars from RRUFF.net/ima-mineral-list).

The resulting MAA algorithm predicted various clays. These clay predictions for Gale crater included predominantly kaolinite, one instance of clinocllore, and a few locations of talc. We assess possible reasons and interpretations for these model predictions and how they speak to model efficacy and how well it represents Mars when trained on earthbound data. The general model accuracy seems to vary between mineral types. However, MAA illustrates potential in expanding insights in Gale crater's mineralogy, as well as locations throughout the solar system.

THE ENERGETICS OF ELECTRICAL DOUBLE LAYERS OVER HETEROGENEOUSLY CHARGED SURFACES

Legg, Benjamin A*¹

¹Pacific Northwest National Laboratory, Richland, WA 99354, USA

Charged solid-solution surfaces are ubiquitous throughout nature, where they regulate surface potential, control ion adsorption, and influence colloidal stability. This has important consequences in diverse geochemical systems, including the adsorption of transition metals, contaminants, and rare earth elements onto mineral surfaces.

The properties of charged interfaces are commonly understood using the modified Gouy Chapman theory and related models, which describe how screening ions accumulate at the interface to generate an electrical double layer (EDL) that regulates the interfacial potential. However, most models focus on simple high-symmetry systems, such as homogeneously charged planes, and neglected lateral variations in surface charge density. This is often a significant oversight, since the charge density of real surfaces can vary widely due to the presence of various crystal terminations, surface defects, surface reconstructions, or adsorbates. Even canonically neutral surfaces like NaCl (001) present an array of positively and negatively charged ions at the atomic scale. Emerging work even suggests that competitions between ion-clustering and electrostatic forces can drive the spontaneous formation of nanostructured interfaces. Models that account for surface charge heterogeneity are needed to understand such systems.

Here we present new simulations on the energetics of heterogeneously charged interfaces, conducted using a finite-volume Poisson Boltzmann solver. We simulate charged interfaces that display stripes of positive and negative surface charge, and then systematically study how variations in ionic strength, surface charge density, and stripe width influence the interfacial energy. We show that stripe-interactions have significant influence over the interfacial energy, and we identify crossover lengths at which the system transitions from being governed by geometric screening to electrolyte screening. Our work also reveals deficiencies in standard paradigms. Whereas traditional models focus almost exclusively on the screening behavior of the electrolyte solution, our simulations show that the dielectric properties of the substrate have significant influence on the energetics of heterogeneously charged substrates. These results provide new insights into mechanisms of ion adsorption, colloidal stability, and the formation of interfacial nanostructures.

ASSESSING PALEOCLIMATE USING PEDOGENIC MINERALS FROM CRETACEOUS PALEOSOLS OF THE DAKOTA FM. IN KANSAS

Andrzejewski, Kate ^{*1}, Dorst, Grace.², and Kalbas, Jay.¹,

¹Kansas Geological Survey, University of Kansas, Lawrence, KS 66047, USA.

²Department of Geology, University of Kansas, Lawrence, KS 66045, USA. *geokate@ku.edu

The Cretaceous deposits of central Kansas preserve abundant paleosols within the Dakota Formation (Albian-Cenomanian) which record paleoclimatic and paleoenvironmental signals during proposed intervals of pervasive greenhouse conditions. By conducting both qualitative descriptions of the paleosols and quantitative mineralogical, geochemical, and isotopic analyses of pedogenic minerals formed within the paleosols, this study provides estimates of both paleotemperature and paleoprecipitation patterns. Furthermore, this unique study applies these techniques to samples collected in both core and outcrop to evaluate modern weathering influence on primary mineralogical and stable isotopic composition. Stratigraphic placement of the samples was conducted using stratigraphic correlations created using the datum “X-bentonite” marker bed in the overlying Graneros Shale and generated stable carbon isotope chemostratigraphic profiles.

Results show similar bulk geochemistry across many of the collected paleosol samples, except for two samples collected in core from the middle of the Dakota Fm. The isolated fine clay fraction (<0.2 μm) shows similar mineralogical composition with a high abundance of kaolinite. Stable hydrogen and oxygen isotope values for isolated clay minerals from outcrop samples ranged from -83‰ to -72‰ and 17.1‰ to 18.2‰ respectively, while stable hydrogen and oxygen isotope values for core samples ranged from -86‰ to -78‰ and 16.7‰ to 19.5‰ respectively. Paleotemperatures calculated by combining mineralogical, stable isotopic, and water-mineral fractionation factors, range from $14 \pm 3^\circ\text{C}$ to $28 \pm 3^\circ\text{C}$. The paleotemperature results reveal a cooling trend, decreasing from $27 \pm 3^\circ\text{C}$ to $14 \pm 3^\circ\text{C}$, from the base to the middle Dakota Fm. This is followed by a warming trend, increasing from $14 \pm 3^\circ\text{C}$ to $28 \pm 3^\circ\text{C}$, from the middle to the upper Dakota Fm. Overall, the results suggest relatively warm and humid paleoclimatic conditions compared to modern day Kansas; however, they also highlight possible cool, dry punctuations across this Cretaceous time interval that should continue to be evaluated with emphasis on constraining geochronological age of the deposits as this would allow for refined comparisons to global paleoclimate records.

UNRAVELING LONG-RANGE NANOCONFINEMENT EFFECTS IN CHARGED LAYERED NANOPORES

Tuan A. Ho and Aditya Choudhary

Sandia National Laboratories, Albuquerque, New Mexico 87185, USA.

The length scale at which nanoconfinement alters aqueous behavior remains highly debated, with reported thresholds ranging from subnanometer to tens of nanometers. These discrepancies arise from differences in materials, surface chemistry, measured observables, and, critically, the choice of reference systems used to separate interfacial effects from true confinement. This challenge is particularly important in charged nanopores, where electrostatic interactions strongly influence ion distributions and water structure. Here, we employ classical molecular dynamics simulations to study aqueous LiCl confined between positively charged Mg/Al layered double hydroxide (LDH) surfaces. We show that the commonly used single-surface geometry with a liquid/vacuum interface is not a valid interfacial reference in charged systems, as it introduces asymmetric ion adsorption and additional structuring from the liquid/vapor boundary. Instead, a sufficiently wide slit pore containing a bulk-like central region provides a consistent interfacial baseline. To isolate nanoconfinement effects from concentration-induced changes, we compare systems with identical ionic strength but different pore sizes. We find that nanoconfinement suppresses counterion accumulation in the Stern layer, with onset at pore sizes of $\sim 50\text{--}60$ Å. At high ionic strength, narrow pores exhibit undercharging, whereas the interfacial limit shows overcharging, revealing distinct electrostatic screening mechanisms under confinement. We further show that nanoconfinement is strongly property-dependent. Water density becomes bulk-like within ~ 10 Å from the surface, while dipole orientation remains sensitive up to $\sim 70\text{--}80$ Å. Importantly, pore-averaged properties can be misleading, suggesting persistent confinement even in large pores, whereas spatially resolved profiles provide a more reliable indicator. These results demonstrate that nanoconfinement in charged nanopores can extend over unexpectedly long length scales and provide a framework for distinguishing interfacial and confinement effects in complex aqueous systems.

This work was supported by the DOE Office of Science, Office of Basic Energy Sciences (BES), Chemical Sciences, Geosciences, and Biosciences Division and by a Laboratory Directed Research & Development (LDRD) project. SNL is managed and operated by NTESS under DOE NNSA contract DE-NA0003525

PALEOCLIMATE RECONSTRUCTIONS USING PALEOSOL CLAY AND COARSE SEDIMENT GEOCHEMISTRY: A MACHINE LEARNING APPROACH

Burgener, Landon*¹, Beggs, Britton¹, Evans, Emily², Griffith, Emily³, Bickmore, Barry¹, and Hyland, Ethan⁴

¹Department of Geological Sciences, Brigham Young University, Provo, UT 84602, USA.

²Department of Math, Brigham Young University, Provo, UT 84602, USA.

³Department of Statistics, North Carolina State University, Raleigh, NC 27695, USA.

⁴Department of Marine, Earth and Atmospheric Sciences, North Carolina State University, Raleigh, NC 27695, USA.

*landon.burgener@byu.edu

Terrestrial paleoclimate reconstructions provide context for modern climate change and help improve projections of future climate conditions. Clay-rich paleosol horizons preserve evidence of past terrestrial climates, yet traditional geochemistry-based “climofunctions” derived from such horizons exhibit limited predictive accuracy. We address these limitations by developing a machine learning-based model to reconstruct four key paleoclimate parameters: mean annual temperature, mean annual range in temperature, mean annual precipitation and mean growing season precipitation from paleosol predictors (Fig. 1). The *paleogeocliM* model can explicitly incorporate soil texture information—quantified as percent clay, silt, and sand—alongside traditional geochemical variables, enabling the model to better relate

pedogenic processes and chemistry to these climate parameters. *paleogeocliM* uses Gaussian Process Regression with a rational quadratic kernel to model nonlinear relationships and associated uncertainties. Model performance is evaluated using 5-fold cross-validation, producing predicted values, residuals, and RMSE metrics. Preliminary results indicate significantly stronger agreement between predicted and observed climate parameters compared to previous paleotemperature climofunctions. Feature attribution and ablation analyses highlight the importance of both geochemical and textural variables as predictor variables. The *paleogeocliM* model represents a more comprehensive and flexible paleoclimate reconstruction framework that significantly improves paleosol-based temperature and precipitation predictions.

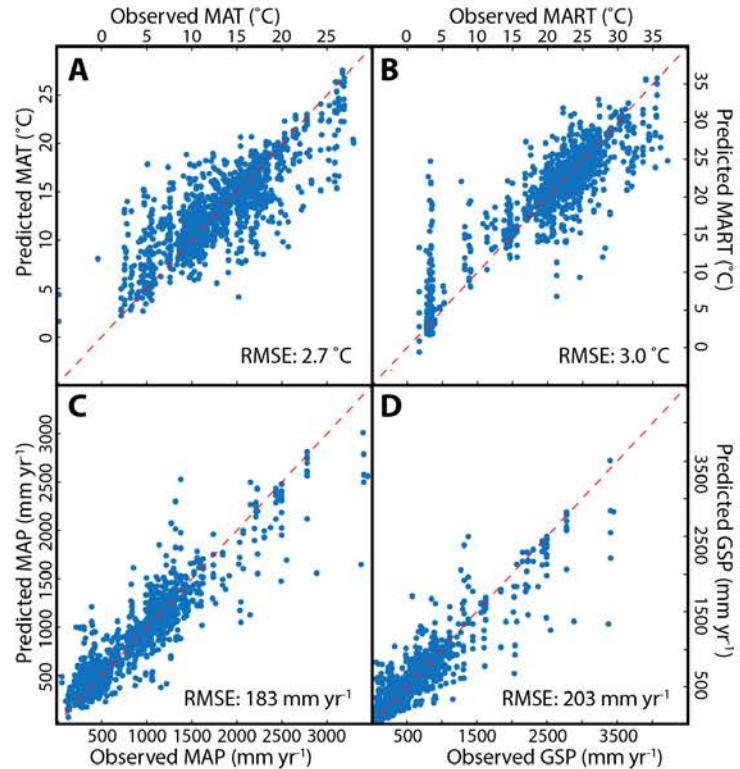


Figure 1. Preliminary results from the *paleogeocliM* model showing observed versus predicted values for A) mean annual temperature (MAT), B) mean annual range in temperature (MART), C) mean annual precipitation (MAP), and D) mean growing season (GSP). Root mean square error (RMSE) reported for each climate parameter.

CLAY ALTERATION IN HIGH SALINITY BRINES: CATION EXCHANGE & ENHANCED ALUMINUM MOBILITY

Elwood Madden, Megan ^{*1}, Geyer, Christopher.², Elwood Madden, Andrew¹; Hodges, Caitlin.², Bishop, Janice³

¹ Michigan State University, East Lansing MI 48824 USA.

² University of Oklahoma, Norman OK 73019 USA.

³ SETI, Mountain View, CA 94043.

*meem@msu.edu

Clay mineral assemblages are observed in a wide range of environments on Earth as well as within surface materials on Mars, Ceres, and other planetary bodies, providing clues to past aqueous conditions. While most studies of clay weathering and diagenesis have focused on relatively dilute systems (salinity \leq seawater) common on Earth, the abundance of salts in meteorites, as well as surface materials observed throughout the Solar System, suggest that many planetary waters likely were/are much saltier. In this study we investigate the effects of high salinity brines on clay alteration to better understand the effects of high ionic strength solutions on clay chemistry and preservation during weathering and diagenesis. We reacted saturated NaCl, Na₂SO₄, CaCl₂, MgCl₂, MgSO₄, and NH₄Cl brines with kaolinite (KGa-2), nontronite (NAu-2), and montmorillonite (SAz-1) at 25 and 100°C and compared the results with experiments using 10% dilutions of the saturated brines or ultrapure water. Trace secondary minerals observed in XRD, Raman, and visible-IR spectroscopy provide evidence of mixed-layer smectite-illite transformation in NAu-2 and SAz-1, residual salts in many of the experiments, and calcium sulfate minerals formed through cation exchange reactions with smectites. Aqueous elemental analyses produced significantly higher Al concentrations in the near saturated brines than in the more dilute solutions. In contrast, Si concentrations were similar in both the dilute and near saturated solutions. Al/Si ratios increase as water activity decreases in the near saturated experiments, likely due to increased Al solubility due to complexation with ions in solution, combined with enhanced Si precipitation at high ionic strength. These results indicate that high salinity brines may significantly alter clay minerals over geologic timescales, with enhanced Al mobility and residual Si-rich weathering signatures likely in high ionic strength solutions common in planetary systems.

WHEN PORES POLARIZE: A BROWNIAN DYNAMICS EXAMINATION OF MEMBRANE POLARIZATION IN HETEROGENEOUSLY CHARGED MEDIA

Underwood, Thomas R. *¹

¹Pacific Northwest National Laboratory, Richland, WA 99354, USA

*thomas.underwood@pnnl.gov

Electrophoresis, the transport of charge carriers and ions under an applied electric field, governs the frequency-dependent electrical response of charged porous media. It is central to interpreting spectral induced polarization (SIP) and electrochemical impedance spectroscopy (EIS) measurements in the sub-MHz regime and connects to terahertz dielectric measurements at much higher frequencies.

In this presentation we examine frequency-dependent electrophoresis in heterogeneous, charged pore networks using Brownian dynamics simulations, with the goal of identifying the origin of the low-frequency SIP response observed in charged porous media such as clay minerals. Our analysis disentangles contributions from bulk conduction, electric double-layer (EDL) polarization, membrane polarization, and correlation effects including overscreening in concentrated electrolytes.

By exploring bulk electrolyte systems, slit pores, and increasingly complex pore-network geometries, we outline how the characteristic frequencies and amplitudes of the polarization response scale with ionic concentration, Debye length, surface charge density, and pore-network geometry. Our results offer a mechanistic opportunity to examine the low-frequency response of SIP with near molecular-level resolution; in doing so, improving our understanding of how impedance spectra relate to mineralogical composition, pore-water chemistry, and the pore-geometry of a sample.

SIMULATION OF ALUMINA AND CLAY MINERALS WITH PH RESOLUTION TO STUDY ELECTROLYTE INTERFACES AND ORGANIC BINDING

Heinz, Hendrik*¹, Zhu, Cheng¹, Kanhaiya, Krishan¹, Mishra, Ratan K.²

¹ Department of Chemical and Biological Engineering, University of Colorado Boulder, Boulder, CO 80301, USA.

² Group Research, BASF SE, Carl-Bosch-Strasse 38, 67056 Ludwigshafen am Rhein, Germany

*hendrik.heinz@colorado.edu

Alumina and clay minerals play a central role in catalysts, coatings, composites, electronics, and biomedical materials, however, predictive molecular models that connect structure, surface chemistry as a function of pH value, and interfacial reactivity have remained elusive.

Here, we introduce a set of INTERFACE Force Field (IFF) parameters and pH-resolved surface models for molecular dynamics simulations of alumina phases— α - Al_2O_3 , γ - Al_2O_3 , diaspore (α - $\text{AlO}(\text{OH})$), boehmite (γ - $\text{AlO}(\text{OH})$), and gibbsite ($\text{Al}(\text{OH})_3$)—with high accuracy across structural, surface, thermodynamic, and mechanical benchmarks along with existing IFF models for clay minerals. The alumina models are compatible with CHARMM, AMBER, OPLS-AA, CVFF, and PCFF, eliminating the need for reparameterization across phases with organic, polymeric, and biomolecular systems.

A database provides over 20 atomistic surface models across the full pH range for solid-liquid interfaces that represent protonated, neutral, and deprotonated alumina interfaces based on experimentally validated titration and zeta-potential data. This level of detail is required to predict the correct order of magnitude of electrolyte and (bio)molecular binding interactions as shown for simulations of the adsorption of p-hydroxybenzoic acid α - Al_2O_3 (0001) in comparison with adsorption isotherms from experiments. More than 10x differences in binding strength across several units in pH values are predicted in excellent agreement between simulations and experiments.

We discuss suitable extension of these pH-resolved models for alumina, along with earlier models for silica, to represent clay mineral surfaces across pH values from 2 to 12. The models are intended as a rigorous foundation for understanding alumina and clay phases in soils, corrosion protection, REE recovery, and functional materials applications.

IS THERE A SMECTITE SIGNATURE OF EUXINIC CHEMICAL WEATHERING OR DIAGENESIS?

Apalara, Itunu T.¹, Sluder, Katherine A.², Hodges, Caitlin¹, Sabisch, Julian C.¹, Elwood Madden, Megan E.², Saneiyani, Sina³, Moehnke, Brittany¹, Storms, Dani¹, Nell, Liam³, Elwood Madden, Andy S.^{2*}

¹ University of Oklahoma, Norman OK 73069 USA

² Michigan State University, East Lansing MI 48824 USA

³ Binghamton University, Binghamton NY 13902 USA

*maddenan@msu.edu

Dynamic iron-sulfide reactions have shaped the history of Earth and planetary systems and continue to be powerful energy sources in modern Earth systems for life, the environment, and technology. Iron-sulfur reactions are critically important for cycling of carbon, metals, critical mineral resources, and other elements associated with aqueous fluids throughout the Solar System. While low-temperature Fe-S reactions dominated Earth's oceans for billions of years; low-temperature sulfidic field environments are difficult to access on modern Earth. Our team has been working to link biogeochemical and geophysical signatures at a methane-rich, low-temperature, sulfidic spring site adjacent to Zodletone 'Mountain', Oklahoma and develop new methods for assessing dynamic Fe-S redox environments on Mars and other planets. As a subset of this work, previously we investigated the mineralogy and chemistry of clay minerals impacted and unimpacted by the euxinic spring water. In this work, we investigated the reaction of Al-rich (SAz-1 "Cheto" montmorillonite) and Fe-rich (SWa-1 ferruginous smectite) smectites over time in the euxinic spring. We found that Fe-rich smectite reductively dissolved and sequestered trace metals, while Al-rich smectite remained relatively unaffected. This corroborates our investigation of smectites extracted from near the spring, where the natural Al-rich smectites were very similar in morphology and chemistry in sulfide-impacted versus unimpacted sediments, although slightly depleted in Fe. Ultimately, we found that Fe-clays would likely not persist long-term in low-temperature sulfidic weathering conditions. These results may inform interpretations of clay-rich deposits observed on Mars, as well as ancient sediments on Earth.

CLAY-ORGANIC INTERACTIONS: EVOLUTION OF *N*-ALKANES DURING EARLY MATURATION OF SEDIMENTARY ORGANIC MATTER

Smolen, Jonathan D.^{1,2,3*}, Hren, Michael T.¹

¹Department of Earth Sciences, University of Connecticut, Storrs, CT 06268, USA.

²Department of Earth and Planetary Sciences, Harvard University, Cambridge, MA 02138, USA.

³Department of Human Evolutionary Biology, Harvard University, Cambridge, MA 02138, USA.

*jonathansmolen@fas.harvard.edu

Clay minerals play a critical, albeit complex, catalytic role in the thermal maturation of sedimentary organic matter, with important implications for hydrocarbon generation potential in natural systems as well as engineered applications. Through anhydrous pyrolysis experiments (100–300°C, up to 30 days) on modern terrestrial organic matter extracts amended with kaolinite and montmorillonite, we isolate mineral-specific effects on bituminous organic matter maturation from the evolution of molecular and isotopic signatures.

In both clay systems, thermal maturation results in the secondary production of *n*-alkanes from larger molecular precursors, resulting in substantial increases in *n*-alkane abundance (~7x for montmorillonite; ~32x for kaolinite) as well as pronounced shifts in their distribution. While average chain length (ACL) decreased systematically at higher T, significant decreases in carbon preference index (CPI) occur earlier and at lower T – thus CPI is a sensitive diagnostic tool for detecting the onset of maturation. These trends define distinct CPI–ACL trajectories relative to clay-free systems, indicating that mineral surfaces mediate precursor degradation pathways. Correspondingly, compound-specific $\delta^{13}\text{C}$ values of *n*-alkanes initially decrease with maturation, reflecting kinetic isotope effects associated with preferential cleavage of ^{12}C – ^{12}C bonds during secondary hydrocarbon generation. Despite broadly similar controls on $\delta^{13}\text{C}$ behavior, δD exhibits distinct responses between clay mineral systems, suggesting separate and mineral-dependent mechanisms of isotopic alteration. Notably, the kinetics of these processes differ between kaolinite and montmorillonite with montmorillonite generating significantly more branched, cyclic, and gaseous hydrocarbons.

Importantly, the kinetics and products of these processes differ between kaolinite and montmorillonite. Montmorillonite generates significantly more branched, cyclic, and gaseous hydrocarbons, while kaolinite produces mostly linear *n*-alkanes and abundant alkenes. These results demonstrate significant hydrocarbon generation from the extractable bituminous organic fraction during early stages of maturation, modulated by matrix effects specific to clay mineralogy. Though temperatures in excess of 150°C were necessary to observe alteration on a laboratory timescale, significantly lower temperatures experienced during burial over geological timescales are likely to produce results similar to those observed here.

NANO-PHASES FORMED AT REDOX INTERFACES IN A SULFIDIC SPRING

Sluder, Katherine^{1*}, Storms, Dani², Apalara, Itunu², Moehnke, Brittany², Nell, Liam³, Saneiyan, Sina³, Hodges, Caitlin², Elwood Madden, Megan¹, and Elwood Madden, Andy⁴

¹Department of Earth and Environmental Sciences, Michigan State University, East Lansing, MI 48823, USA.

²School of Geosciences, University of Oklahoma, Norman, OK 73019, USA.

³Department of Earth Sciences, Binghamton University, Binghamton, NY 13902, USA.

⁴Center for Advanced Microscopy, Michigan State University, East Lansing, MI 48823, USA.

* sluderk1@msu.edu

Colloids play a large role in the chemical and physical composition of groundwater and surface water systems. Through the transport of nutrients, trace elements, and sorbed organic matter, along with serving as electron acceptors/donors, colloids influence organisms and biogeochemical cycling. Zodletone, an artesian euxinic spring in western Oklahoma, is a natural laboratory where we investigate the composition of colloids formed and transported and at the redox interface of deeply sourced, reduced, S-rich spring water with the surrounding meteoric groundwater. Zodletone serves as an analog site for Proterozoic oceans and potential extraterrestrial ecosystems due to the interface of salty, sulfidic water with the oxygenated atmosphere, and organisms such as purple sulfur bacteria. Our research objective is to examine the distribution, mineralogy, chemistry, and textural relationships of colloids and elucidate changes in the colloids in relation to the groundwater chemistry at the Zodletone spring site. By examining the mineral components of this colloidal system using x-ray diffraction (XRD), scanning electron microscopy (SEM), and transmission electron microscopy (TEM), we have characterized the bulk colloidal composition and have begun to investigate individual particles and groundwater chemistry. Silicates (quartz, feldspars, and clays) and carbonates are present in all sediment and colloid samples; whereas sulfides, elemental sulfur, and sulfates are only present in the spring water impacted sediments and colloid samples. This suggests that the sulfides and sulfate minerals, pyrite, gypsum, and barite are formed through interactions at the euxinic-oxic interface and/or are transported with the spring water. Currently, we are collecting major and trace element concentration data of the groundwater at different size filter intervals (0.45, 0.22, 0.10 μm) at each well. By examining how chemistry changes in relationship to these size fractions, we can better understand what elements are traveling as the dissolved fraction (operationally defined as $<0.10 \mu\text{m}$) and what is traveling in association with the colloidal material at these different size fractions. Ultimately, these results will clarify the role of colloidal minerals, including clays and sulfur species, in biogeochemical cycling and the transportation of trace elements across redox gradients in hydrologic systems.

DIFFERENTIATING LITHIUM-BEARING CLAYS USING ORBITAL AND AIRBORNE HYPERSPECTRAL DATA

Meyer, John M.^{*1}, Kokaly, Raymond F.¹, Pfaff, Katharina¹, Ensign, Derek B.¹, Orkild-Norton, A. Rae Ann¹, Key, Erica L.², Wesoloski, Catherine E.², Swayze, Gregg A.¹, Stillings, Lisa L.³, Hoefen, Todd M.¹, and Cox, Evan¹.

¹United States Geological Survey, Denver, Colorado, USA.

²California Geological Survey, Sacramento, California, USA.

³United States Geological Survey, Reno, Nevada, USA.

*jmmeyer@usgs.gov

Lithium has been designated as a critical mineral by the U.S. Geological Survey (USGS) due to its overall risk of supply disruptions and importance to the United States economy. Currently, lithium is primarily extracted from brines of arid sedimentary basins and granitic pegmatites. However other occurrences, such as Li-rich clays and zeolites, are additional potential sources of lithium. Remote sensing data may enable exploration for, and characterization of lithium in clays exposed at the surface. While hectorite is the most common Li-bearing clay, other Mg-silicate clays such as stevensite, may contain Lithium. Past studies have identified a mixed hectorite and lower-Li-grade Mg-smectite footprint, such as saponite or stevensite, in the Barstow Formation of California. Currently deployed imaging spectrometers such as the Airborne Visible/InfraRed Imaging Spectrometer (AVIRIS-Classic), the Airborne Visible/InfraRed Imaging Spectrometer - 5 (AVIRIS-5), and the Earth Surface Mineral Dust Source Investigation (EMIT) imaging spectrometer, were used to create spectral-based mineral maps, to identify potential new sources of lithium, and to improve our understanding of known lithium resources. We applied the USGS's Material Identification and Characterization Algorithm (MICA) to data from these three imaging spectrometers. MICA uses spectral feature matching of diagnostic absorption features in more than 140 reference spectra to identify the spectrally dominant mineral(s) in each pixel of an imaging spectroscopy data set. Initial spectral-based mineral maps produced using EMIT, AVIRIS-Classic, and AVIRIS-5 imaging spectroscopy data identified possible occurrences of hectorite, saponite, and sepiolite in the Amargosa Valley, NV, and an area near Barstow, CA. However, because stevensite was not included in the reference spectra used to generate these maps, no stevensite was mapped in the area. Thirty-nine field samples were collected and returned to USGS laboratories and analyzed using bulk chemical and XRD analysis. These analyses confirmed the presence of stevensite with elevated Lithium content and led to a revision of the MICA command file to include a reference spectrum for stevensite. New spectral-based mineral maps were then generated, which identified areas of hectorite and stevensite. The XRD and bulk chemistry analyses were used to validate the revised spectral-based mineral maps. The addition of stevensite to the MICA command file resulted in more accurate spectral-based mineral maps and this revised MICA command file will be applied to other remotely sensed data to identify potentially Li-bearing stevensite in other localities.

A GENERALIZED STRUCTURE-CHEMISTRY-ACTIVITY RELATIONSHIP FOR SMECTITE-CATALYZED RNA POLYMERIZATION IN PREBIOTIC CHEMISTRY ON EARLY EARTH-LIKE PLANETARY BODIES

Sahai, Nita *^{1,2,3,4,5}, Villafañe-Barajas, Saul¹, Bickmore Barry R.⁶, Ruf, Reghan⁵, Namani, Trishool¹, Hu, Ruibo¹, Gao Y.¹, Chipman, Aaron⁶, Parkinson, Natalie⁶, and Hoban, Christopher⁶

¹School of Polymer Science and Polymer Engineering, University of Akron, Akron, OH 44325

²Department of Geoscience, University of Akron, Akron, OH 44325, USA

³Department of Biology, University of Akron, Akron, OH 44325, USA

⁴Integrated Bioscience Program, University of Akron, Akron, OH 44325, USA

⁵Integrated Bioscience Program, University of Akron, Akron, OH 44325, USA

⁶Department of Geological Sciences, Brigham Young University, Provo, UT 84602, USA

*sahai@uakron.edu

Minerals have long been proposed as catalysts in promoting prebiotic biomolecule synthesis and self-organization, ultimately, leading to the Origins of Life. Clays are often claimed to catalyze nonenzymatic RNA. Since smectites were widely distributed on early Earth, found on Mars and on chondrites, it may be surmised that prebiotic RNA polymerization was widespread in the solar system. In fact, only some montmorillonites (mmte), that are acid-preactivated with 0.5 M HCl and neutralized to pH 7, can promote polymerization of RNA monomers, in the presence of “polymerization salts” (75 mM MgCl₂ and 100 mM NaCl), and the monomers have to be pre-activated with phosphorimidazole leaving groups. The mechanisms of mmte acid-activation and how the chemical-structural changes affect RNA polymerization, and catalytic potential of other smectites have never been described. The goals of the present study were to establish (i) precise chemical-structural changes in mmte by acid-treatment; (ii) their effects on RNA polymerization efficiency; and (iii) a generalized smectite chemistry/structure-catalytic activity relationship.

Results of XRD, FTIR, TGA and zeta potential analyses on mmte (Wyoming-Volclay® SPV-200) treated with [HCl] = 0-1.0 M along with ICP-OES solution analyses showed greater leaching of octahedral versus tetrahedral cations. Al/Fe oxyhydroxides partially reprecipitated as interlayer “islands”, i.e., partial chloritization. The extent of leaching and Al/Fe oxyhydroxide island formation increased with acid concentration, finally showing some destruction of lateral crystal planes and silica precipitation at [HCl] > 0.5 M. Concomitantly, RNA polymerization efficiency increased from tetramers to octamers with [HCl] > 0-0.1 M, and decreased to heptamers at [HCl] = 1 M. We propose that Mg²⁺ from the polymerization salts adsorb to the interlayer Al/Fe oxyhydroxide pillars and release H⁺s that protonate the imidazole of the activated RNA monomer, rendering the P center more susceptible to nucleophilic attack by the 3'-OH of the next monomer, thus catalyzing polymerization. Further, other smectites were shown to promote RNA polymerization or not, depending on: (i) their leachability and dioctahedral or trioctahedral structure, which control the extent of Al/Fe oxyhydroxide pillar formation; and (ii) interlayer cation identity and octahedral or tetrahedral charge, which control how much RNA monomers can enter the interlayer sites. These results provide the first detailed mechanistic rationale for predicting prebiotic smectite-catalyzed RNA polymerization on early Earth and other solid bodies.

LITHIUM-BEARING CLAY MINERAL ASSEMBLAGES IN THE MCDERMITT CALDERA, OREGON-NEVADA, USA: IMPLICATIONS FOR LACUSTRINE DIAGENESIS AND LOCALIZED HYDROTHERMAL ENRICHMENT

Day-Stirrat, Ruarri J.*¹, Scarberry, Kaleb C.*^{1,2}

¹Oregon Department of Geology and Mineral Industries, 800 Northeast Oregon Street, Suite 965, Portland, Oregon 97232, USA. *Ruarri.Day-Stirrat@dogami.oregon.gov

²College of Earth, Ocean, and Atmospheric Sciences, Oregon State University, 104 CEOAS Admin. Bldg., Corvallis, Oregon 97331, USA.

Li-bearing trioctahedral smectite are a common occurrence in the basin and range of the Western United States. The McDermitt caldera, a ~16.4 Ma super volcano, hosts one of the most important lithium-claystone systems recognized in North America and is a natural laboratory for evaluating mineralogical controls on lithium enrichment in caldera-related lacustrine sediments. Early work established that lithium in the caldera is associated with authigenic clay minerals in altered volcanoclastic and sedimentary units (Rytuba and Glanzman, 1978, 1979). More recent work showed that basin-scale lithium enrichment is commonly associated with Li-bearing trioctahedral smectite, whereas the highest-grade interval identified near Thacker Pass reflects a later hydrothermal overprint that converted earlier smectitic assemblages to Li-rich illite (Benson et al., 2023). Published data indicate that caldera-wide smectite-dominated intervals commonly contain on the order of 1000 to 4000 ppm Li in whole-rock assays.

Using the McDermitt Caldera as the type example, this abstract emphasizes the clay-mineral system rather than the resource statement alone. Lithium enrichment in the Oregon part of the caldera is associated with laminated clay-altered mudstone and ash-tuff intervals, elevated magnesium, and a strong inverse relationship between lithium and gallium. The working mineralogical interpretation is that restricted-basin conditions, high pH brines, low detrital dilution, and abundant Mg-Si activity favored precipitation of trioctahedral smectite clay minerals broadly comparable to hectorite; these conditions are consistent with experimental and sedimentological models for Mg-silicate formation in saline alkaline lakes (Tosca and Masterson, 2014).

The principal questions are where lithium resides in the clay fraction, how Mg-smectite evolves with burial and fluid-rock interaction, and under what conditions illitization or other diagenetic overprints increase or redistribute lithium. In that context, McDermitt is best interpreted as a composite lacustrine-hydrothermal clay system in which depositional restriction established the precursor Li-rich smectite assemblage and later localized fluid flow enhanced mineralogical and grade variability. This framework is directly useful for exploration because it shifts emphasis from bulk lithium assays alone to clay-mineral mapping, basin evolution, accommodation space creation, and process-relevant mineral characterization.

ELEMENTAL GEOCHEMISTRY OF THE MOWRY SHALE AS A PREDICTIVE TOOL FOR HYDROCARBON EXPLORATION

Hudson, Samuel M.*¹, Greenhalgh, Brent², Taylor, Brad¹, Toner, Austin¹, Kewish, Charles¹, Morgan, McKay¹, and Gray, Adam¹

¹ Department of Geosciences, Brigham Young University, Provo, UT 84602, USA.

² Wexpro, Enbridge Gas, Salt Lake City, UT, 84145.

The clay-rich Cretaceous Mowry Shale is a proven hydrocarbon source rock in fields across Wyoming, northeastern Utah and northwestern Colorado. It sources multiple conventional hydrocarbon reservoirs such as the Frontier and Dakota formations, and is a prolific unconventional hydrocarbon play in the Powder River Basin of eastern Wyoming. Moving to the west, Mowry strata progressively feels the influence of the Sevier Orogeny as a source of terrestrial detrital material. This influx in terrestrial matter can be seen in the inorganic and organic chemistry of the Mowry Shale. A recent increase in interest towards the Mowry Shale as a more regional unconventional play makes understanding these spatial variations crucial for continued resource development.

This study involved a comprehensive sampling strategy across multiple geological settings, including five outcrops, five cores, and two well cuttings along the western margin of the Greater Green River Basin, proximal to the Sevier orogenic front. Of the five outcrops, four were complete stratigraphic sections, while one represented only the upper portion of the formation. In these outcrops, samples were systematically collected at approximately 1.5-meter intervals. The five cores analyzed did not encompass the full thickness of the Mowry Shale; however, their relative positions within the formation were well established, allowing for contextualized sampling at approximately 1-meter intervals. Additionally, two sets of well cuttings were examined, with samples obtained across 10-foot intervals. Each sample was analyzed using high temperature Rock-Eval pyrolysis and elemental geochemical analysis using X-ray fluorescence (XRF) in order to quantify major and minor elements indicative of depositional conditions.

The average total organic carbon (TOC) of all samples is 2.02% ($\pm 1.56\%$), with regional TOC values increasing overall toward the northeast. The majority of samples contain type II/III to type III mixed marine/terrestrial kerogens, but indicators become more marine-dominant (Type II) moving to the northeast. This reflects a decrease in terrestrial organic matter (TOM) input basinward to the east and north moving away from paleoshoreline. Elemental geochemistry supports this trend, with Ti/Al ratios indicating higher detrital input in western and southern regions. Redox-sensitive ratios suggest oxic to suboxic depositional conditions, where hydrocarbons are preserved through rapid burial or high primary productivity rather than anoxia. Thin section analysis and elemental data reveal a significant biogenic silica component (17–25%), reinforcing high productivity as the primary preservation mechanism. Understanding these spatial and geochemical variations is essential for refining paleoenvironmental reconstructions and improving subsurface predictions for future hydrocarbon production.

MECHANICAL ACTIVATION OF UNDERCLAY FOR ENHANCED LITHIUM EXTRACTION AND AMORPHOUS SILICA PRODUCTION

Ogunsunlade, Toluwalase S.*¹, and Ogunmodimu, Olumide S.¹

¹Department of Energy and Mineral Engineering, Pennsylvania State University, State College PA 16802, USA.

*tso5091@psu.edu.

Lithium-bearing coal underclays represent an underutilized unconventional resource for both critical mineral supply and low-carbon cementitious materials. Lithium is structurally bound within phyllosilicate lattices (e.g., kaolinite, muscovite, cookeite), limiting its accessibility to direct leaching. This study evaluates high-energy mechanical activation as a low-temperature pretreatment to induce structural disorder, amorphization, and particle-size reduction in Pennsylvania Mercer underclay, with the dual objective of enhancing lithium extraction and producing reactive amorphous aluminosilicates for supplementary cementitious material (SCM) applications.

Representative samples were subjected to controlled planetary ball milling at 400–600 rpm for 30–120 min. Structural and physicochemical evolution was characterized using X-ray diffraction (XRD), Fourier transform infrared spectroscopy (FTIR), thermogravimetric analysis (TGA/DTG), scanning electron microscopy (SEM), and BET surface area analysis. Lithium extraction using mild lixiviants was quantified by inductively coupled plasma optical emission spectroscopy (ICP-OES), while cementitious reactivity was evaluated through amorphous phase development and isothermal calorimetry (ASTM C1897).

Mechanical activation progressively disrupted long-range crystallographic order, evidenced by peak broadening, intensity loss, and amorphous hump formation, alongside hydroxyl-band attenuation and silicate framework distortion. These changes coincided with particle fragmentation and increased surface area, enhancing lithium liberation during leaching. Lithium recovery increased with milling intensity and duration, reaching up to 97%, while activated samples achieved cumulative heat release of ~450 J/g at 600 rpm and 120 min, confirming strong dependence on the degree of amorphization. These structural (XRD) and morphological (SEM) changes are illustrated in Figure 1, which shows intensity reduction and phase transformation.

This study demonstrates that mechanical activation is an effective, low-temperature strategy for the dual valorization of coal underclay, simultaneously enhancing lithium extraction and generating reactive amorphous silica for sustainable cementitious use.

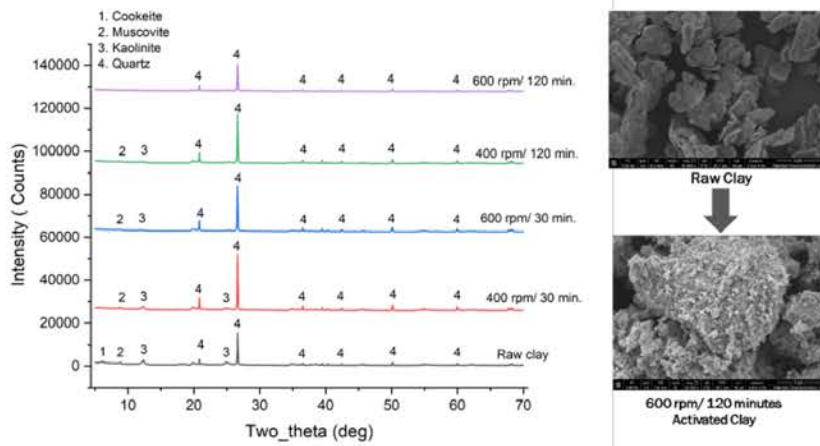


Figure 1. Structural evolution of Mercer underclay during mechanical activation: XRD (left) shows peak broadening and intensity loss with increasing milling (400–600 rpm; 30–120 min), while SEM (right) shows transformation from platy crystals to fragmented, aggregated, disordered particles at 600 rpm/120 minutes.

EVALUATING THE EFFECTS OF SMECTITE SPECIES AND EXCHANGEABLE CATIONS ON SOLID BITUMEN MATURATION IN HYDROUS PYROLYSIS EXPERIMENTS

Stokes, M. Rebecca ^{*1}, Hackley, Paul C.¹, Jubb, Aaron M.¹

¹U.S. Geological Survey, Reston VA, 20192

Hydrous pyrolysis experiments were performed using two solid bitumen (SB) samples (SB_{low}: R_o=0.04±0.003% and SB_{high}: R_o=0.85±0.04%), and two smectites: low-charge Wyoming smectite (SWy-3) and high-charge Otay smectite (SCa-3), both exchanged with Na⁺, K⁺, and Ca²⁺ cations. Fourteen samples including 12 clay-SB mixtures (1:1 weight ratio) and two SB-only samples were pyrolyzed in the presence of deionized water at 350°C for 96 hours. The post-pyrolysis residues were evaluated using programmed temperature pyrolysis, Raman spectroscopy, reflectance, and gas chromatography (GC) analysis. Solid bitumen reflectance values of the clay-SB mixture residues are consistently ~0.35% lower than SB-only residues. T_{max} values for the clay-SB_{high} residues are similar (~457°) and lower than the SB_{high} only value (470°). In contrast, T_{max} values for the clay-SB_{low} mixtures are variable, 443–452°, and the SB_{low} only sample value is 448°. The G peak full-width at half-maximum (G-FWHM) values, an indicator of aromaticity, from Raman spectroscopy for the clay-SB_{high} mixtures are similar at ~60±0.5 cm⁻¹, but the G-FWHM values for the clay-SB_{low} mixtures are variable (61–96 cm⁻¹). Notably, the G-FWHM is lowest for the two K⁺-exchanged smectite-SB_{low} mixtures. GC results from the residues show that the aromatic fraction was undetectable in the SB_{low} mixtures except for K⁺-exchanged SCa-3-SB_{low}, whereas the SB_{high} mixtures are relatively aromatic with the K⁺-exchanged smectite-SB_{high} mixtures showing the highest values. GC results for the saturate fractions are complex, but in general, the shorter chain hydrocarbons (C₈–C₂₀) are lower by an order of magnitude in the clay-SB_{low} mixtures relative to the clay-SB_{high} mixtures. The C₂₁–C₄₀ hydrocarbons are more abundant in the clay-SB_{low} mixtures relative to the clay-SB_{high} mixtures but show a consistent trend between different exchangeable cation types where Na⁺>K⁺>Ca²⁺. In summary, the results obtained from this study show that development of aromaticity in SB in the presence of both high-charge and low-charge smectite is suppressed and no consistent differences between the type of smectite are observed. However, SB_{low} mixture residues with Na⁺- and K⁺-exchanged smectite are generally more aromatic and produce more long- and short-chain hydrocarbons relative to the Ca²⁺-exchanged clay-SB mixtures. These results suggest that the hydration enthalpy of the exchangeable cations (Ca²⁺>>Na⁺>K⁺), and thus the availability of H₂O, has a discernable influence on the aromatization of SB and production of hydrocarbons.

APPLICATION OF CLAY-POLYMER NANOCOMPOSITES FOR THE REMOVAL OF TOXIC CYANOBACTERIA AND OTHER PHYTOPLANKTON FROM WATER

Rytwo, Giora^{1*}, Tsveher, Yehezkel¹, Viner-Mozzini, Yehudith², and Sukenik, Assaf²

¹Environmental Physical Chemistry Lab, Tel Hai- University of Kiryat Shmona, Kiryat Shmona, 1220800, ISRAEL

²Kineret Limnological Institute, Israel Oceanographic & Limnological Research, Migdal, ISRAEL

*rytwo@telhai.ac.il

Climate change, particularly rising temperatures, and increased CO₂ levels further contribute to algal bloom frequency. Phytoplankton generally behaves as suspended particles with low density and surface colloidal charge resulting in very slow sedimentation.

While traditional coagulation and flocculation methods can promote settling, their use in drinking water is limited by regulatory consideration, treatment rate and cost, and concerns over cell lysis and toxins release.

Polymer clay nanocomposites may offer a promising alternative. The polymer neutralizes colloidal charge and bridges particles, while the clay increases density, accelerating sedimentation. In previous studies this method has shown effectiveness in wastewater pretreatment. This study evaluated nanocomposites based on Polydiallyldimethylammonium chloride (PolyDADMAC, PD) and various clay minerals, testing different ratios and doses based on particle charge detector (PCD) measurement and past experimental knowledge. Water quality was assessed one hour after treatment by measuring turbidity and chlorophyll fluorescence, whereas toxin concentrations were analyzed via HPLC.

Results showed over 95% removal of turbidity and chlorophyll in water containing *Microcystis aeruginosa*, at lower-than-expected nanocomposite doses, a very interesting effect that additional tests indicate that can be attributed to specific interactions between the polymer and the specific cyanobacteria. The effect was less significant in *Aphanizomenon ovalisporum* and not observed at all in *Chlorella* sp. Nanocomposites based on kaolinite clay mineral showed slightly better performance than those based on sepiolite. However, too high nanocomposite concentrations were associated with increased microcystin levels, possibly due to cell lysis. Modelling this effect remains challenging due to limitations in meeting key assumptions.



Clarification in *Aphanizomenon* (APH), *Microcystis* (MIC) or *Chlorella* (CHL) suspensions 5 minutes after addition of clay polymer nanocomposites at doses equivalent to neutralize only 25% of the relevant charges.

THE EFFECT OF *pH* ON THE INTERACTIONS BETWEEN RARE EARTH ELEMENT IONS AND GIBBSITE NANOPARTICLES

Molnar, Zsombor ^{*1}, Song, Shuhong.¹, Park, Hyoju.¹, Mergelsberg, Sebastian ¹, and Legg, A. Benjamin¹

¹Pacific Northwest National Laboratory, Physical Sciences Division, Richland, WA 99354, USA.

*molnar.zsombor@pnnl.gov

Sedimentary rare earth element (REE) deposits are among the most significant sources of REEs because they are readily accessible and relatively inexpensive to extract. In these deposits, trivalent REE ions are commonly considered as individually adsorbed ions (e.g., outer sphere complexes) on the surfaces of different clay minerals, such as kaolinite and different swelling clay minerals. Recent studies on trivalent metal cations and mica surfaces showed that charged mineral surfaces attract and adsorb metal cations, facilitating the formation and stabilization of novel, quasi-two-dimensional surface phases. We hypothesize that similar phenomena significantly influence the behavior of REE ions and the subsequent formation of REE surface species and precipitates, with environmental factors (such as pH) acting as a primary driver of these interactions. To study how the REE ions adsorbed on charged minerals surfaces we used gibbsite ($\text{Al}(\text{OH})_3$) as a reference material. Gibbsite is also one of the major mineralogical components of sedimentary-hosted REE deposits, and it could provide important implications to the behavior of the octahedral layer of sheet silicates.

To test our hypothesis, we investigated the impact of pH and dissolved REE concentrations on the surface charges of synthetic gibbsite ($\text{Al}(\text{OH})_3$) nanoparticles using a dynamic light scattering (DLS) instrument connected to an autotitrator. We correlated the measured ζ -potential values with the results of bulk adsorption experiments and with the observations from high resolution scanning transmission electron microscopy (STEM) analyses. Our findings showed that the adsorbing REE ions significantly modified the surface potentials of gibbsite, suggesting that adsorption proceeds via surface complexation, which subsequently promotes aggregation of gibbsite particles. We observed a distinct pH-dependency in these mechanisms: at low pH, we observed individual REE ion on the surface of gibbsite. Above neutral pH, ions assemblies and REE oligomeric clusters appeared especially on the edges of gibbsite nanoparticles. As the pH increased, from around neutral pH we observed a few nm large REE containing oligomers, and the sizes of the clusters rapidly increased with the increasing pH. These findings imply that complex REE containing forms could also play an important yet overlooked role in REE adsorption processes.

MODELING THE GEOMECHANICAL EFFECTS OF LAYERED BENTONITES IN PRODUCTION OF THE MOWRY SHALE

Fischer, Timothy*¹, Hossain, Md Mahruf.², Mollah, Md Mahmudul Hasan², and Zhang, Xiang²

¹Center for Economic Geology Research, School of Energy Resources, University of Wyoming, Laramie, WY 82071, USA.

²Department of Mechanical Engineering, University of Wyoming, Laramie, WY, 82071, USA.

*tfische2@uwoyo.edu

The Mowry Shale, underlying most of Wyoming, contains the largest unexploited oil and gas resource in the state. An estimate from 2009 indicates the Mowry Total Petroleum System contains up to 300 million barrels of oil in the Powder River Basin and a recent USGS report estimates as much as 450 million barrels in the Greater Green River Basin. Because Wyoming receives a large fraction of its state budget from mineral severance tax, this reservoir is vitally important to the state. With such an important resource to extract, why has it not happened already? The short answer is that there are easier resources to go after. The Mowry underlies the Niobrara and Frontier Formations, which have long been large and, importantly, relatively shallow oil reservoirs. But maybe the more daunting challenge is the geological complexity of the Mowry. Laid down in the mid-Cretaceous on the western edge of the Western Interior Seaway, the silicious shale layers are interspersed with many bentonite layers. These layers can be anywhere from millimeters to several feet in thickness. The bentonites cause two major problems: 1) a significant drilling hazard and 2) uncertainty in the stimulated rock volume due to the lack of geomechanical knowledge and how fractures propagate during hydraulic fracturing.

The University of Wyoming is attempting to solve both of these problems with what is known as the Mowry Project. State funded to the tune of \$3MM, the program consists of 13 research projects across 6 departments. This presentation will touch on those, but highlight the work done in the Mechanical Engineering department on modeling the fracture behavior between the brittle shale layers and the ductile bentonites.

We use a penalty-enforced Lipschitz regularization for local continuum damage models to address mesh dependence in local damage modes. This regularization, together with multiple selected continuum damage models are implemented and tested in the Multiphysics Object-Oriented Simulation Environment (MOOSE). One continuum damage model, the Simo-Ju model, is employed to simulate fracture initiation and growth under coupled hydro-mechanical conditions for both the shale and bentonite layers, with a different set of material parameters to distinguish the brittle vs ductile behavior in the shale and bentonite. A 2D simulation domain, which represents the plane perpendicular to the horizontal well, is considered, with a simplified bentonite layer positioned at different distances and/or orientations relative to the injection point. The model aims to capture how the mechanical mismatch and low permeability of the bentonite layer influence the stress distribution, pressure evolution, and fracture development during fluid injection under different bentonite layer configurations. The modeling framework established in this work is intended to support future investigations involving thermal and chemical processes relevant to the realistic hydraulic fracture modeling, and the incorporation of interfacial effects between the bentonite layer and the shale, and eventually model validation and hydraulic fracture design.

CLAY MINERAL CONTROLS ON REE DISTRIBUTION AND RECOVERY IN GEORGIA KAOLIN MINE TAILINGS

Ellis, Shannon*¹ and Schroeder, Paul A.¹

¹Department of Geology, University of Georgia, Athens, GA, 30602, USA.

*shannon.ellis@uga.edu

Georgia kaolin systems produce a clay-dominated continuum of materials ranging from natural weathering profiles to rejects generated during mining and beneficiation, allowing rare earth element (REE) behavior to be evaluated across linked natural and industrial environments. Initial work focuses on a 120-ft kaolin core from central Georgia (GM24), where twenty-seven samples were analyzed using powder X-ray diffraction and lithium metaborate/tetraborate fusion ICP-MS to relate mineral assemblages to REE distribution. This framework is being extended to mine waste materials from Wrens (GW25) and Macon (GM26) areas of Georgia, including tailings, processing streams, and overburden, to evaluate how beneficiation redistributes clay-rich fractions and associated REEs.

Results from the GM24 core indicate that total REE concentrations are highest in kaolinite- and gibbsite-rich intervals, whereas quartz-rich sands show lower REE abundances but relatively higher HREE/LREE ratios. Iron oxide-rich intervals exhibit Ce anomaly behavior consistent with redox influences. Ongoing work integrates mineralogical and geochemical analyses of mine materials, including bulk X-ray diffraction and targeted ICP-MS, to determine REE partitioning among clay fractions, oxide phases, and heavy minerals. This study establishes a mineralogical framework for interpreting REE behavior across kaolin weathering systems and beneficiation products, with implications for evaluating clay-rich mine wastes and recycled materials.

SMECTITE–ILLITE TRANSFORMATION AND KAOLINITE FORMATION FROM OFFSHORE AFRICA: IMPLICATIONS FOR THERMAL EVOLUTION AND FLUID–ROCK INTERACTION

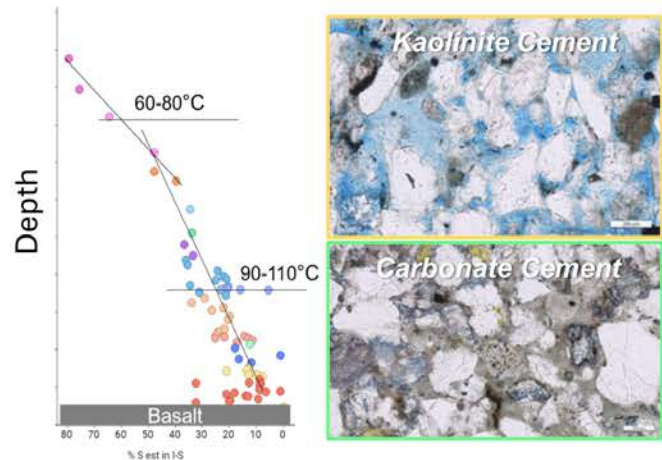
Cheshire, Michael^{1*}, Svihlik, Nik¹, Zhou, Jie¹, Matthews, Jessica¹, Christensen, Brad¹, Dockrill, Ben¹, Locklair, Robert¹, Little, Jessica¹, Valencia, Luis¹

¹ Chevron Corporation, Houston, Texas 77042, USA. *michael.cheshire@chevron.com

A well recently drilled by Chevron from offshore Africa provides information that documents progressive clay mineral transformations across a broad stratigraphic interval. This study focuses on key diagenetic processes central to basin evolution, and reservoir and seal quality: illitization and kaolinite authigenesis. These mineralogical indicators constrain thermal gradient, fluid migration pathways, and redox conditions that shaped the basin's burial history and have implications for reservoir permeability and seal integrity (capillary and mechanical).

Progression from smectitic materials in the shallower Campanian sections towards illite-dominant Barremian assemblages with depth is the prominent mineralogical trend in this area. This 38 Ma trend correlates strongly with thermal maturation (i.e., vitrinite reflectance). Thermal modeling using mineral stability relationships yields an average geothermal gradient of ~32 °C/km, consistent with regional gradients. A notable inflection in the transition suggests a shift in either basin heat flow or fluid flux.

Authigenic kaolinite reflects localized geochemical processes rather than basin-wide thermal gradients. Textural and mineral evidence supports formation in acidic, reducing conditions generated from kerogen or hydrocarbon degradation likely played a major role in driving feldspar alteration. In zones with early Fe-calcite cement, kaolinite occurrence is minimal, emphasizing the importance of relative timing of diagenetic conditions locally controlling clay diagenesis.



The mineralogical transformations documented illuminate a basin evolving from carbonate-rich depositional conditions toward more clay-rich environments, culminating in thermally driven illitization at depth. The combination of illitization and kaolinite authigenesis provides constraints on thermal history, fluid–rock interactions, mechanical and reservoir properties, and diagenetic timing. Together, these processes highlight the complex interplay between burial diagenesis, organic geochemistry, and sediment composition in shaping clay mineral evolution, seal integrity, and reservoir performance in frontier offshore basins.

HISTORY OF GEORGIA AND CORNWALL KAOLIN PRODUCTION AND NEW INSIGHTS FOR CO-PRODUCTION OF CRITICAL MINERALS

Schroeder, Paul A.*¹ Carney, Hugh C.¹, and Ellis, Shannon¹

¹Department of Geology, University of Georgia, 210 Field St., Athens, GA 30602-2501, USA

*schroe@uga.edu

China clay (kaolin) has been used for more than 2,000 years to produce porcelain, a material that some consider the first high-tech, human-made product. It was near Jingdezhen in China that kaolin was transformed into prized ceramics described as “thin as paper, bright as a mirror, and white as jade.” For centuries, trade along the Silk Road brought prosperity to the West and introduced fine porcelain dinnerware and sculpted objects that rang with musical tones when struck. European fascination with these materials led William Cookworthy to discover kaolin deposits in Cornwall, United Kingdom, enabling domestic porcelain production. Earlier, however, Josiah Wedgwood imported consignments of kaolin from Georgia, USA, to the UK, helping drive advances in kiln technology and establishing the distinguished legacy of Wedgwood porcelain. Today, kaolin is an essential ingredient in high-tech applications, including paper coatings, ceramics, pigments, plastics, rubber, and pharmaceuticals. The global kaolin market is now valued at nearly \$5 billion annually, with Georgia accounting for approximately \$1 billion of that total.

Looking ahead, the demand for advanced materials with specialized thermal and electrical properties increasingly depends on rare earth elements (REEs). Opportunities may exist to co-produce REEs from existing kaolin mining operations, commonly referred to as brownfields. Kaolin brownfields in Georgia and the United Kingdom may provide such opportunities through the recovery of REEs from waste ponds, overburden, and reject streams generated during kaolin beneficiation. Preliminary assessments suggest that economically meaningful concentrations occur within kaolin processing streams. Advancing the technology readiness levels required to extract and refine REEs for high-tech supply chains remains challenging. Key considerations include energy demand, environmental sustainability, workforce development, and engagement with stakeholders affected by the full lifecycle of resource extraction and processing.

THE CHARACTERISTICS AND GENESIS OF SECONDARY MINERALS IN THE GRANITIC ROCK REGOLITH IN SOUTH CHINA

Tan, Wei ^{*1,2}, Luo, Lianying^{1,2,3}, and He, Hongping ^{1,3}

¹State Key Laboratory of Deep Earth Processes and Resources, Guangzhou Institute of Geochemistry/ Guangdong Provincial Key Laboratory of Mineral Physics and Materials, Guangzhou Institute of Geochemistry, Chinese Academy of Sciences, Guangzhou 510640, China

²Guangdong Research Center for Strategic Metals and Green Utilization, Guangzhou 510640, China.

³University of Chinese Academy of Sciences, Beijing 100049, China

*tanwei@gig.ac.cn

The warm and humid climatic conditions prevailing in South China strongly facilitate the chemical weathering of granitic rocks, resulting in the development of thick regolith. Within these regolith, primary rock-forming minerals (*e.g.*, feldspar and mica) undergo complex transformation sequences, giving rise to diverse secondary mineral assemblages, predominantly comprising clay minerals and iron oxides. Elucidating the evolutionary characteristics and principal controlling factors of these secondary minerals is essential for understanding the dynamic mechanisms governing elemental cycling and mass transfer in supergene environments. Nevertheless, current knowledge remains insufficient regarding the synergistic control exerted by chemical weathering intensity and hydrodynamic conditions on secondary mineral evolution, particularly concerning the mechanisms through which different hydrodynamic stratifications regulate secondary mineral phase transformations and crystallization behaviors. This study systematically investigates representative regolith profiles in South China through an integrated approach combining mineralogical analysis, elemental geochemistry, and hydrogeological characterization.

The results demonstrate that the evolution of secondary minerals within the regolith follows a progressive sequence. With increasing chemical weathering intensity, primary rock-forming minerals (K-feldspar, plagioclase, and biotite) are initially transformed into 2:1-type clay minerals (illite and smectite) accompanied by the formation of abundant ferrihydrite, and subsequently further transformed into 1:1-type clay minerals (kaolinite and halloysite) along with hematite and goethite. Concurrently, against the context of overall enhanced chemical weathering, the transformation and spatial distribution patterns of secondary minerals are significantly governed by the hydrodynamic conditions prevailing within the thick regolith. Based on the vertical hydrodynamic stratification of the regolith, which comprises, from top to bottom, the vadose zone, capillary fringe, and saturated zone, the distinct seepage velocities and water content characteristic of each zone exert a fundamental control on the evolutionary trajectories of secondary minerals within the regolith. Regarding clay minerals, the alternating wetting-drying regime within the capillary fringe provides favorable kinetic conditions for the intercalation of water molecules into the interlayers of kaolinite and the subsequent transformation of kaolinite to halloysite, resulting in a marked decrease in both the structural order and abundance of kaolinite. Regarding iron oxides, the relatively humid conditions prevailing in the saturated zone and capillary fringe favor the preservation of goethite, whereas

REHYDRATION BEHAVIOUR OF SMECTITES AND BENTONITES

Rybka, Karolina*¹

¹Institute of Geological Sciences, Polish Academy of Sciences, Senacka 1, 31002, Kraków, Poland.

*ndrybka@cyf-kr.edu.pl

Smectite clays possess a remarkable ability to take up and release water reversibly, a property central to their behavior in natural environments and industrial applications alike. Yet this reversibility is not unconditional - heating can permanently alter smectite structure, limiting how much water the mineral can recover and how fast this process will be. In this study, homoionic smectites (a high charge SCa-3 “Otay” obtained from the CMS Source Clay Repository) with interlayer K^+ , Na^+ , Ca^{2+} , Mg^{2+} , and several natural bentonites from worldwide deposits were subjected to heating at $T_d = 100$ or 200 °C and exposed to rehydration under $RH = 30\%$ and temperatures (T_r) varying between 10-40 °C. Thermogravimetric analysis showed that rehydration was never fully reversible relative to the pre-dehydration state [1]. The degree of rehydration reflected an interplay between dehydration temperature, interlayer cation type, and the resulting structural changes - most notably a reduction in effective layer charge (measured by the O-D method). Rehydration began immediately upon humidity exposure and was relatively rapid; the initial stage was well-described by contracting geometry and diffusion models. In natural bentonites, the degree of rehydration corresponded primarily to the dominant interlayer cation, with higher recovery in those containing divalent species. Monovalent cations led to the irreversible layer collapse during dehydration, based on the observation of $d(001)$ reflection shift in X-ray powder diffraction, confining rehydration largely to non-interlayer sites [2]. In turn, divalent cations supported interlayer reopening to varying degrees depending on dehydration temperature. Near-infrared spectroscopy captured accompanying changes in $(\nu+\delta)OH$ combination mode at ~ 4500 cm^{-1} , reflecting progressive relaxation of the clay lattice, which proceeded relatively slower than the recovery of the $(\nu+\delta)H_2O$ band envelope at ~ 5200 cm^{-1} which reflects the total H_2O [2]. This indicated that rehydration is a spatially heterogeneous process, where adsorption of water at different sites in smectite proceeds with varying rates.

[1] Rybka K., Kuligiewicz A., Kaufhold S., Dohrmann R., Derkowski A. (2025) Kinetics of rehydration in smectite and its application to water resorption in bentonites. *Applied Clay Science*, 271, 107813

[2] Rybka K., Siranidi E., Skiba M., Chryssikos G.D., Derkowski A. (unpublished) Mechanism of rehydration in smectite studied by in-situ near-infrared spectroscopy and X-ray powder diffraction

STRUCTURE AND REACTIVITY OF CLAY MINERALS AND ITS ENVIRONMENTAL AND ENGINEERING APPLICATIONS

XI YUNFEI *

State Key Laboratory of Advanced Environmental Technology & Guangzhou Institute of Geochemistry, Chinese Academy of Sciences, Guangzhou, China.

*xiyf@gig.ac.cn

Clay minerals are abundant, low-cost, and environmentally compatible resources with diverse structural features. These characteristics provide significant potential for applications in environmental remediation and construction materials. However, their complex composition, structural heterogeneity, and poorly defined structure–property relationships have long constrained efficient utilization.

Systematic efforts have elucidated key structural factors governing mineral reactivity and enabled the development of structure-regulation strategies. Three primary controls on mineral surface activity have been identified: interlayer environments, surface functional groups, and microstructure. Based on these insights, modification approaches including intercalation engineering, structural reconstruction (e.g., thermal activation and acid treatment), and mineral–nanomaterial hybridization have been established. These strategies enhance both adsorption and catalytic performance, enabling efficient removal and degradation of organic and inorganic contaminants. The development of multifunctional mineral-based materials capable of co-removal of mixed pollutants and promoting redox cycling represents a significant advance. In parallel, mineralogical principles have been applied to understand and optimize mineral-based construction materials. Integrated characterization has clarified the roles of clay minerals in high-temperature processes, including the effects of water content, fluxing elements, elemental composition, and crystallinity on phase transformation, pore evolution, and mechanical properties. These results establish a unified framework linking composition, reaction pathways, and macroscopic performance. Building on these advances, a new paradigm integrating mineralogy with data-driven approaches has been proposed. Machine learning now enables performance prediction, transforming empirical materials design into intelligent and sustainable strategies. This work establishes a framework for understanding and controlling mineral reactivity across environmental and engineering systems, providing new opportunities for advanced functional materials design and sustainable development.

KAOLIN MEMBRANES FOR HYDROGEN PRODUCTION AND GAS SEPARATION: THERMAL AND CHEMICAL MODIFICATION FOR NICKEL NANOPARTICLE NUCLEATION

Olaleye, Olorunfemi P.^{*1}, Ricote, Sandrine², Coors, Grover³, Staerz, Anna F.¹, and Reimanis, Ivar¹

¹Metallurgical and Materials Engineering, Colorado School of Mines

²Mechanical Engineering, Colorado School of Mines

³Hydrogen Helix, Golden, CO.

*olorunfemi_olaleye@mines.edu

Ethanol steam reforming (ESR) is a promising route for sustainable hydrogen production, but efficient separation of hydrogen from reaction by-products remains a key challenge. Clay-derived porous membranes offer a low-cost solution, combining selective gas transport with a stable platform for catalyst deposition. This study provides a comprehensive overview of the development, microstructural evolution, and performance of Edgar Plastic Kaolin membranes designed for both Knudsen diffusion-based gas separation and nickel catalyst support. Kaolin membranes were fabricated by slip casting and bisque-fired at temperatures from 800 to 1000°C, spanning the transition from amorphous metakaolin toward mullite. To further optimize pore architecture, membranes underwent two post-firing chemical modification routes: acid leaching with hydrochloric acid drove dealumination and significantly increased specific surface area, while alkaline treatment with sodium hydroxide induced desilication and the hydrothermal nucleation of LTA Zeolite directly on the membrane framework.

Membrane microstructure, phase evolution, and transport properties were characterized using permeance testing, nitrogen gas adsorption, X-ray diffraction, and scanning electron microscopy. Permeance testing with helium and argon confirmed size-selective gas transport driven by Knudsen diffusion, where lighter gases permeate preferentially through the controlled nanopores. Acid treatment increased specific surface area from approximately 25 m²/g to over 100 m²/g under optimal conditions, reflecting the development of an extensive mesopore network. When evaluated as catalyst supports, both acid- and alkali-modified membranes successfully supported the formation of nickel nanoparticles via incipient wetness impregnation, with chemical treatment shown to directly influence nickel reducibility and dispersion. These results demonstrate that targeted thermal and chemical processing of kaolin membranes enables simultaneous control of gas permeance, pore size distribution, and catalyst-support interactions, establishing a scalable foundation for efficient membrane reactors in ESR-based hydrogen production.

IN-SITU MONITORING OF MICRO-MORPHOLOGY AND SWELLING PRESSURE OF NA-SMECTITE AT ELEVATED TEMPERATURES

Deng, Youjun*¹, Sanchez-Avellaneda, Camilo^{1,2}, Rivers, Mark³, Yakovlev, Maxim A.³, Mitchell, Chven A.⁴, Greathouse Jeffrey A.⁴, and Sanchez, Marcelo².

¹Department of Soil & Crop Sciences, Texas A&M University, College Station, TX 77843, USA,

²Zachry Department of Civil and Environmental Engineering, Texas A&M University, College Station, TX, 77843, USA.

³Center for Advanced Radiation Sources, The University of Chicago, Chicago, IL, 60637 USA

⁴Nuclear Waste Disposal Research & Analysis Department, Sandia National Laboratories, Albuquerque, New Mexico 87185, USA

*yjd@tamu.edu

Bentonite clays are used as engineered barriers in geological repositories for high-level nuclear waste. Recent studies have revealed significant gaps and discrepancies between experimental observations of swelling pressure and theoretical models, particularly when temperatures exceed 100 °C and when the dominant exchangeable cation in saline solutions shifts from Na to Ca. These inconsistencies indicate that current model parameters require refinement or revision. The overall objective of this study is to investigate the effects of elevated temperatures (up to 200 °C) and saline chemistry on the swelling behavior of compacted bentonites. High-purity smectite was isolated from a Texas bentonite and fully saturated with either Na or Ca. Swelling pressure, along with pore- and aggregate-scale structural evolution, was examined for Na-smectite specimens with a dry density of 1.4 g cm⁻³, a diameter of 6.0 mm, and a height of 4.0 mm. Measurements were conducted *in situ* as functions of hydration time and temperature using a miniature triaxial apparatus at the ANL Advanced Photon Source (APS). A maximum swelling pressure of 16 MPa was observed, which is three to four times higher than that typically measured for natural Na-bentonite, highlighting the critical role of smectite content in governing bentonite swelling behavior. Despite attempts to constrain sample volume, an axial expansion of approximately 5% was recorded. Analysis of aggregate and pore evolution over the 11-hour monitoring period indicates continuous, though incomplete, hydration and aggregate disintegration. Fluctuations in swelling pressure during heating were also observed and warrant further detailed analysis. Quantitative morphological analyses are ongoing and will be reported.

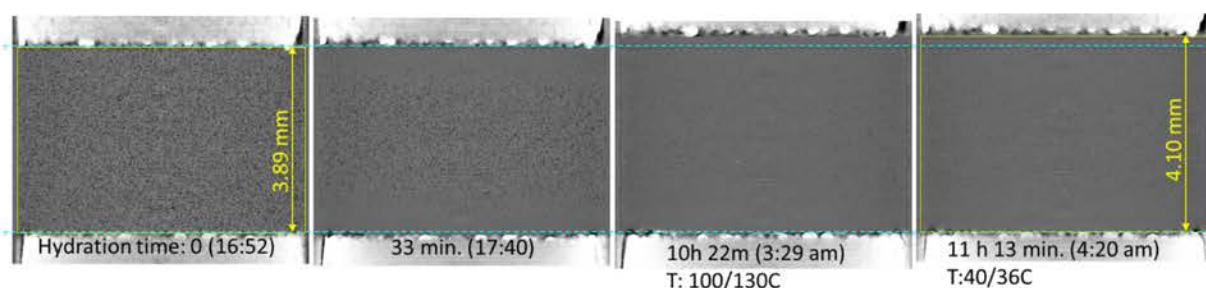


Figure 1. Evolution of middle slice of Na-Sm during hydration and heating.

Sandia National Laboratories is managed and operated by NTESS under DOE NNSA contract DE-NA0003525.

EVALUATING ZINC AND COBALT DOPING OF LAYERED DOUBLE HYDROXIDES ON THEIR EFFICIENCY OF LITHIUM EXTRACTION FROM BRINES

Siwek, Krzysztof¹, Matusik, Jakub*¹, Seftel, Elena M.², Cool, Pegie³

¹AGH University of Krakow; Faculty of Geology, Geophysics and Environmental Protection; al. Mickiewicza 30, 30-059 Krakow, Poland.

²MATCH – CAST, VITO Flemish Institute for Technological Research, Boeretang 200, B-2400, Belgium.

³Laboratory of Adsorption and Catalysis, Department of Chemistry, University of Antwerpen (CDE), Universiteitsplein 1, 2610 Wilrijk, Antwerpen, Belgium.

*jmatusik@agh.edu.pl

The demand for lithium is rapidly increasing, driven by the advancement of electric vehicles and energy storage technologies. Consequently, the development of more efficient methods for lithium extraction from brines is essential to meet the needs of this expanding industry. Direct lithium extraction (DLE) technologies, particularly those based on lithium-selective adsorbents, offer significant advantages, including high selectivity and applicability to a wide range of brine compositions.

This study examines the effect of Zn and Co incorporation into Li/Al layered double hydroxides (LDHs) on their lithium extraction performance. The materials were synthesized via coprecipitation at room temperature using Li, Al(III), Zn(II), and Co(II) salts (chlorides or nitrates), maintaining a Li/Al molar ratio of 1:2. Partial substitution of Al(III) with Zn(II) and/or Co(II) was achieved at levels of 5% and 10%. Two synthesis routes were employed. In the first, the metal precursor solution was added dropwise (5 mL/min) to distilled water, with the pH controlled at 5–6 using 3 M NaOH. In the second approach, the same solution was added dropwise to 8 M NaOH until the pH decreased to 5. The precipitates were aged for either 30 minutes or 24 hours, then collected by centrifugation, washed with water, and dried at 60°C.

X-ray diffraction analysis confirmed the formation of LDH structures in all samples, with basal spacings of approximately 9.0 Å for nitrate-intercalated LDHs and 7.7 Å for chloride forms. No visible differences in XRD patterns were observed between the samples doped with transition metals as well as pure Li/Al-LDH. The chemical analysis indicated Zn(II) and/or Co(II) presence in the synthesized structures. Adsorption–desorption studies revealed that synthesis conditions significantly influenced performance. The materials synthesized in 8 M NaOH exhibited higher lithium release ($\sim 3.0 \pm 0.5$ mg/g) in 5 studied cycles. Moreover, high selectivity of Li adsorption was noticed in relation to co-occurring Na^+ , K^+ , Ca^{2+} , and Mg^{2+} ions. However, no clear improvement of Li adsorption/desorption was observed between the doped LDHs. The presentation will additionally discuss the influence of Zn(II) and Co(II) incorporation on the structural stability of LDHs in brine environments.

This project was supported by the National Science Centre, Poland under the OPUS call in the Weave programme No. 2023/51/I/ST11/00368. The authors acknowledge the Fund for Scientific Research – Flanders for financial support FWO-WEAVE G000425N.

CHROMIUM OXIDATION ON FERRIHYDRITE UNDER ATMOSPHERIC CONDITIONS WITH ULTRAVIOLET IRRADIATION: TRENDS AND MECHANISMS

Lin, Li-Pang¹, Kung, Yu-Yu¹, Liu, Yu-Ting¹, and Hsu, Liang-Ching*¹

¹Department of Soil and Environmental Sciences, National Chung Hsing University, Taichung, 40227, Taiwan. *hsulc@nchu.edu.tw

This study explores the redox behavior of chromium in particulate matter derived from soil dust, emphasizing the role of ferrihydrite in simulating particulate matter composition. Using an oxidation flow reactor, the research investigates chromium transformation under varying atmospheric conditions by simulating hydroxyl radical formation and examining how these radicals promote chromium(III) oxidation to toxic chromium(VI) via interactions with iron oxides, which are common inorganic components of particulate matter. The study also evaluates how humidity influences hydroxyl radical generation and chromium redox reactions. Ferrihydrite was used to adsorb chromium(III), forming chromium-ferrihydrite complexes, and photoreactions were examined under different relative humidity levels (20%, 40%, 55%, and 70%).

Results show that increasing humidity reduces chromium(VI) formation in chromium-ferrihydrite systems, while chromium without ferrihydrite exhibits enhanced chromium(VI) production at higher humidity. This contrast suggests that iron in chromium-ferrihydrite modulates chromium oxidation, particularly under low humidity conditions where chromium(VI) formation is most pronounced. Ultraviolet light absorption by water vapor reduces light intensity but enhances iron(III) to iron(II) photoreduction, thereby increasing chromium(III) reactivity with iron(II) and hydroxyl radicals. The accumulation of iron(II) also promotes chromium(VI) reduction. These findings demonstrate the dual influence of atmospheric humidity and iron oxides on chromium redox cycling. Overall, the study confirms that atmospheric hydroxyl radicals can oxidize chromium(III) to chromium(VI), with iron playing a critical role in regulating this process under light irradiation. The results provide new insights into heavy metal transformation in atmospheric particulate matter and support strategies to mitigate health risks associated with chromium(VI) exposure.

FUNCTIONAL EVALUATION OF CLAY MINERALS AND CARBON-BASED ADSORBENTS FOR ANTIMICROBIAL AND CYTOPROTECTIVE EFFECTS IN A POULTRY DISEASE MODEL.

Agada E. Samuel*¹, Caldwell Denise², Allen J. Byrd², Farnell Morgan¹, Youjun Deng³, Timothy Phillips⁴, McElroy Audrey¹, Oladokun Samson¹

¹Department of Poultry Science, Texas A&M AgriLife Research, College Station, TX.

²U.S. Department of Agriculture, Agricultural Research Service, Southern Plains Agricultural Research Center, College Station, TX.

³Department of Soil and Crop Sciences, Texas A&M AgriLife Research, College Station, TX.

⁴Department of Veterinary Physiology and Pharmacology, Texas A&M University.

[*samuellagada@tamu.edu](mailto:samuellagada@tamu.edu)

Necrotic enteritis (NE), caused by *Clostridium perfringens* (CP), remains a major threat in antibiotic-free poultry systems, yet effective strategies remain limited. This study investigated the direct antimicrobial and cytoprotective and antioxidant effects of seven natural adsorbents (NA): clays (Kaolinite, Bentonite 4x, Wyoming Mx, Sodium montmorillonite), Graphite, Wood biochar, and Agricultural waste biochar. Samples (n=6) of each natural adsorbent in 3 independent experiments were used for all assays. Antibacterial activity against CP was evaluated using microbroth dilution and agar diffusion assays, while cell viability was evaluated using MTT assay and quantification of intracellular reactive oxygen species (ROS) levels using the DCFDA/H₂DCFDA assay using primary chicken intestinal epithelial cells derived from the duodenum, jejunum, and ileum. Agar diffusion showed that sodium montmorillonite, graphite, kaolinite, bentonite, and both biochar types inhibited (P<0.05) CP growth in a dose-dependent manner. Sodium montmorillonite, hardwood biochar, and agricultural-waste biochar also exhibited the strongest (p<0.05) antibacterial activity at 100, 50, and 25 mg/mL using agar well diffusion. A marked reduction (p < 0.05) in ROS generation in adsorbent-treated cells compared to negative controls was also observed, with the most pronounced antioxidant effect observed in graphite, bentonite, and wood biochar treatments across all intestinal segments. The MTT data indicates that kaolinite, sodium montmorillonite and wood biochar maintained high cell viability at the lowest concentrations of tested concentration range (3.125–100 mg/mL). Collectively, these findings suggest that specific natural adsorbents particularly graphite, sodium montmorillonite, bentonite, and hardwood biochar based on demonstrated antimicrobial and cytoprotective effects could be potential therapeutic agents against NE in poultry

PROBING STRUCTURAL CHANGES OF SEPIOLITE AND ZEOLITIC WATER DYNAMICS WITH TEMPERATURE-DEPENDENT INFRARED SPECTROSCOPY AND MOLECULAR SIMULATIONS

Bidemi Fashina^{1,2}, Randall T. Cygan¹, Md Wasek Foysal¹, and Youjun Deng^{1*}

¹Department of Soil and Crop Sciences, Texas A&M University, College Station, TX 77843-2474, USA

²Geochemistry Department, Sandia National Laboratories, P.O. Box 5800-0754, Albuquerque, New Mexico 87123, United States

*yjd@tamu.edu

Fibrous, modulated 2:1 clay minerals palygorskite and sepiolite are composed of unique tunnel structures with siloxane surfaces serving as the ceiling and floor and with structural M-OH₂ water groups of the octahedral sheet as the side walls. The tunnel-confined water appeared to have different physical and chemical properties from the bulk water that the mineral suspended in. These sub-nanometer features enable the selective adsorption of certain compounds such as indigo dye and a virulence factor pyocyanin to the tunnels. The determinative roles of the tunnel structure, surface polarity, confined water or the structural OH₂ groups on the selectivity of the pigments, toxins, or similar compounds are poorly understood. Studying the dehydration of sepiolite and palygorskite surfaces and tunnels can elucidate the structure, dynamics, and reactivity of confined water in these minerals. Sepiolite, a hydrated magnesium silicate with tunnel-like structures, contains zeolitic water (H₂O), bound water (OH₂), and structural hydroxyl group (OH), which influence its thermal and structural properties. The objective of this study was to investigate the dehydration dynamics of sepiolite using *in situ* variable-temperature infrared (IR) spectroscopy (25–300°C) and classical molecular dynamics (MD) simulations. The IR spectra reveal that most of the zeolitic water molecules (ν 3375 cm⁻¹ and δ 1660 cm⁻¹) are lost at ~100°C, and the residual zeolitic water molecules are lost at ~200°C. Confinement in tunnels makes zeolitic waters more thermodynamically stable than surface-adsorbed waters (ν 3252 cm⁻¹), which are completely lost by 100°C. The gradual evacuation of the tunnel results in a shift in the stretching vibration of structural waters from 3690 to 3675 cm⁻¹ due to diminished repulsion from the hydrogen atoms of zeolitic waters. The bound waters (ν 3616, ν 3565 and δ 1620 cm⁻¹) are stable until 300°C and subsequent loss induced the folding of layers. The MD simulations of a 4a x 2b x 10c supercell (Sep-8H₂O to Sep-0H₂O zeolitic water hydration states) show a ~1.2% tunnel height reduction upon dehydration, consistent with weakened Si–O–Si ribbons (1210 shifts to 1195 cm⁻¹). The zeolitic water molecules form 4, 3, and 2 structured layers in Sep-8H₂O, Sep-4H₂O, and Sep-2H₂O, respectively, with diffusion coefficients increasing from 5.0 x 10⁻¹⁰ m²/s to 7.5 x 10⁻⁹ m²/s as hydrogen bonding decreases. These findings elucidate the coordinated interplay of water types and structural changes in sepiolite, offering insights into its thermal stability and potential applications in catalysis and adsorption.

DEVELOP A CLAY-BASED PLATFORM AS AN ANTIBIOTIC ALTERNATIVE TO DISARM *PSEUDOMONAS AERUGINOSA*

Foysal, Md Wasek^{*1}, Hu, Jialin¹, Gentry, Terry¹, Cannon, Carolyn L², Deng, Youjun¹

¹Dept. Soil and Crop Sciences, Texas A&M University, College Station, Texas, 77843, USA

² Dept. Microbial Pathogenesis and Immunology, Texas A&M Univ., Bryan, Texas, 77807, USA

*wasek_foysal@tamu.edu

Pseudomonas aeruginosa is a widely distributed opportunistic pathogen responsible for serious hospital-acquired infections, including ventilator-associated pneumonia and surgical site infections. Patients with cystic fibrosis (CF), immuno-compromised individuals or burn victims are vulnerable to these bacteria. This bacterium produces several critical virulence factors, including pyocyanin, a redox-active phenazine that generates reactive oxygen species and causes oxidative damage to host cells, and iron-scavenging siderophores such as pyoverdine and pyochelin. New approaches of disrupting bacterial iron metabolism show promising antimicrobial effects. Our recent studies suggested that clay minerals, smectite and sepiolite can effectively adsorb and hold pyocyanin within their interlayer space or structural tunnels. We propose a synergistic approach of binding virulence factors and disrupting iron metabolism by the clay minerals. The objectives of the research were to assess the effects of the modified and synthesized clay minerals on 1) *P. aeruginosa* growth, 2) virulence factor production, and 3) gene expression.

A sodium smectite (Na-Sm), a modified smectite, sepiolite, and a layered double hydroxide (LDH) were prepared and added to Luria-Bertani (LB) medium containing *P. aeruginosa* PAO1. Bacterial growth was monitored at OD₆₀₀, pyocyanin was extracted with chloroform and quantified at 520 nm. Pyoverdine was measured by fluorescence spectroscopy. For RNA sequencing, *P. aeruginosa* cultures were grown aerobically in LB broth under shaking conditions without clay or with low and high concentrations of the clays. Cultures were harvested at the late-exponential to early stationary phase. RNA sequencing was performed on Illumina NovaSeq X Plus platform, and differential expression analysis was conducted to evaluate virulence factor-associated gene expression.

At 0.5 mg/mL, Na-Sm and sepiolite had minimal effects on bacterial growth and virulence factor production. In contrast, at the same concentration, modified Sm and LDH achieved 54% and 96% growth inhibition, respectively. In addition to inhibiting bacterial growth, these two materials also reduced virulence factors production. RNA-seq identified 5,698 genes and revealed significant transcriptional shifts under the modified Sm and LDH treatments. The modified Sm exhibited concentration-dependent regulation of pyoverdine (*pvd*) genes, with 0.2 mg/mL decreasing and 0.025 mg/mL increasing expression relative to the control. LDH at 0.025 mg/mL suppressed the expression of both *pvd* and pyocyanin (*phz*) genes, whereas 0.0125 mg/mL LDH had minimal effects. In contrast, sepiolite at 1 mg/mL increased *pvd* and *phz* expression, while Na-Sm had minimal effects. Additionally, LDH suppressed genes related to adhesion and motility, and modified Sm, LDH (0.025 mg/mL), and sepiolite (1 mg/mL) reduced quorum sensing-related gene expression. These findings highlight the potential of modified smectite and LDH as non-antibiotic alternatives for mitigating virulence in *P. aeruginosa*.

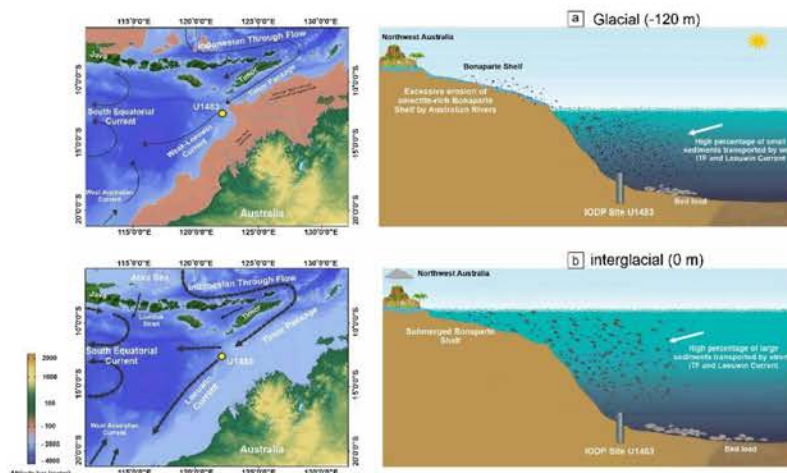
QUATERNARY REORGANIZATION OF THE INDONESIAN THROUGHFLOW AND ITS INFLUENCE ON REGIONAL SEA LEVEL AND MONSOON DYNAMICS

Sarim Muhammad*¹

¹State Key Laboratory of Continent Evolution and Early Life, Department of Geology, Northwest University, Xi'an, 710000, China.

*sarimmuhammad@nwu.edu.cn

Understanding how low-latitude ocean circulation and hydroclimate respond to glacial-interglacial forcing is essential for improving future sea-level projections, particularly in regions where ocean-atmosphere coupling and land-ocean sediment fluxes influence regional sea-level variability. The Indonesian Throughflow (ITF), the only low-latitude gateway between the Pacific and Indian Oceans, plays a key role in regulating heat transport, regional sea level, and the Australian summer monsoon (ASM), yet its long-term sensitivity to climate forcing remains poorly constrained. Here we reconstruct Mid-Late Quaternary (~800 kyr) variability of the ITF and ASM using high-resolution clay mineral assemblages, Sr-Nd-Pb isotopes, and grain-size records from IODP Site U1483 along the northwest Australian margin. Clay minerals are dominated by smectite, with moderate kaolinite and illite and minor chlorite. Combined clay mineral and radiogenic isotope ($^{87}\text{Sr}/^{86}\text{Sr} = 0.730\text{-}0.720$; $\epsilon\text{Nd} = -8.22$ to -10.73 ; $^{206}\text{Pb}/^{204}\text{Pb} = 19.25\text{-}18.95$) indicate that sediments were primarily derived from the Victoria and Ord Rivers of the Kimberley region, with some contributions from the Timor region via the ITF. Time-series records show pronounced glacial-interglacial cyclicity, with finer grain size, higher smectite, and low kaolinite and illite during glacials, and coarser sediments with increased kaolinite and illite during interglacials. Ratios of kaolinite/smectite, and clay/silt track variations in river discharge, monsoon intensity, and ITF strength, indicating a stronger ASM and intensified ITF during interglacials, and weakened conditions during glacials. A distinct shift at ~450 ka coincides with the Mid-Brunhes Event, marking the onset of extreme glacial-interglacial variability and an enhanced imprint of high-latitude forcing (65°S). Orbital-scale variability shows power in the 100-kyr, 41-kyr, and 23-kyr bands, reflecting that ice-sheet-driven climate cycles and low-latitude insolation forcing jointly regulated ITF-ASM dynamics. These results provide long-term process-based constraints relevant for improving representations of low-latitude circulation and regional sea-level variability in future projection frameworks.



PROTECTIVE EFFECTS OF A BIO-CLAY PRODUCT ON GROWTH, JEJUNAL HISTOMORPHOLOGY, BACTERIOME, AND METABOLITES IN AFLATOXIN-CHALLENGED BROILERS

Oluseyifunmi Iyabo W.¹, Phillips Timothy², Isakeit Thomas³, Deng Youjun⁴ and Oladokun Samson¹

¹*Department of Poultry Science, Texas A&M University, College Station, TX, 77843*

²*Department of Veterinary Physiology and Pharmacology, Texas A&M University*

³*Department of Plant Pathology and Microbiology, Texas A&M University*

⁴*Department of Soil and Crop Sciences, Texas A&M University, College Station, TX*

iyabo.oluseyifunmi@ag.tamu.edu

Aflatoxin (AF) remains a major threat to poultry health and performance, prompting growing interest in natural adsorbents such as clay minerals to mitigate its toxic effects. In a 28-day study, 240 day-old off-sex Cobb-500 chicks were used to evaluate the ameliorative effects of dietary Bio-clay (a sodium-rich montmorillonite conjugated with ZnO) against the toxic impacts of aflatoxin (AF). Birds were assigned to 4 treatments with 8 replicate cages each: (1) control (corn–soy diet), (2) control + clay (8 g/kg), (3) AF challenge (2 mg/kg), and (4) AF challenge + clay (2 mg/kg AF + 8 g/kg clay). Growth performance was assessed on days 0, 7, 14, 21, and 28. Jejunal tissues and contents were collected on day 21 for histomorphology and full-length 16S rRNA sequencing, while cecal samples were collected on days 21 and 28 for short-chain fatty acid (SCFA) analysis. From days 0–7, the weight gain (WG), final weight gain (FBW), and feed conversion ratio (FCR) were not significantly ($P > 0.05$) influenced by treatments. From days 7–14, birds in the control and unchallenged clay groups had greater ($P < 0.05$) WG and FBW and lower FCR than other groups, although AF-challenged birds receiving clay achieved FI and FBW comparable to both unchallenged groups. Across days 14–21, 21–28, and cumulatively from 0–28, WG and FBW remained higher ($P < 0.05$) and FCR lower in the control and unchallenged clay-fed birds, while challenged birds fed clay-maintained FI similar to the control. SCFA concentrations at day 21 were not significantly affected; however, branched-chain fatty acids (isovalerate, isobutyrate) were higher ($P = 0.001$) in the unchallenged birds fed dietary clay at day 28. Jejunal histomorphology and bacterial diversity (alpha & beta) were not significantly ($P > 0.05$) altered. Linear discriminant analysis effect size (LEfSe) indicated a tendency ($P = 0.068$) for clay to increase family *Streptococcaceae* abundance under unchallenged conditions. Overall, these findings indicate that while Bio-clay did not fully counteract AF-induced growth depression, it was able to sustain feed intake, maintain gut integrity, and microbial diversity in AF-challenged birds.

Keywords: Aflatoxin, Bio-clay, Growth performance, Microbiome, Short-chain fatty acids

THE MINERALOGY, GEOCHEMISTRY, AND GENESIS OF THE SILICON RIDGE CLAY DEPOSIT, UTAH COUNTY, UTAH, USA

Gerratt, Tyler ^{*1}, Zeitoun, Andre ², Colledge, Preston ², Christiansen, Eric ¹, Kalan, Ravi ², and Bickmore, Barry ¹

¹Department of Geological Sciences Brigham Young University, Provo, UT 84602, USA.

²Ionic Mineral Technologies, Provo, UT, 84601, USA.

*tg297@byu.edu

The Silicon Ridge clay deposit (traditionally known as the Fox clay deposit) is located on the southern flank of Lake Mountain, Utah, within the Paleogene White Knoll Member. It contains abundant halloysite alongside elevated concentrations of critical metals. While noted in historical literature, the deposit lacked a comprehensive evaluation. To address this gap, this study establishes a spatial, mineralogical, and geochemical framework for the deposit using an extensive suite of drill chip and core samples (100+ drill holes).

Our analytical approach integrates X-ray diffraction, X-ray fluorescence, and inductively coupled plasma mass spectrometry, supplemented by stable isotope measurements ($\delta^{18}\text{O}$, δD , $\delta^{13}\text{C}$, $\delta^{34}\text{S}$). Collectively, these mineralogical, geochemical, and isotopic indicators are used to reconstruct the original host lithologies and evaluate competing mechanisms of alteration—specifically determining the relative contributions of low-temperature weathering by meteoric water versus hydrothermal or magmatic fluid inputs..

Our findings indicate that the Silicon Ridge clay deposit formed through alteration of volcanic ash lenses interlayered with travertine mounds and fluvio-lacustrine cobble beds in a paleosurface lacustrine-margin setting. Pyrite and marcasite, together with oxidized sulfate phases including gypsum, alunite, and jarosite, are common within distinct stratigraphic intervals. Isotopic and mineralogical data indicate that low-temperature meteoric waters (we only have a few datapoints in the shallow part of the drilling) contributed to late-stage alteration of volcanic ash to clay; however, elevated concentrations of As, Cs, and W cannot be explained by near-surface weathering alone and point to an additional hydrothermal or magmatic-fluid component. These results resolve the stratigraphic context of the deposit and support a hybrid genetic model in which volcanic ash alteration, meteoric fluid interaction, and hydrothermal-metal enrichment collectively contributed to halloysite formation and critical-metal anomalism at Silicon Ridge.

LC-OD: A PORTABLE R-BASED APPLICATION FOR SMECTITE LAYER CHARGE CALCULATION USING THE OD METHOD

Kuligiewicz, Artur*¹

¹Institute of Geological Sciences, Polish Academy of Sciences, Krakow, Poland.

*ndkuligi@cyf-kr.edu.pl

With the development of the OD method, a new spectroscopic technique for measuring the smectite layer charge (LC) has become available. This method uses the position of a sharp, high-frequency O–D stretching mode (ν O–D), present in the attenuated total reflectance infrared (ATR-IR) spectrum of D₂O vapor-saturated smectite, as an LC proxy. One of the crucial steps in the OD method workflow is the precise determination of ν O–D. This is commonly achieved using built-in algorithms of the spectroscopic software provided with FTIR spectrometers. As the OD method has been demonstrated to be sensitive to very small changes in the apparent LC of smectitic surfaces, small differences produced by various algorithms used in ATR-IR data processing become non-negligible.

LC-OD is an R-based application designed to calculate LC from ATR-IR spectra of D₂O-saturated smectites or other smectite-bearing materials. It operates via a browser-based graphical user interface (GUI) using the Shiny package. Comparison of ν O–D positions determined with LC-OD and OMNIC software (Thermo Fisher Scientific) shows that LC-OD returns ν O–D positions comparable to the commercial program within ± 0.2 cm⁻¹, which is similar to the differences between ν O–D positions determined with OMNIC and OPUS (Bruker Optics GmbH) (Figure 1). The user has full access to the LC-OD code and complete control over the algorithm. The LC-OD program is available from a GitHub repository (<http://bit.ly/4bUBpbj>) as a portable R application that does not require installation of the R environment.

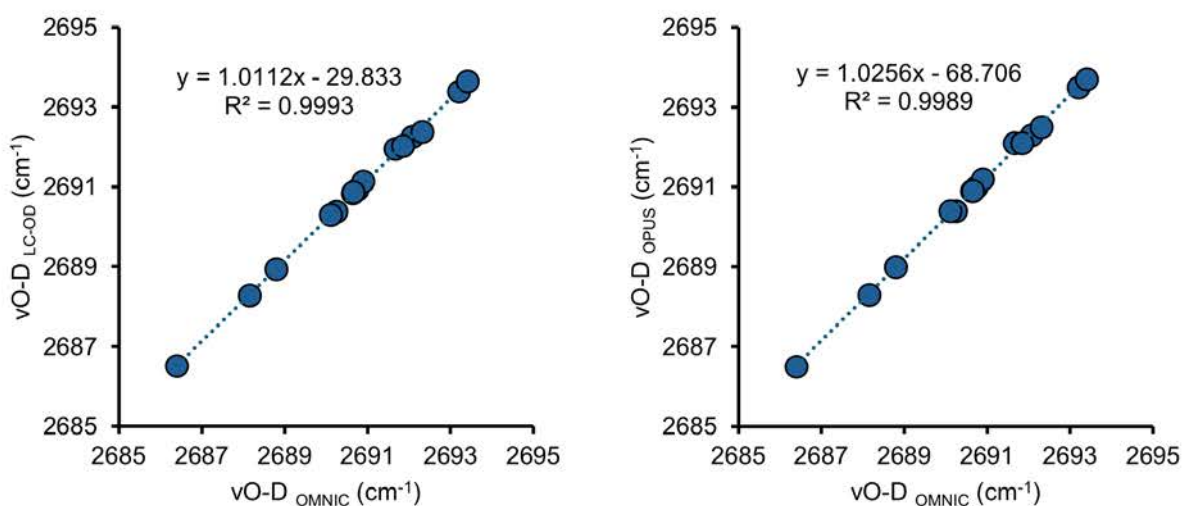


Figure 1. Comparison of ν O–D positions determined with OMNIC, OPUS, and LC-OD.

A PEAK-MODELING PROGRAM FOR THERMOGRAVIMETRIC ANALYSIS

Teeples, Sky^{*1}, Bickmore, Barry R.¹, Evans, Emily J.²

¹Department of Geological Sciences, Brigham Young University, Provo, UT 84606, USA.

²Department of Mathematics, Brigham Young University, Provo, UT 84606, USA.

*komeumai@student.byu.edu

Thermogravimetric analysis (TGA) is a standard technique for identifying and quantifying minerals (including clay minerals) that undergo weight loss due to degassing as they are heated. A sample is continuously weighed inside a furnace while the temperature is steadily ramped, and the data is displayed in terms of the percentage of the initial mass ($Wt\%$) as a function of temperature (T). Inflections in the weight loss curve indicate distinct processes, e.g., dehydroxylation events for different minerals, which occur in different temperature ranges.

The temperature ranges for different processes may overlap, however. Overlapping degassing processes can more easily be identified by plotting the negative temperature derivative of the $Wt\%$ vs. T curve as a function of T , where individual processes can be seen as peaks. To estimate the weight loss associated with overlapping processes, some peak deconvolution strategy must be applied, after which the separated peaks can be integrated.

To address this need, we have created AnalyzeTGA, a computer program for fitting peaks to derivative TGA data to estimate weight loss associated with individual processes. The program loads TGA data, applies appropriate smoothing, displays both the weight loss and derivative curves, allows the user to select approximate peak locations, fits the peaks to the derivative data, and calculates the weight loss associated with each peak. New peaks can be added until the data is closely modeled.

It is common for Gaussian peaks to be used, but peaks in derivative TGA curves are very often asymmetric. In that case, it might take multiple Gaussians to adequately model a peak representing a single process. Therefore, AnalyzeTGA allows the user to model the derivative curve with either Gaussian or split pseudo-Voigt peaks.

MATLAB or standalone (Windows or Mac) versions of the program can be downloaded from <http://epiphaneia.byu.edu>, and a browser-based web application can be accessed at <https://geologymatlab.byu.edu:9988/webapps/home/>.

MACHINE LEARNING FOR MINERAL IDENTIFICATION

Evans, Emily J.*¹, Bickmore, Barry R.², and Chandler, Spencer S.¹

¹Department of Mathematics, Brigham Young University, Provo, UT 84602, USA.

²Department of Geological Sciences, Brigham Young University, Provo, UT 84602, USA.

*evanse@byu.edu

Quantitative phase analysis (QPA) of whole rocks and sediments using X-ray powder diffraction (XRPD) is a standard, workhorse technique for many types of geologists and soil scientists, and there are a number of methods for accomplishing this. Regardless of the method, however, the main source of analytical error in QPA is usually the likelihood of inexperienced analysts choosing inappropriate phases for modeling a sample XRPD pattern. The algorithms employed by standard XRPD analysis software to help the user choose phases to include typically involve simple peak-matching routines, which cannot mimic the sorts of background knowledge expert analysts use to make such decisions (e.g., the relative prevalence of different minerals, which minerals are likely to occur together, and the results of other analytical techniques).

RockJockML is a full-pattern summation QPA program for analyzing XRPD patterns of geological materials, based on the original RockJock program created by D.D. Eberl of the U.S. Geological Survey in Microsoft Excel. We have updated the software to provide dramatically increased processing speed, an intuitive workflow, and a number of features, including machine learning tools, designed to help the user more accurately pick phases for inclusion in the analysis. MATLAB or standalone (Windows or Mac) versions of the program can be downloaded from <http://epiphaneia.byu.edu>, and a browser-based web application can be accessed at <https://geologymatlab.byu.edu:9988/webapps/home/>.

The current version of RockJockML contains several options for automated phase selection including some that utilize models generated by machine learning (ML) algorithms. The first ML algorithm is a forward method (adding one phase at a time) that utilizes association rules that quantify the likelihood of co-occurrence of minerals. This algorithm can also be used in conjunction with a user-driven workflow for a semi-automated analysis. The second ML algorithm is a trained deep learning model that identifies crystalline phases in mineral mixtures with high accuracy.

EMMALAB: A TOOL FOR SEDIMENT UNMIXING

Bickmore, Barry R.^{*1}, Thompson, Alyssa N.¹, Evans, Emily J.², Carling, Gregory T.¹

¹Department of Geological Sciences, Brigham Young University, Provo, UT 84606, USA.

²Department of Mathematics, Brigham Young University, Provo, UT 84606, USA.

*barry_bickmore@byu.edu

Detrital sediments and sedimentary rocks form via deposition of eroded material from previously existing rock bodies. Determining the provenance of those sediments (i.e., the extent to which different rock bodies contributed material to the sediment in question) can be an important tool for reconstructing paleoflow directions for rivers, glaciers, ocean currents, and sea ice. If we assume minimal precipitation, dissolution, or alteration of material during and after transport, this becomes essentially a mixing problem.

Andrews and Eberl (2012) created SedUnMix, a Microsoft Excel-based tool for calculating the contributions of sediment sources (endmembers) in a sediment mixture using the results of quantitative X-ray powder diffraction analysis. That is, the mineralogical compositions of proposed endmembers and the mixture are determined, and SedUnMix estimates the fractional contributions of each endmember to the mixture. Mathematically, this essentially involves the solution of a system of linear equations in which the mixture's fractional content of each mineral is described as a linear combination of that mineral's content in the proposed endmembers.

Unfortunately, Microsoft Excel's macro language is not backwards compatible, rendering the SedUnMix program obsolete. It turns out, however, that a program we created for hydrograph separation will also work for sediment unmixing. EMMALAB implements and streamlines Christopherson and Hooper's (1992) endmember mixing analysis (EMMA) in a MATLAB-based application available on Hydroshare (<https://www.hydroshare.org>). It is available in MATLAB or standalone (Windows or Mac) versions, and a browser-based web application can be accessed at <https://geologymatlab.byu.edu:9988/webapps/home/>.

There are many tools included in EMMALAB to streamline the process and make informed judgements about modeling choices, such as which potential endmembers to choose, and which minerals to use as tracers. It also obviates the need for certain restrictions (e.g., the maximum number of endmembers) built in to SedUnMix.

Andrews, JT, and Eberl, DD (2012) Determination of sediment provenance by unmixing the mineralogy of source-area sediments: The "SedUnMix" program, *Marine Geology* 291-294, 24-33.

Christopherson, N, and Hooper, RP (1992) Mixing analysis of stream water chemical data: The use of principal components analysis for the end-member mixing problem, *Water Resources Research* 28, 99-107.

THE TERRESTRIAL PALEOCLIMATE DATABASE: AN OPEN-ACCESS RESOURCE FOR SEDIMENTOLOGIC AND GEOCHEMICAL PALEOCLIMATE STUDIES

Burgener, Landon*¹, Hayes, Sebastian², McKay Morgan¹, Santibañez, Santiago¹, Beggs, Britton¹, Haynes, Haylee¹, Mason, Eldon¹, Trejo, Camila¹, and Tay, Albert²

¹Department of Geological Sciences, Brigham Young University, Provo, UT 84602, USA.

²Department of Electrical and Computer Engineering, Brigham Young University, Provo, UT 84602, USA.

*landon.burgener@byu.edu

Reconstructing Earth's past climate is essential for understanding climate system behavior under greenhouse and icehouse conditions and for improving predictions of future climate change. However, proxy-based paleoclimate data remain highly fragmented, inconsistently formatted, and often inaccessible, limiting their quantitative integration and comparison with climate model outputs. To address this challenge, we are developing a new open-access paleoclimate proxy database designed to standardize, integrate, and expand global proxy records across geologic time.

The database currently contains >40,000 samples spanning the past ~300 million years and incorporates both quantitative geochemical proxies and semi-quantitative lithologic indicators such as mean annual temperature reconstructions based on the isotopic composition of clay minerals and mean annual precipitation reconstructions based on clay mineral elemental compositions. By integrating these diverse proxy types within a unified relational framework, the database enables users to query and analyze paleoclimate information by age, location, proxy type, and original data source. This structure facilitates the identification of samples and geographic regions where clay minerals have been used as paleoclimate indicators, as well as the identification of prior paleoclimate studies relating clay mineralogy and sediment composition to ancient environmental conditions.

For the clay minerals community, this resource provides a new tool to utilize previously dispersed datasets, evaluate spatial and temporal trends in clay mineral proxies, compare paleoclimate reconstructions from clay-based proxies to other lithologic and geochemical proxies, and support new quantitative paleoclimate reconstructions. The associated web-based interface will allow users to explore data through interactive mapping, filtering, and download tools, promoting broader accessibility and interdisciplinary collaboration.

Importantly, the database is designed for long-term growth. Future development will include community-driven data contributions, allowing researchers to upload new datasets through a standardized submission and quality-control workflow. By centralizing and expanding access to paleoclimate proxy data, this project establishes critical infrastructure for advancing paleoclimate research and enhancing the role of clay minerals in reconstructing Earth's climate history.

FINITE ELEMENT ANALYSIS OF PILED RAFT TUNNEL INTERACTION UNDER CHANGING CLAY CONDITIONS

AL-LABAN, Haider Ehssan

Assistant Head of Department of Structures and Water Resources, University of Kufa, Najaf, 54001, IRAQ.

haidere.allaban@uokufa.edu.iq

ABSTRACT:

This paper presents a finite element analysis to investigate the behavior of the piled-raft tunnel system in clay soil. The aim of this study is carried out to contact the elements model between the piled-raft tunnel and clay soil by Abaqus software CAE. This approach has characteristics that are conducted by the group's (1×2) piled raft tunnel; the clearance distance (H) is 130 mm from the pile tip to the top of the surface of the tunnel, and the pile length (L) is 200 mm. The tunnel features a square cross-section measuring 100 × 100 mm, subjected to forces along the z-axis of the model, with a thickness of 2 mm. The vertical distance from the base of the pile group is 5 mm. The behavior of the clay structure interface affected the stresses and displacements of the piled rafts in the tall building and tunnel. In addition, the sensitivity of clay soil to swelling and shrinkage under changing water conditions was observed.

KEYWORDS: finite element analysis, clay soil, swelling and shrinkage, clay structure interface, piled raft foundation, tunnel.

A CLAY-BASED PLATFORM TO SEQUESTERATE VIRULENCE FACTORS PRODUCED BY *CLOSTRIDIUM PERFRINGENS* TO REGULATE THE PATHOGEN'S GENE EXPRESSION

Foyosal, Md Wasek^{*1}, Hu, Jialin¹, Gentry, Terry¹, Oladokun, Samson², Agada, Samuel E.², Deng, Youjun¹

¹Department of Soil and Crop Sciences, Texas A&M University, College Station, Texas, 77843, USA

²Department of Poultry Science, Texas A&M University, College Station, TX 77843, USA

*wasek_foysal@tamu.edu

Clostridium perfringens is a Gram-positive, drug-resistant, anaerobic bacterium and the primary producer of alpha-toxin. This toxin is a zinc-dependent C-type phospholipase (PLC) enzyme that disrupts eukaryotic cell membranes, leading to severe effects such as sudden death syndrome in domestic animals and necrotic enteritis in broiler chickens. There is an urgent need for safe and economical alternatives of antibiotics to battle this drug-resistant pathogen. We hypothesized that alpha-toxin adsorption within the smectite interlayer would induce protein unfolding and conformational changes, thereby neutralizing its enzymatic toxicity. The adsorption of the toxins may induce gene expression changes in the pathogen.

The objectives of this study were to: (1) determine the adsorption capacity, affinity, and bonding mechanism of clay minerals with alpha-toxin; (2) examine post-adsorption enzymatic activity; and (3) evaluate the impact of clays on virulence factor production and gene expression. For this study, Lyophilized PLC from *C. perfringens* (37 units/mg) was equilibrated with Na-smectite (Na-Sm), Ca-smectite (Ca-Sm), Zn-smectite (Zn-Sm), and sepiolite. Access of the toxins to the interlayer gallery in smectites and tunnel in sepiolite were investigated using X-ray diffraction (XRD) and Fourier Transform Infrared Spectroscopy (FTIR). Virulence factor production will be quantified via ELISA, and PLC activity will be measured using the EnzChek Direct Phospholipase C Assay Kit. *C. perfringens* cultures for RNA sequencing were grown anaerobically in Thioglycollate broth with clay treatments at 0, 0.25, 0.5, and 2 mg/mL. Cultures were harvested after 8 h of incubation. RNA sequencing was performed on Illumina NovaSeq X Plus platform and was analyzed to evaluate virulence factor-related gene expression.

The Zn-Sm exhibited the highest PLC adsorption capacity of 12% of its dry mass. The PLC molecules successfully intercalated into the smectite interlayer space. In sepiolite, although size restrictions limited internal tunnel entry, variable-temperature XRD and FTIR analysis demonstrated that the toxin binds at and blocks the tunnels. Given the adsorption of PLC with clay minerals, it is expected that clay minerals also would reduce the concentration of virulence factors and enzyme activity in bacteria cultures. RNA-seq analysis identified a total of 3,663 genes and demonstrated that clay treatments significantly altered overall gene expression patterns relative to the control. Ca-Sm and Zn-Sm suppressed the expression of alpha-toxin (*cpa*) and NetB (*netB*) genes relative to the control, whereas Na-Sm and sepiolite showed minimal effects or even increased expression. These findings highlight the potential of specific clay minerals as non-antibiotic solutions for mitigating bacterial toxins through both direct adsorption and suppression of virulence gene expression.

HALLOYSITE-REINFORCED NANOCOMPOSITE HYDROGEL AS MULTIFUNCTIONAL INJECTABLE WOUND DRESSING

Wong, Li Wen ^{*1,2}, Tan, Joash Ban Lee², Pasbakhsh, Pooria^{3,4}

¹School of Environmental Science and Engineering, Guangdong University of Technology, Guangzhou 510006, P.R China.

²School of Science, Monash University Malaysia, 47500 Subang Jaya, Selangor, Malaysia.

³School of Engineering, Monash University Malaysia, 47500 Subang Jaya, Selangor, Malaysia.

⁴Department of Infrastructure Engineering, The University of Melbourne, Melbourne, VIC 3010, Australia.

*vivianwongliwen@gdut.edu.cn

Nanocomposite hydrogels, formed by crosslinked polymer networks reinforced with clay minerals, offer versatile platforms for biomedical applications. This study reports the fabrication of an injectable nanocomposite hydrogel incorporating halloysite nanotubes (Hal), a naturally occurring aluminosilicate clay mineral, into a polymer matrix of oxidized bacterial cellulose and gelatin. Hal, an abundant and low-cost mineral resource, serves multiple complementary roles within the hydrogel system: (1) facilitating the sol-gel transition required for injectability, (2) acting as a sustained-release carrier for antimicrobial drugs, and (3) leveraging its inherent hemostatic properties to accelerate clot formation at wound sites. The resulting Hal-reinforced nanocomposite hydrogel enables targeted, sustained antibiotic delivery to infection sites while simultaneously promoting wound recovery through enhanced hemostasis. Its injectable nature allows for minimally invasive administration, conforming to irregular wound geometries while providing structural support, combating bacterial infection, and controlling bleeding, all in a single formulation. This work demonstrates the utilization of halloysite for biomedical applications, offering a multifunctional platform integrating infection management, bleeding control, and wound dressing tailored for diverse wound types.

SURFACE AND INTERLAYER ENGINEERING OF SMECTITES FOR EFFICIENT REMOVAL OF MYCOTOXINS: ZEARALENONE, ALTERNARIOL AND ENNIATIN B

Matusik, Jakub^{*1}, Dziwińska, Klaudia¹, Deng, Youjun², Matras, Aneta³, Borowska, Dominika³, Jedziniak, Piotr³, Gbylik-Sikorska, Małgorzata³

¹AGH University of Krakow; Faculty of Geology, Geophysics and Environmental Protection; al. Mickiewicza 30, 30-059 Krakow, Poland.

²Department of Soil and Crop Sciences, Texas A&M University, College Station, TX 77843-2474, United States.

³Department of Chemical Research of Food and Feed, National Veterinary Research Institute, al. Partyzantow 57, Pulawy, 24-100, Poland.

*jmatusik@agh.edu.pl

The adsorption behavior of three chemically distinct mycotoxins: zearalenone (ZEN), alternariol (AOH), and enniatin B (ENN B) was investigated using modified smectites in aqueous systems and simulated gastric fluid (GF). Unmodified or smectites treated via cation exchange and/or calcination showed limited adsorption for the hydrophobic ZEN and AOH molecules. An exception was ENN B for which the removal was improved after Mg(II) exchange followed by mild heating. These treatments lowered layer charge, introduced hydrophobic domains and Lewis acid sites which most likely were responsible for additional ion–dipole and hydrogen bonding interactions apart.

In contrast, the modification with organic modifiers significantly improved the uptake of ZEN and AOH. This effect was attributed to expanded interlayer spacing and increased hydrophobicity. Among the tested modifiers, hexadecyltrimethylammonium bromide (C16) was the most effective due to its high loading. Moreover, part of the C16 molecules were present in neutral form and were held through hydrophobic chain-chain interactions with the electrostatically stabilized C16 molecules. Such arrangement created a dense coverage of the mineral support, dominated by the alkyl chains of hydrophobic nature. This favoured partitioning of mycotoxins. Other modifiers, such as ethyl lauroyl arginate (LAE®) and cocamidopropyl betaine (CAPB), were less efficient, probably because of steric hindrance effects which limited their incorporation into smectites' interlayer space. Functionalization with vitamin B1 also enhanced adsorption, particularly for the Na-smectite. Adsorption data followed the Freundlich model, indicating a partition-driven process. The performance remained high under acidic conditions but generally declined in alkaline media, except for the C16-modified samples. Additionally, the C16- and B1-modified smectites were less affected by pepsin in GF, whereas ENN B adsorption decreased markedly in all cases. Overall, the adsorption was governed by surface and interlayer chemistry rather than specific surface area of the adsorbents, highlighting the importance of targeted material design.

This project was partially supported by the National Science Centre Poland, under a research project awarded by Decision No. 2021/43/B/ST10/00868.

FUNCTIONALIZATION OF HALLOYSITE NANOTUBES FOR BIOMEDICAL APPLICATION

Liu Mingxian*¹, CheXiangyu¹, Shuiqing Zhou¹, Feng Yue¹.

¹Department of Materials Science and Engineering, College of Chemistry and Materials Science, Jinan University

Guangzhou 511443, PR of China

*liumx@jnu.edu.cn

Halloysite clay (Chinese medicine name: Chishizhi), manifested as one-dimensional aluminum silicate nanotubes (halloysite nanotubes, HNTs), has gained applications in hemostasis, wound repair, gastrointestinal diseases, tissue engineering, cosmetics, detection and sensing, and daily chemicals formulations, like tablets. Various biomedical applications of HNTs are derived from hollow tubular structures, high mechanical strength, good biocompatibility, bioactivity, and unique surface characteristics. This natural nanomaterial is safe, abundantly available, and may be processed with environmentally safe green chemistry methods. This review describes the structure and physicochemical properties of HNTs relative to bioactivity. We discuss surface area, porosity and surface defects, hydrophilicity, heterogeneity and charge of external and internal surfaces, and biosafety. The paper provides comprehensive guidance for the development of this tubule nanoclay and its advanced biomedical applications for clinical diagnosis and therapy.

References:

- [1] Feng Yue, Luo Xiang, Li Zichun, Fan Xinjuan, Wang Yiting, He Rong-Rong, Liu Mingxian. A ferroptosis-targeting ceria anchored halloysite orally drug delivery system for radiation colitis therapy, *Nature Communications*, 2023, 14: 5083.
- [2] Feng Yue, Zhang Di, Chen Xiangyu, Zhou Changren, Liu Mingxian. Confined-synthesis of ceria in tubular nanoclays for UV protection and anti-biofilm application, *Advanced Functional Materials*, 2024, 34(7): 2307157.
- [3] Zhao Puxiang, Hu Jiaojiao, Feng Yue, Wu Feng, Tan Cuiying, Chen Xiaodan, Liu Mingxian. Cu₃-xP nanocrystals filled halloysite nanotubes for chemodynamic therapy of breastcancer, *Journal of Colloid and Interface Science*, 2023, 655: 736-747.
- [4] Yue Feng, Xiangyu Chen, Rong-Rong He, Zhongqiu Liu, Yuri Lvov, Mingxian Liu. The Horizons of Medical Mineralogy: Structure-Bioactivity Relationship and Biomedical Applications of Halloysite Nanoclay, *ACS Nano*, 2024, 18(31): 20001-20026.

EDIBLE CLAY FOR THE MITIGATION OF TOXIC ENVIRONMENTAL CHEMICALS DURING OUTBREAKS, EMERGENCIES AND DISASTERS

Phillips, Timothy*¹, Wang, Meichen², Oladele, Johnson¹, Jackson, Steven¹, and Deng, Youjun³

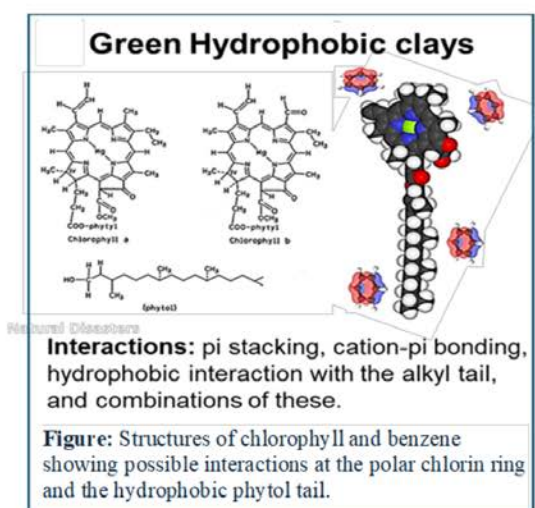
¹Department of Veterinary Physiology and Pharmacology, Texas A&M University, College Station, TX 77843, USA.

²Department of Environmental Health Sciences, University of Massachusetts Amherst, Amherst, MA 01003, USA

³Department of Soil and Crop Sciences, Texas A&M University, College Station, TX 77843, USA.

*tphillips@cvm.tamu.edu

Research has focused on the development and characterization of clay-based materials that can be used as dietary supplements to decrease toxin bioavailability and systemic exposure in vulnerable populations of humans and animals living near the site of outbreaks, emergencies and disasters. For example, soil and sediment containing toxic chemicals can be mobilized during flooding and redistributed into urban, rural and agricultural zones. Also, drought stress can increase the level of hazardous mycotoxins in the diet. Field-practical and cost-effective strategies to reduce health risks following these emergencies are highly desirable. The central hypothesis for most of my work has been to engineer edible, clay-based materials that can be used to decrease toxin exposure from contaminated diets, water, soil, and sediment. In earlier work, *in vitro*, *in silico* and *in vivo* studies were designed to validate the efficacy and affinity of toxin adsorption to basal and interlayer surfaces. Earlier work in Texas and Africa demonstrated that calcium montmorillonite clay (added to the diet) was effective in reducing aflatoxin bioavailability and molecular biomarkers of aflatoxin exposure from urine and blood.



This work has facilitated the engineering of clay-based materials that will bind diverse environmental chemicals and mixtures of concern. These materials are composed of nutrients and nutraceuticals derived from thermodynamic studies and computational predictions of potential interactions of clay surfaces with important toxins such as PFAS, PCBs, PAHs, mycotoxins and multidrug-resistant microbes. Previous reports from our laboratory have demonstrated the potency of green-engineered clays for diverse chemicals including benzene, PFAS and polystyrene (Figure). We have also investigated the binding and detoxification potential of chlorophyll-amended montmorillonite clays for aflatoxin B₁ (AFB₁).

In addition to analyzing binding metrics including affinity, capacity, free energy, and enthalpy, the sorption mechanisms of AFB₁ onto the surfaces of engineered clays were also investigated. Computational and experimental studies were performed to provide mechanistic insights, as well as to validate the efficacy and safety of these, and other adsorbent materials.

FROM MINERAL SURFACES TO MYCOTOXIN BREAKDOWN: UV-ACTIVATED SEMICONDUCTORS SUPPORTED ON KAOLIN-GROUP MINERALS

Dziewiątka, Klaudia^{*1}, Matusik, Jakub¹, Kuncewicz, Joanna², Błachowski, Artur¹, Sobańska, Kamila², Kuc, Joanna³

¹Faculty of Geology, Geophysics and Environmental Protection, AGH University of Krakow, al. Mickiewicza 30, 30-059 Krakow, Poland.

²Faculty of Chemistry, Jagiellonian University, Gronostajowa 2, 30-387 Krakow, Poland.

³Faculty of Chemical Engineering and Technology, Cracow University of Technology, Warszawska 24, 31-155 Krakow, Poland.

*dziewiatka@agh.edu.pl

Fusarium mycotoxins such as deoxynivalenol (DON) and zearalenone (ZEN) are globally widespread contaminants of cereals and water systems, posing serious risks to food safety and animal and human health. Their persistence and poor removal by conventional treatments necessitate advanced degradation strategies. In this context, kaolin-group minerals serve as robust supports for photoactive semiconductors enhancing toxin preconcentration, strengthen interfacial interactions, suppress nanoparticle aggregation, and promote uniform dispersion of active phases [1].

A series of kaolin-group minerals differing in morphology, texture and structural order was selected as supports, including a kaolinite-rich material (M), synthetic calcined kaolinite nanotubes (MNC), commercial halloysite (HS), and a halloysite-bearing sample (HD). These mineral matrices were functionalized (~20 wt%) with TiO₂, g-C₃N₄, or TiO₂/g-C₃N₄ for the degradation of ZEN, and with TiO₂, Fe₂O₃, or TiO₂/Fe₂O₃ for DON removal. ZEN elimination was carried out under photocatalytic conditions, whereas DON degradation required activation with peroxymonosulfate (2 mM).

The incorporation of aluminosilicate nanotubes as supports significantly improved textural properties and enhanced charge separation at the mineral-semiconductor interface. Electrochemical analyses revealed reduced charge-transfer resistance and extended charge-carrier lifetimes, confirming improved interfacial electron dynamics. Consequently, the MNC-based composites containing g-C₃N₄ and TiO₂/g-C₃N₄ achieved up to 98.8% ZEN removal within 25 min of UV irradiation. ZEN degradation was mainly driven by reactive oxygen species, particularly O₂⁻ and •OH, proceeding via isomerization and cleavage of functional groups and the aromatic ring to form oxygenated intermediates. For DON degradation, SEM and Mössbauer spectroscopy confirmed well-dispersed nanosized maghemite on the MNC surface, providing abundant redox-active sites for PMS activation. Accordingly, the MNC-supported TiO₂/Fe₂O₃ composite showed the best performance, achieving 98.8% DON degradation within 45 min, compared to 66.1% and 46.0% for the TiO₂-MNC and Fe₂O₃-MNC, respectively. Electrochemical measurements indicated a p-type character of the TiO₂-MNC and TiO₂/Fe₂O₃-MNC, consistent with enhanced charge transfer, while EPR identified •OH and ¹O₂ as the dominant radicals.

This project was supported by the National Science Centre Poland, under a research project awarded by Decision No. 2021/43/B/ST10/00868.

[1] K. Dziewiątka et al. (2025) Chemical Engineering Journal 506, 160198, <https://doi.org/10.1016/j.cej.2025.160198>.

EVALUATING AND CORRECTING THE ACCURACY OF THE FULL-PATTERN SUMMATION METHOD

Bickmore, Barry R.*¹, Evans, Emily J.²

¹Department of Geological Sciences, Brigham Young University, Provo, UT 84602, USA.

²Department of Mathematics, Brigham Young University, Provo, UT 84602, USA.

*barry_bickmore@byu.edu

Full-pattern summation (FPS) is a popular method of quantitative phase analysis (QPA) for X-ray powder diffraction (XRPD) data on mixtures of geological materials. Its usefulness is especially evident for mixtures containing disordered clays and amorphous substances, because FPS is based on linear combinations of empirically obtained diffractograms from pure reference materials. That is, diffractograms of disordered clays and amorphous substances can be difficult to simulate from known structures, as is needed for Rietveld analysis. Instead, FPS employs reference intensity ratios (RIRs) calculated relative to an internal standard (usually corundum) on the basis of the integrated area under the diffractogram over a certain 2θ range.

A number of factors negatively affect the accuracy of FPS. Some of these can be mitigated with careful, consistent sample preparation and instrumental setup, but the phenomenon of microabsorption presents a different problem. Microabsorption effects can be related to too-large particle size, but it can occur even when particles are sufficiently fine if there is a large contrast in linear absorption coefficients between phases. This can cause diffraction intensity to respond nonlinearly to weight fraction, in contradiction to the main assumption of RIR-based QPA methods [1].

The U.S. Geological Survey recently released an updated database of XRPD diffractograms with associated RIR values for use with FPS on clay-bearing samples [2]. The RIR values were calculated by comparing XRPD patterns collected on the same diffractometer for 1) a corundum standard, 2) the pure phase in question, 3) a filler phase, and 4) a mixture (usually 40:40:20) of the pure phase, a filler, and the corundum standard. The filler was quartz for clay standards and disordered kaolinite (KGa-2) for non-clays.

We have used the database to recalculate the RIR values, while at the same time calculating the weight fraction of the fillers based on consistent RIR values for those phases. This allows us to evaluate, at least at a certain weight fraction, how accurate we can expect FPS to be for quartz and kaolinite, which can serve as proxies for other phases.

In addition, we are examining the database to see if Brindley corrections [1] based on the linear absorption coefficients of the phases present could be used to make the FPS method more accurate for a wider variety of phases.

[1] Taylor JC and Matulis CE (1991) Absorption contrast effects in the quantitative XRD analysis of powders by full multi-phase profile refinement, *J. Appl. Cryst.* 24, 14-17.

[2] Kane TJ, Campbell-Hay KM, and Eberl DD (2021) An updated X-ray diffractogram library of geologic materials, DOI: 10.5066/P9ID8IX1.

□

RESULTS OF THE STUDY ON ADSORPTIVE QUALITY OF ZEOLITE BY ARTIFICIALLY INCREASING RUMEN CUD AMMONIA CONCENTRATION IN LAMBS

Dorjgoo Purevtsogt¹, Tsogtbaatar Lkhagvajav¹, Sukhbat Banzragch¹, Davaasuren Ulzii-Uchral¹, Bazarragchaa Tumenjargal¹, Shirchin Demberel¹, Majigsuren Zolzaya*¹

¹Research Institute of Veterinary Medicine, MULS, Ministry of Economy and Development, Mongolia

*E-mail: mzoloo97@gmail.com

Keywords: natural zeolite, fistula, rumen vein, rumen cud, blood

INTRODUCTION

Mongolian grazing livestock typically lose over 20% of their autumn weight during the harsh winter–spring period due to prolonged feed shortages and severe environmental conditions. During this time, they rely on body reserves, leading to intensified rumen–hepatic nitrogen circulation and increased accumulation of toxic compounds such as ammonia and methane, which contribute to endogenous toxicosis. Natural zeolite may help neutralize these effects. Therefore, this study investigates the impact of zeolite on artificially elevated rumen ammonia levels in one-year-old lambs.

MATERIALS AND METHODS

□

Four one-year-old lambs (22.00 ± 1.17 kg) were fitted with a rumen fistula and left rumen vein catheter. After recovery, rumen and blood samples (rumen and jugular veins) were collected before feeding (0 h) and at 90, 180, and 360 minutes post-feeding to determine ammonia concentrations using the phenol-hypochlorite method; these served as baseline values.

Ammonia levels were then experimentally increased by administering 40 ml of 2M $(\text{NH}_4)_2\text{SO}_4$ on day 1 and 80 ml on day 2 via the fistula, with sampling at the same time points. In the following phase, the same dosing was repeated (40 ml on day 1, 80 ml on days 2 and 3), after which zeolite (1 g/kg) was administered 30 minutes later. Samples were collected and analyzed as in the control.

RESULTS AND DISCUSSION

□

Before giving 80 ml 2M sulfate ammonium solution, 1 g/kg zeolite and feed via rumen fistula or at hour 0, the rumen cud ammonia concentration was 20.97 ± 1.79 mmol/L, then increased gradually after the experiment start reaching 22.10 ± 1.57 mmol/L at 90 minute and 25.39 ± 1.03 mmol/L at 180 minute and finally a tendency of drop was found in the last samples stabilized at the level of 24.29 mmol/L. Comparison of this result to those in the experiment using 80 ml 2M sulfate ammonium solution demonstrates ammonia production reduces significantly by 34.7% at 90 minute and 28.2 to 20.9% at 180 to 360 minutes. It is seen that statistically significant decrease of artificially caused high concentration of ammonia with 2 M $(\text{NH}_4)_2\text{SO}_4$ solution in experimental lambs by use of 1 g/kg zeolite has proved the hypothesis propounded from practical trials and laboratory experiments.

Thus, results of the present study reveal the use of zeolite has positive effects on decrease of concentrations ammonia circulating in both rumen and peripheral venous blood.

INTERPRETABLE MACHINE LEARNING FOR PREDICTING BRICK STRENGTH FROM KAOLINITE AND ILLITE

Wang, Sen ^{*1}, Diao, Enmao², Gainey, Lloyd³, Liu, Lihui⁴, Zeng, Zijun⁵, Zhu, Runliang¹, and Xi, Yunfei^{1,6}

¹State Key Laboratory of Advanced Environmental Technology & Guangdong Provincial Key Laboratory of Mineral Physics and Materials, Guangzhou Institute of Geochemistry, Chinese Academy of Sciences, Guangzhou, China.

²DreamSoul, Chengdu, Sichuan 610000, China

³Brickworks Limited, Rochedale, QLD 4123, Australia

⁴School of Environmental and Municipal Engineering, Lanzhou Jiaotong University, Lanzhou, Gansu 730070, China

⁵School of Chemistry and Physics, Faculty of Science, Queensland University of Technology (QUT), QLD 4001, Australia.

⁶School of Mechanical, Medical and Process Engineering, Faculty of Engineering, Queensland University of Technology (QUT), QLD 4001, Australia.

*wangsen@gig.ac.cn

Quantifying the relationship between clay mineralogy and the mechanical properties of fired bricks is critical for industrial optimization, yet remains challenging due to the complex mineralogical reactions during firing. This study develops an integrated research paradigm combining machine learning (ML), SHapley Additive exPlanations (SHAP), and multi-scale mineralogical characterization to evaluate the specific roles of kaolinite and illite in brick strength development.

By leveraging a meticulously curated dataset of 70 laboratory samples, our model achieved high predictive accuracy, with validation and test R^2 values reaching 0.854 and 0.801, respectively. Notably, SHAP analysis quantified the hierarchical influence of key variables on compressive strength (CS): firing temperature (SHAP value = 0.56) was identified as the dominant factor, followed by the kaolinite/clay minerals ratio (0.29) and total clay mineral content (0.11).

Notably, the synergistic integration of advanced mineralogical characterizations with SHAP analysis provides a high degree of model interpretability, effectively transforming the predictive model from a “black box” into a transparent mineralogical mechanism. Unlike previous studies that rely on massive datasets of hundreds or thousands of samples, this work demonstrates that high predictive performance can be achieved with a relatively small but high-quality dataset through the integration of leave-one-out cross-validation and reasonable experimental design.